LAPPEENRANTA UNIVERSITY OF TECHNOLOGY

LUT School of Engineering Science

Master's Programme in Chemical Engineering

Oula Kotilainen

COOLING CRYSTALLIZATION OF CARBONATE SOLUTIONS

Examiners: Professor Tuomo Sainio

Professor Marjatta Louhi-Kultanen

Instructors: D.Sc. (Tech.) Bing Han

M.Sc. (Tech.) Juhani Vehmaan-Kreula

ABSTRACT

Lappeenranta University of Technology

LUT School of Engineering Science

Master's Programme in Chemical Engineering

Oula Kotilainen

Cooling crystallization of carbonate solutions

Master's thesis

2017

97 pages, 55 figures, 15 tables and 1 appendix

Examiners: Professor Tuomo Sainio

Professor Marjatta Louhi-Kultanen

Instructors: D.Sc. (Tech.) Bing Han

M.Sc. (Tech.) Juhani Vehmaan-Kreula

Keywords: Cooling crystallization, recausticizing, white liquor, green liquor

The purpose of this master's thesis is to increase the sodium hydroxide concentration of synthetic white liquor and industrial green liquor by separating sodium carbonate with cooling crystallization. In order to find the retention time for the liquor in a continuous process, two different cooling rates were studied.

The literature part of thesis presents the theory of cooling crystallization, which includes kinetics and mechanisms of crystallization, solubility and different crystallizer designs. In addition, recausticizing process is briefly presented.

In the experimental part of thesis both synthetic white liquor and industrial green liquor were crystallized using a batch cooling crystallizer. Different analysis were carried out for liquid phase and solid phase. The obtained crystals were analyzed with XRD, SEM, and CSD to examine the crystal composition, morphology and size distribution respectively. The liquid phase was analyzed by titration and ICP.

It was concluded that cooling crystallization offers a plausible technology to remove sodium carbonate from both liquors. Cooling rate was found to have little or no effect to the sodium carbonate to sodium hydroxide ratio.

TIIVISTELMÄ

Lappeenranta University of Technology

LUT School of Engineering Science

Master's Programme in Chemical Engineering

Oula Kotilainen

Karbonaatteja sisältävien liuosten jäähdytyskiteytys

Diplomityö

2017

97 sivua, 55 kuvaa, 15 taulukkoa ja 1 liite

Tarkastajat: Professori Tuomo Sainio

Professori Marjatta Louhi-Kultanen

Ohjaajat: TkT Bing Han

DI Juhani Vehmaan-Kreula

Hakusanat: Jäähdytyskiteytys, kaustisointi, valkolipeä, viherlipeä

Diplomityön tarkoituksena on kasvattaa natriumhydroksidin konsentraatiota synteettisessä valkolipeässä ja teollisessa viherlipeässä erottamalla niistä natriumkarbonaattia jäähdytyskiteytyksellä. Kahta eri jäähdytysnopeutta tutkittiin, jotta lipeän viipymäaika voitaisiin arvioida jatkuvatoimisessa prosessissa.

Kirjallisuusosassa on esitelty jäähdytyskiteytyksen teoriaa, kuten liukoisuutta, erilaisia jäähdytyskiteyttimiä, kiteytyksen kinetiikkaa ja mekanismeja. Lisäksi kaustisointiprosessi on esitelty lyhyesti.

Kokeellisessa osassa synteettistä valkolipeää ja teollista viherlipeää kiteytettiin panosjäähdytyskiteyttimessä. Nestefaasi ja kiteet analysointiin useilla eri menetelmillä. Kiteistä analysointiin muun muassa niiden morfologia, kokojakauma ja koostumus. Nestefaasi analysointiin titraamalla ja ICP:llä.

Tulosten perusteella jäähdytyskiteytystä voidaan pitää mahdollisena teknologiana natriumkarbonaatin erottamiseen synteettisestä valkolipeästä ja teollisesta viherlipeästä. Jäähdytysnopeudella ei ollut merkittävää vaikutusta natriumkarbonaatin suhteesta natriumhydroksidiin.

FOREWORDS

I thank the support from Juhani Vehmaan-Kreula, Taina Lintunen, Tuomo Sainio, Marjatta Louhi-Kultanen, and Bing Han for this thesis. Special thanks to Bing Han for the help in laboratory and to Marta Bialik and Anja Jensen for the chemical equilibrium simulation results. LUT laboratory staff members are acknowledged for helping with AAS, ICP, XRD, CSD, and SEM measurements.

Table of Contents

APPENDIX

I SEM Pictures of Produced Crystals

SYMBOLS

A	constant, -
A_C	surface area of the crystal, m^2
A_P	area of the particle, m^2
a	volume of the consumed HCl at the first turning point, ml
b	volume of the consumed HCl at the second turning point, ml
c	actual solution concentration, mol dm^{-3}
c^*	equilibrium saturation value, mol dm^{-3}
$c(Na_2CO_3)$	concentration of Na_2CO_3 in the liquor, mol dm^{-3}
$c(NaOH)$	concentration of NaOH in the liquor, mol dm^{-3}
$c(HCl)$	concentration of the HCL, mol dm^{-3}
DC	degree of causticizing, %
E_G	activation energy, kJ mol^{-1}
G	overall growth rate, m s^{-1}
g	constant, -
J	nucleation rate, -
K_g	growth constant typically, kg/(s m^2 $(kg_{solute}/kg_{solvent})^g$)
k	Boltzmann constant, $1.3805 \cdot 10^{-23}$ J K^{-1}
k_g	growth constant typically, m/(s$(kg_{solute}/kg_{solvent})^g$)
L	characteristic dimension, m
$M(Na_2CO_3)$	molar mass of Na_2CO_3, g mol^{-1}
$M(NaOH)$	molar mass of NaOH, g mol^{-1}
m	mass of the particle, kg
$m(beginning)$	initial mass of dried crystals and container, g
$m(container)$	mass of the container, g
$m(final)$	final mass of anhydrous Na_2CO_3 and container, g
$m(Na_2CO_3)$	mass of Na_2CO_3 in the liquor, g l^{-1}
$m(NaOH)$	mass of NaOH in the liquor, g l^{-1}
R	gas constant, 8.3145 J mol^{-1} K^{-1}
R_G	mass deposition rate, kg m^{-2} s^{-1}
r	radius corresponding to equivalent sphere, m
S	degree of supersaturation, -
T	temperature, K

TWF	total water fraction, %
V(sample)	volume of titrated sample, ml
v	molecular volume, m^3
α	volume factor, -
β	surface shape factor, -
γ	interfacial tension, J m^{-2}
ΔC	difference between bulk and interfacial concentrations, mol dm^{-3}
Δc	concentration difference, mol dm^{-3}
ΔG	overall excess free energy, J
ρ	crystal density, kg m^{-3}
σ	relative supersaturation, -

1 Introduction

Crystallization is a very old unit operation which dates back thousands of years. The earliest use for crystallization was the production of salt from sea water. Hence, crystallization can be regarded as the oldest separation technology in chemical engineering. When designing and operating a crystallizer one must consider numerous properties of the produced solids such as separation of the two or more phases. This is not specific for crystallization processes. In fact, almost all separation method involves the formation of a second phase from a feed stream. Relationships between function, process, phenomena, and product relevant in crystallization are represented in figure 1 (Seidel, 2007).

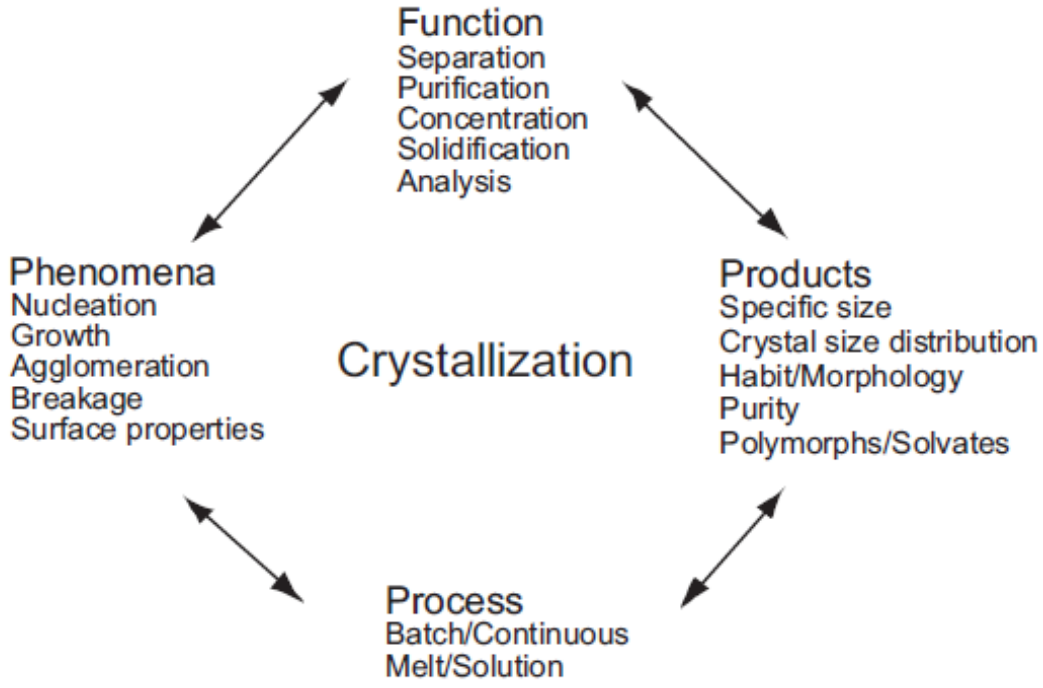

Figure 1. Crystallization (Seidel, 2007)

The possible functions achieved by crystallization are shown in figure 1. They include but are not limited to separation, concentration, and purification. For example, sodium carbonate, known in the industry as soda ash, can be recovered from brine. Crystallization acts as a separation method in this process (Seidel, 2007).

During the last four decades the attraction to more efficient recycles in a pulp mill has increased significantly. For instance, bleach plant effluent has been successfully recycled back to the evaporation plant. On the other hand, high recycle rates cause a problem: accumulation of nonprocess elements in the mill. Usually, this problem is solved by utilizing purge streams in key locations in the process (Jaretun and Gharib, 2000).

Recausticizing is a part of the chemical recovery cycle in kraft pulping process which is an important part in the production of white liquor. The recausticizing converts sodium carbonate (Na_2CO_3) in green liquor to sodium hydroxide (NaOH) which is one of the main active compounds in white liquor. White liquor is used in kraft pulping process to separate lignin and hemicellulose from cellulose fiber. The separation occurs because white liquor breaks the bonds between cellulose and lignin. Green liquor is a mixture of molten smelt from a kraft recovery boiler and weak wash liquor. Both white and green liquors are very alkaline solutions (pH>13) and get their name from their colour (Gullichsen and Fogelholm, 2000; Theliander, 1992).

1.1 Background

This Master's thesis is made for ANDRITZ Oy. ANDRITZ Oy is one of the leading global suppliers of systems, equipment and services for the pulp and paper industry, for instance, wood processing, fiber processing, chemical recovery and stock preparation. In addition, ANDRITZ Oy provides services to hydropower plants, steel and other metal strip foundries, and various separation technologies. This thesis is carried out for Fiber and Chemical Division located in Kotka, Finland.

This thesis is a part of a larger project which aims to develop and optimize a sustainable process for the production of regenerated cellulose. According to the background information of this project, one of the suggested methods for above process is based on cold alkali dissolution of pre-treated cellulose mixed with zinc and surfactants. Subsequently, the mixture passes through coagulation where Na_2CO_3 is the main salting-out component. The large potential for an easy recovery

and recycle of the process chemicals makes this technique extremely appealing. It was found earlier, however, that even small traces of Na_2CO_3 have a negative effect on the cold alkali dissolution process, particularly on the dissolution stage. As a result, the concentration of Na_2CO_3 present in the regenerated alkali stream must be of a minimum acceptable level in order to make the whole process technically feasible. Furthermore, both literature and previous results indicate that traditional recausticizing process is inadequate to produce white liquor containing the desired low concentration of Na_2CO_3, because recausticizing reaction is an equilibrium reaction which limits the conversion of CO_3^{2-} to OH^-. Furthermore, typically the white liquor used in the industry has a significantly lower concentration of OH^- than the equilibrium value. Therefore, an additional separation step is needed to purify the regenerated alkali stream. Multiple solutions to the above problem were suggested, but the most plausible one is a cooling crystallizer. When the solution is cooled to a subzero temperature the remaining CO_3^{2-} in the solution should crystallize as $Na_2CO_3 \cdot 10H_2O$ which is separated and recycled. Furthermore, the effect of cooling crystallization to the zinc found in the synthetic liquor is investigated because the zinc is a key species in the proposed process.

As a summary, the aim of this thesis is to provide a literature review of the cooling crystallization of carbonate solutions and in the experimental part to separate $Na_2CO_3 \cdot 10H_2O$ crystals from synthetic liquor and from industrial green liquor in low temperatures. In addition, existing data on the cooling crystallization of industrial green liquor below 10°C is not available. Therefore, cooling crystallization in lower temperature range below 10°C will be studied experimentally in this work as well.

2 Saturation and supersaturation

Solubility specifies the equilibrium concentrations of both the solid solute and liquid solvent. This knowledge enables calculation of the maximum yield of the produced crystals. This mass balance is an essential part of process design, development, and experimentation of any crystallization process. However, it does not provide anything about the rate at which the crystals are generated and the time

needed to this formation of solids. The reason is because thermodynamics provides the equilibrium states but not reaction rates. Moreover, Myerson describes crystallization as a rate process which means that the crystallization time is depended on a driving force. In the case of crystallization this driving force is referred as supersaturation. The main methods for generating supersaturation are represented in figure 2 (Myerson, 2002).

Arpe *et al*. describe saturated solution as a solution that is in thermodynamic equilibrium with the solid phase of its solute at a certain temperature. Still, solutions often contain more dissolved solute than that predicted by the equilibrium saturation value. These solutions are described as supersaturated. Concentration difference Δc, is generally used to express the degree of supersaturation:

$$\Delta c = c - c^* \tag{2.1}$$

Where, Δc = concentration difference, mol dm^{-3}
c = actual solution concentration, mol dm^{-3}
c^* = equilibrium saturation value, mol dm^{-3}

According to Arpe *et al*. supersaturation S and relative supersaturation σ are also common expressions of supersaturation. Both of these expressions are dimensionless and presented in equations (2.2) and (2.3) (Arpe *et al*., 2012).

$$S = \frac{c}{c^*} \tag{2.2}$$

$$\sigma = \frac{\Delta c}{c^*} = S - 1 \tag{2.3}$$

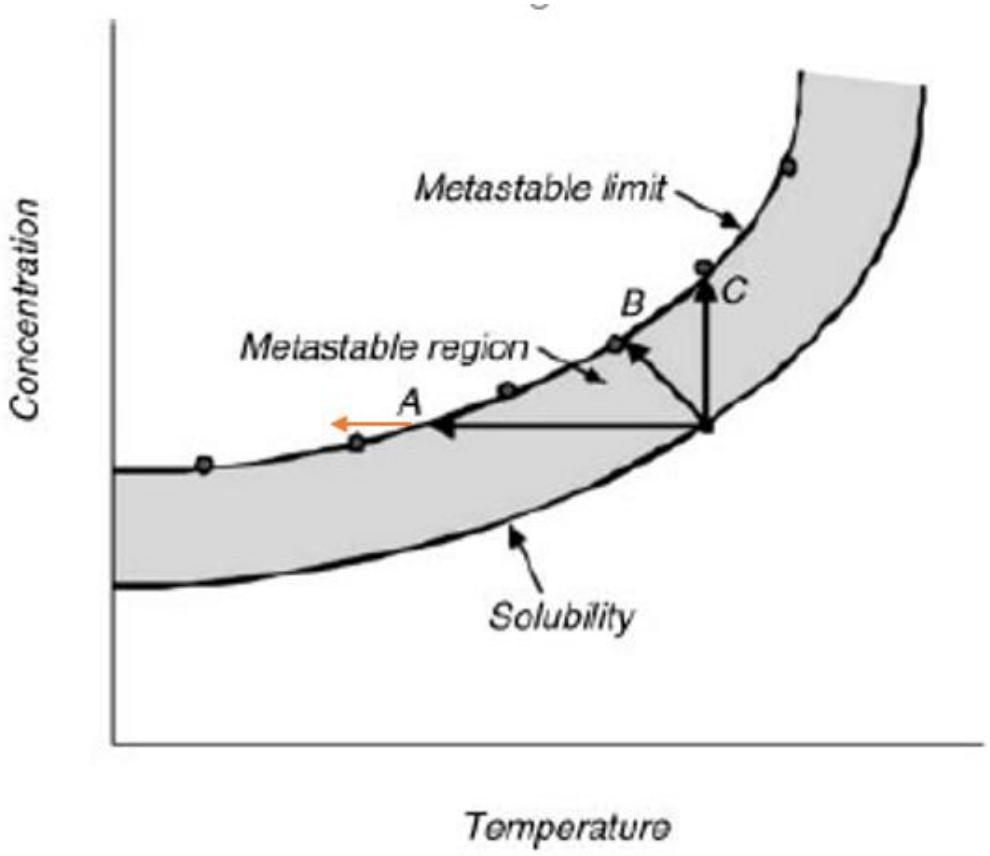

Figure 2. Main methods for generating supersaturation, (A) by cooling crystallization, (B) by evaporative crystallization (isothermal), (C) by evaporative-cooling crystallization (adiabatic). Adapted from Seidel, 2007 (modified).

Figure 2 helps to understand supersaturation, for instance, if a solution is cooled to point A it becomes saturated. If the solution is cooled slightly beyond point A (orange arrow), the solution will probably stay homogeneous. However, if the solution is agitated or left alone for a prolonged period of time, crystals will eventually form inside the system. As mentioned above, supersaturated solution is a solution in which the concentration of a solute surpasses the equilibrium solute concentration at a certain temperature. These supersaturated solutions are metastable. Figure 3 is provided in order to clarify what metastable means. An unsaturated solution is represented in figure 3a and shows as a minimum. This means that a large shock is required to change the state in this case. On the other hand, in figure 3b is represented a saturated solution which is the exact opposite of an unsaturated solution. This saturated solution is represented by a sharp maximum. As a result, only small disturbance is needed to change the state of the system. Finally, a metastable solution is shown in figure 3c, where a small change is

required to change the state of the system, but this change is conditioned (Myerson, 2002).

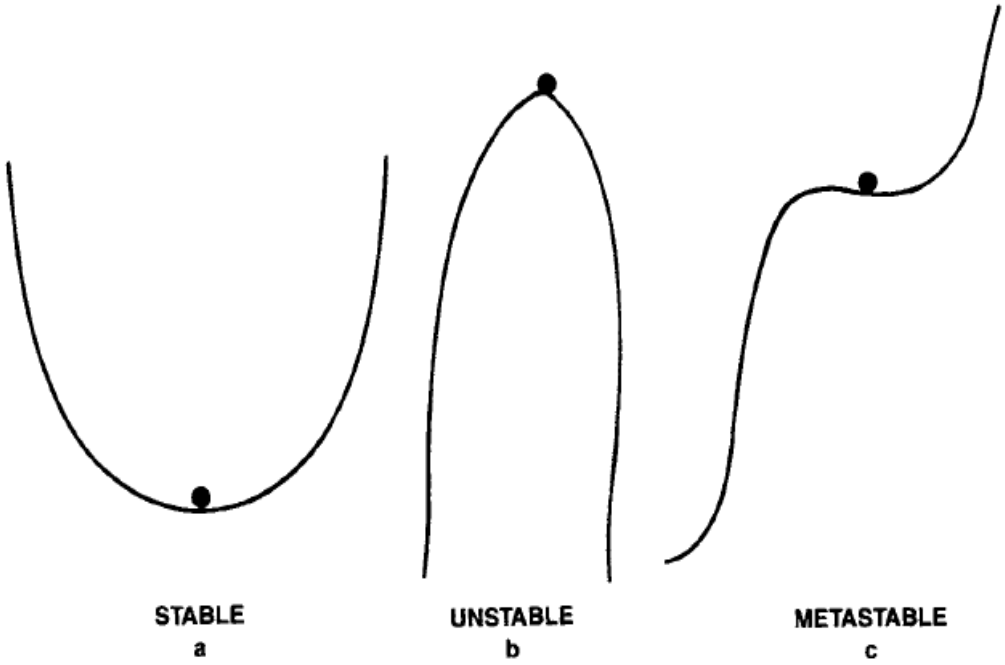

Figure 3. Stability states (Myerson, 2002).

3 Kinetics and mechanisms of crystallization

3.1 Nucleation

According to Mullin, neither supersaturation nor supercooling alone is adequate to start the crystal growth in a system. Crystals cannot develop unless there are lots of minute solid bodies, embryos, nuclei or seeds acting as cores for crystallization. There are two ways to start the nucleation of a supersaturated system: by delivering a disturbance to the system or waiting a period of time due to the spontaneous nature of nucleation. However, it is not always clear whether the nucleation happened spontaneously or whether it was induced artificially (Mullin, 2001).

Mullin lists several methods for causing nucleation in solutions and melts. These methods include, but are not limited to, agitation, friction, mechanical shock, and extreme pressures. In addition, the unpredictable consequence of external influences such as magnetic and electric fields, spark discharges, X-rays, UV-light,

and ultrasonic radiation have been investigated over the decades. However, none of the studied methods have yielded any significant application in industry-scale crystallization processes. Moreover, cavitation in an undercooled liquid may induce nucleation. The cause is probably a mixture of the above stated effects. Mullin reports that the nucleation takes place during the implosion of the cavity rather than the expansion of the cavity. That is because, as the cavity collapses the sudden change in pressure lowers the temperature of the solution and nucleation results (Mullin, 2001).

Nucleation, i.e., the generation of crystalline material within a supersaturated solution, is a complicated, usually unclear process, and nuclei may be formed by various mechanisms. Numerous classification schemes for describing nucleation have been suggested over the years. Most of these schemes, however, are divided into two main categories which are primary nucleation and secondary nucleation. Usually, the term primary nucleation is used when nucleation occurs in the absence of any crystalline matter. However, it is not uncommon that nuclei are formed in the proximity of crystalline material within the supersaturated liquid. This phenomenon is known as secondary nucleation and it takes place in the presence of crystals (Arpe *et al.*, 2012; Mullin, 2002). A simplified scheme of nucleation categorization is presented in figure 4.

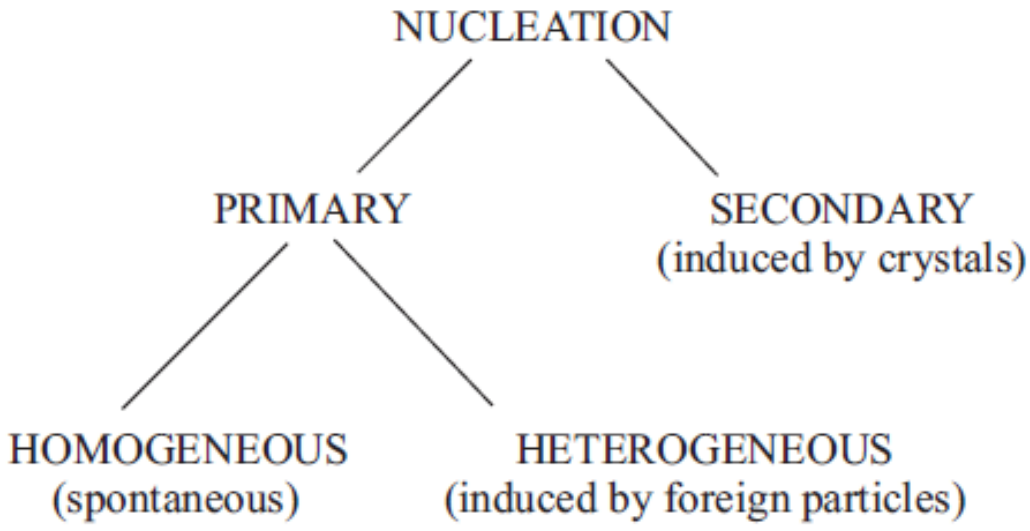

Figure 4. Nucleation categorization (Mullin, 2002).

According to Mullin, the nucleation rate which describes the number of nuclei generated per unit time per unit volume, can be expressed in the form of the Arrhenius reaction velocity equation. Arrhenius equation for reaction velocity is usually used for the rate of a thermally activated process (Mullin, 2002).

$$J = A \exp\left(-\frac{\Delta G}{\mathrm{k}T}\right) \qquad (3.1)$$

Where, J = nucleation rate, -

k = Boltzmann constant, $1.3805 \cdot 10^{-23}$ J K^{-1}

ΔG = overall excess free energy, J

A = constant, -

T = temperature, K

Nucleation rate can be also expressed as:

$$J = A \exp\left(-\frac{16\pi\gamma^3 v^2}{3k^3T^3(\ln S)^2}\right) \qquad (3.2)$$

Where, γ = interfacial tension, J m^{-2}

S = degree of supersaturation, -

v = molecular volume, m^3

How this is done is presented in J.W. Mullin's Crystallization Fourth Edition pages 184-185. Equation (3.2) shows that interfacial tension, also known as surface tension, degree of supersaturation, and temperature are the three major parameters that govern the rate of nucleation (Mullin, 2002).

As described above, the generation of new crystals, which is known as nucleation, refers to the start of the phase separation process. The solute molecules have generated the most minimal sized particles possible under the present conditions in the system. Subsequently, these formatted crystals begin to grow larger by the

addition of solute molecules from supersaturated liquid. According to Myerson, this phase of the crystallization process is generally called crystal growth. Crystal growth is discussed in detail in the following chapter (Myerson, 2002).

Nucleation and growth kinetics control, along with operating variables of the crystallizer, such crystal characteristics as crystal size distribution (CSD), modification of polymorphs or solvates, purity, and morphology. Seidel describes the crystal nucleation as the generation of an ordered solid phase from an amorphous or liquid phase. Furthermore, nucleation is the most important component as far as crystallizer design and CSD are concerned because it sets the character of the crystallization process (Seidel, 2007).

3.2 Crystal growth

Once a stable nucleus has been formed in a supersaturated liquid, it is able to grow into a crystal. This growth may be simplified to a two-step process which involves mass transport, either by convection or diffusion from the mother solution to the crystal face. Subsequently, a surface reaction occurs which integrates the growth units into the crystal lattice. The overall growth process may be contributed to either of above steps. On the other hand, convective mass transport is insignificant for very small crystals (diameter smaller than 10 μm) because they are rarely affected by turbulent eddies and diffusional mass transport predominates (Arpe *et al*., 2012).

Crystal growth and nucleation determine the final size distribution of the product crystals. Furthermore, the final product purity and the crystal habit are strongly influenced by the conditions and rate of crystal growth. Therefore, knowledge of crystal growth theory and experiments regarding crystal growth from solution are significant and extremely helpful in the development of industrial crystallization process (Myerson, 2002).

Generally, crystal growth is defined by the difference in some dimension of the crystal with time. This phenomenon is known as the linear growth rate. However,

the knowledge of a linear growth rate alone is not very useful because it can mean various things. Moreover, crystals consist of several faces which can grow at different rates. As a result, linear growth rate of a specific face is a fundamental expression of the crystal growth rate (Myerson, 2002).

Although face growth rates are an important topic in the fundamentals of crystal growth, they are not usually used to express the overall crystal growth. Different way of determining the growth rates of crystals is to measure the change in mass of a crystal. However, there is no easy or universally accepted method for expressing the growth rate of a crystal, because it is complicatedly affected by temperature, supersaturation, agitation, etc. Still, for thoroughly defined conditions crystal growth rate can be expressed as an overall growth rate G, mass depositions rate R_G, or a mean linear velocity v. The increase in mass as time passes is generally applied and can be directly linked to the overall linear growth velocity. The relationships between these quantities are presented in equation (3.3).

$$R_G = \frac{1}{A_C}\frac{dm}{dt} = 3\frac{\alpha}{\beta}\rho G = 3\frac{\alpha}{\beta}\rho\frac{dL}{dt} = 6\frac{\alpha}{\beta}\rho\frac{dr}{dt} = 6\frac{\alpha}{\beta}\rho v \quad (3.3)$$

Where, R_G = mass deposition rate, kg m^{-2} s^{-1}
A_C = surface area of the crystal, m^2
α = volume factor, -
β = surface shape factor, -
ρ = crystal density, kg m^{-3}
L = characteristic dimension, m
r = radius corresponding to equivalent sphere, m

The volume and surface shape factors, α and β, respectively, are defined in equations (3.2) and (3.3). For spheres and cubes $6\alpha/\beta = 1$ (Mullin, 2002).

$$m = \alpha\rho L^3 \quad (3.4)$$

Where, m = mass of the particle, kg

L = some characteristic size of the particle, m

$$A_P = \beta L^2 \tag{3.5}$$

Where, A_P = area of the particle, m^2

Eq. (3.3) shows that both the volume and surface shape factors must be known or estimated in order to calculate linear growth rates from mass growth rates. It is a common practice to make the assumption that the crystal shape is sphere and thus calculate growth rates based on a corresponding spherical geometry. Depending on the crystal's truly existing shape, this assumption can be an acceptable estimate or can be fairly substandard. Any accessible kinetic data on the crystal growth helps the development and operation of industrial crystallization process. The kinetic data can be utilized in process models, process and crystallizer design, and may help to understand empirical knowledge of the system (Myerson, 2002).

Numerous crystal growth theories provide a theoretical basis for the interactions of experimental crystal growth data and the identification of kinetic parameters from the experimental data to be utilized in models of large-scale crystallizers. Two basic models are often used to express the correlation between supersaturation and crystal growth. These expressions are shown in equations (3.6) and (3.7) (Myerson, 2002):

$$G = k_g \Delta C^g \tag{3.6}$$

Where, G = overall growth rate, m s^{-1}

k_g = growth constant typically, $m/(s(kg_{solute}/kg_{solvent})^g)$

g = is normally between 1 and 2

ΔC = difference between bulk and interfacial concentrations, mol dm^{-3}

$$R_G = K_g \Delta C^g \tag{3.7}$$

Where, K_g = growth constant typically, kg/(s m^2 ($kg_{solute}/kg_{solvent}$)^g)

Linear crystal growth velocity, length per time, is shown in equation (3.6) and mass rate of crystal growth, mass per area per time, is shown in equation (3.7). The growth constants (K_g and k_g) in equations (3.6) and (3.7) can be connected to each other, which is shown in equation (3.8) (Myerson, 2002):

$$K_g = 3\frac{\alpha}{\beta}\rho k_g \tag{3.8}$$

Both of the growth constants (K_g and k_g) are usually temperature-dependent. The Arrhenius equation can be used to acquire a universal model for growth rate. Growth constant k_g can be expressed using Arrhenius equation as a function of temperature (Myerson, 2002):

$$k_g = A \exp(-E_G/RT) \tag{3.9}$$

Where, A = constant, -
E_G = activation energy, kJ mol^{-1}
R = gas constant, 8.3145 J mol^{-1} K^{-1}
T = temperature, K

By combining equation (3.9) with equation (3.6), a complete crystal growth expression is obtained that takes into account both the temperature and supersaturation effect on the growth rate. This general expression is shown in equation (3.10):

$$G = A \exp\left(-\frac{E_G}{RT}\right) \Delta C^g \tag{3.10}$$

4 Factors affecting solubility

One of the basic physical properties of any ionic compound is their solubility. Theory behind this phenomenon suggests that ionic crystals in a saturated solution are in equilibrium with the hydrated ions. This equilibrium leads to increased solubility by reduction in lattice energy and by reduction in the energy of hydration of the ions. The prediction of an ionic compound solubility is complicated due to the competition of the above factors. Still, tables based on empirical data which predict solubility of ionic compounds have been generated and are repeatedly published in academic textbooks. On the other hand, the solubility of an individual species has proven extremely difficult (Hurst and Fortenberry, 2015).

4.1 Effect of impurities on solubility

It is uncommon to find so-called pure solutions outside laboratory conditions, and even then the impurities can cause measurement errors. However, industrial solutions are in most cases always impure. Moreover, the impurities usually have various effects on the solubility of the main solute and, in most cases; low impurity levels have major effects on crystal growth, morphology, and nucleation. Particularly, in industrial crystallization processes the impurities can complicate any improvements based on optimizing the process parameters, such as temperature, supersaturation, and residence time. Traditionally, the effect of impurities and solvents in industrial crystallization has been dealt with empirical knowledge. Nowadays, advanced modelling tools, kinetic data, and more accurate methods of determining crystals structure have provided better knowledge of crystal surfaces and the interactions between impurities, crystal surfaces and solvents (Mullin, 2001; Myerson, 2002).

According to Mullin, the impurities can have four different effects to a saturated binary solution. In his example a small amount of component *C* (soluble in *B*) is added to a saturated binary solution of *A* (a solid solute) and *B* (a liquid solvent). First effect, in rare cases, is that nothing happens and the system remains in its initial saturated state. Second effect is that component *C* reacts or combines otherwise

with *A* and the generated complex alters the nature of the original system. Third possible effect is that component *C* makes the solution supersaturated with regarding solute *A*, which would then be precipitated. In the fourth case, the solution becomes unsaturated with regards to *A*. Salting-out and salting-in terms are generally used to describe the last two cases, especially when electrolytes are involved (Mullin, 2001).

Seidel notes that, usually, impurities decrease the growth rates of crystalline materials and contamination of feed solutions often results in the production of smaller crystals than desired. Therefore, in order to minimize the occurrence of impurities in the crystallizer, unit operations before the crystallizer ought to be operated very precisely. In addition, the monitoring of composition of recycle streams is extremely important. This is done to prevent the accumulation of impurities in the recycle streams. Moreover, kinetic data used in scale up ought to be obtained from experiments on solutions analogous to those expected in the full-scale process (Seidel, 2007). The growth rate reduction of NaCl caused by $MgCl_2$ is shown in figure 5.

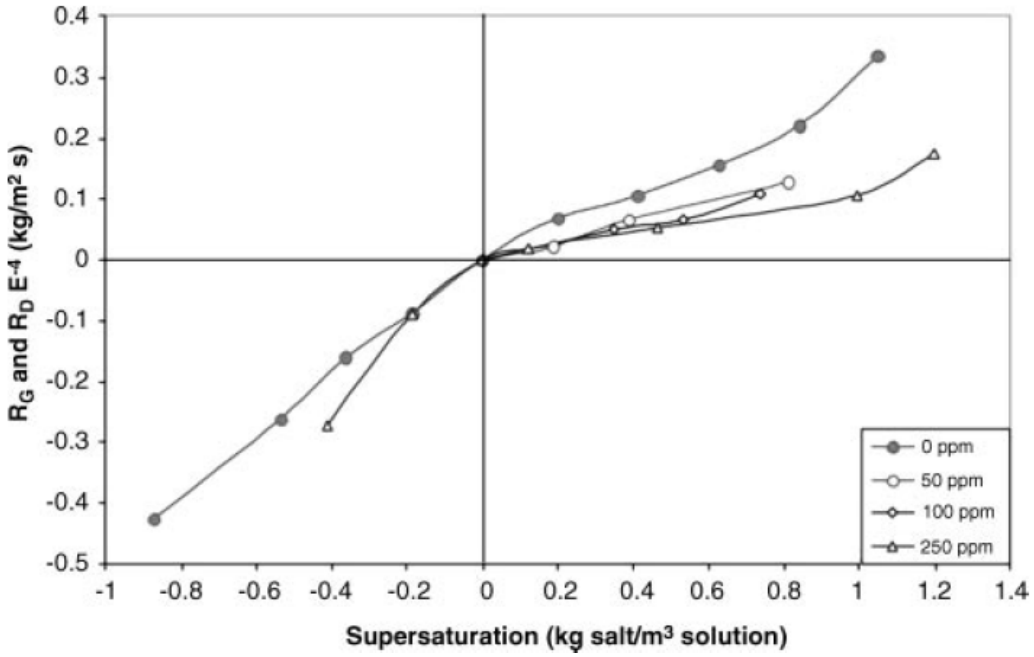

Figure 5. Growth rate of NaCl crystals with different concentrations of $MgCl_2$ (Seidel, 2007).

As shown in figure 5, the concentration increase of $MgCl_2$ reduces the growth rate of NaCl. According to Seidel, however, the solubility of any compound is strongly influenced by used solvent. This information is, particularly, used in the fine chemicals and pharmaceutical industries. For instance, poor solubility of another solvent results in low yield of the desired product. Besides, the solvent may result in weak crystal morphology or to the wrong polymorph (Seidel, 2007).

Crystallization is regularly used to influence separation process. Purification of materials that do not have impurities in the parts per million stage is achieved by crystallization due to the ordered lattice of a crystal, and more accurately, the energetic penalties for altering this order. In order for an impurity to penetrate the lattice substitutionally, impurity molecules must take place of host molecules at lattice sites. The different points of imperfection in crystal lattice are shown in figure 6. However, if the size, shape, or chemical composition difference between the host and impurity molecules is significant this substitution can only be accomplished at the cost of altering the crystal lattice. Usually, crystal lattice distortions cost lots of energy, and therefore are unfavorable from energy point of view, i.e., the total energy of the solid mixture is greater than the energy of the two pure solids, each in an undistorted crystalline state. As a result, true solid solutions are uncommon in organic systems. Moreover, they are only anticipated in systems where both host and impurity molecules are identical in size and shape, i.e., isomorphous. Of course there are several exceptions to the above statement, but they represent a small minority. For example, caproic acid and adipic acid which are isomorphous pair of organic molecules, and thus separate poorly by crystallization (Myerson, 2002).

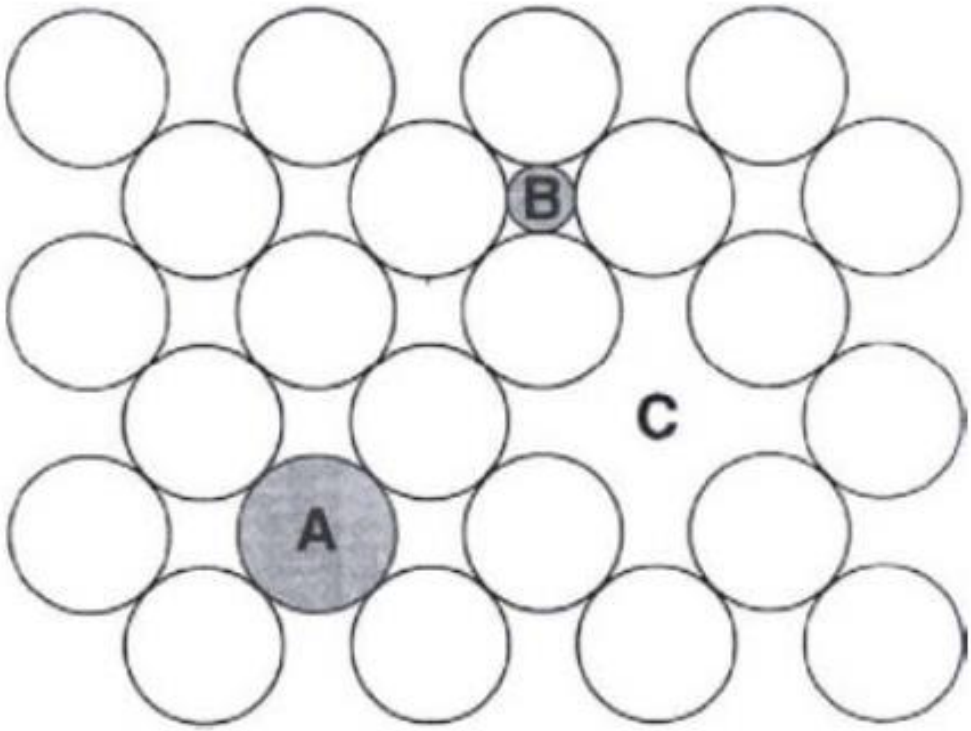

Figure 6. Points defects in crystalline lattice: (A) substitutional; (B) interstitial; and (C) vacancy. Adapted from Myerson, 2002.

4.2 Solubility of zinc oxide in aqueous sodium hydroxide solution

One of the proposed methods for the production of regenerated cellulose is based on cold alkali dissolution in the presence of zinc and surfactants. It is important to know how the zinc reacts as it passes through the chemical recovery cycle. Chen *et al*. have studied the solubility of zinc in Na_2O-ZnO-H_2O system at different temperatures (figure 7). It is visible from figure 7 that temperature has a major influence on the maximum value of zinc oxide solubility. Chen *et al*. conclude that ZnO in the alkaline solution on the left side of the equilibrium curve (line OB) cannot be obtained but $NaZn(OH)_3$ in alkaline solution on the right side of equilibrium curve can be obtained. However, in the case of Neocell the concentration of ZnO is around 1%wt. Therefore, according to Chen *et al*. the zinc should remain dissolved in the solution (Chen *et al*., 2012).

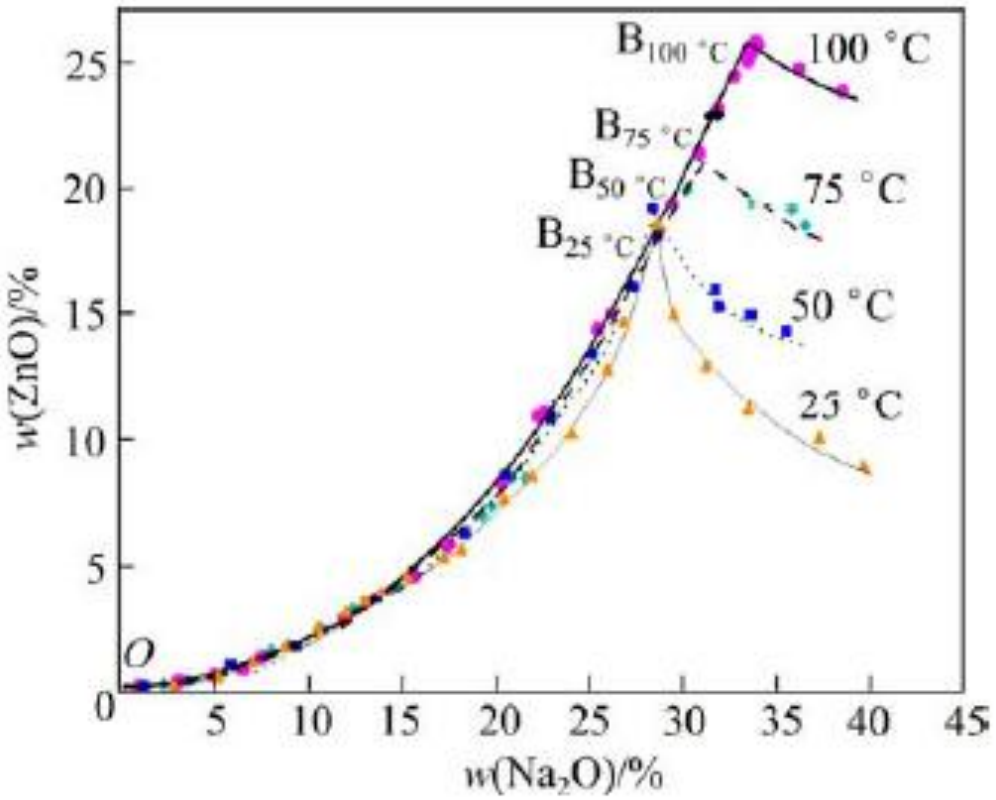

Figure 7. Solubility of zinc in Na_2O-ZnO-H_2O system. Adapted from Chen *et al.*, 2012.

4.3 Chemical equilibrium simulations

In order to have a better understanding of the effects of impurities in crystallization several simulation tools have been produced. These tools are used to estimate the amount of equilibrium liquid and solid compounds upon cooling. For example, OLI Studio Stream Analyzer software by OLI systems and Pitzer equations are these simulation tools.

OLI systems Stream Analyzer software is used for simulating aqueous-based chemical systems by utilizing a predictive thermodynamic framework for calculating the physical and chemical properties of multi-phase, aqueous-based systems (OLI Systems, 2017). Moreover, it predicts the composition in each phase, i.e. vapor, 2nd liquid, and solid. In addition, the simulation yields several thermophysical properties such as pH and density. The software calculates single points, surveys, mix, and separate operations. In this work, simulation data

regarding cooling of a carbonate solution was acquired. The used simulation conducted a temperature survey at constant pressure and feed composition. The temperature range was between −15°C and 25°C. Stream analyzer has two separate databases of thermodynamic parameters: Aqueous Databanks (AQ) and Mixed Solvent Electrolyte Databanks (MSE). The simulation was finished using both of the above mentioned databanks. However, it was noticed that AQ lacks the required parameters for the solid phase at low temperatures. Therefore, the simulation with MSE databank was assumed to be the reference case and the values from AQ simulation were included for comparison. The results from these simulations are represented in figures 26-29 which are found in the experimental part of this thesis.

5 Crystallization from solution or melt

Nowadays, there are numerous different crystallizers for industrial solutions. However, they can be classified into a few universal categories using different methods. Most commonly used method is to classify crystallizers according to the method by which supersaturation is achieved, i.e., cooling, evaporation, reaction, vacuum, etc., crystallizers. In addition, specific terms, such as batch or continuous, agitated or non-agitated, controlled or uncontrolled, classifying or non-classifying, can be used to further describe the crystallization process. Most of these classes are obvious, but some need description. For instance, supersaturation control is referred by the term control. The term classifying refers to the production of a specific product size by classification which takes place in a fluidized bed of crystals (Mullin, 2001).

Crystallization techniques can be categorized based on the methods which are used to form supersaturation in the solution. Supersaturation acts as a driving force for crystal formation. In the cases of cooling, evaporative, and adiabatic evaporative-cooling crystallizers the way to accomplish the supersaturation can be seen from the solubility line. The most commonly used methods for achieving driving force in solution crystallization are shown in figure 2. The term precipitation is used when the nucleation occurs only at very high supersaturation levels and is linked with fast

occurrence and crystal nucleation rates. Therefore, precipitation can be described as fast crystallization (Seidel, 2007).

Cooling crystallizers utilize a heat sink to extract both the sensible heat from the feed stream and the heat of crystallization dispensed as crystals are generated. Several different heat sinks are used in cooling crystallization from the ambient surroundings to cryogenic cooling agent. Evaporative crystallizers form driving force by evaporating solvent, therefore, increasing solute concentration in the mixture. Generally, evaporative crystallizers utilize a vacuum pump as a part of the unit, but other systems also exist. In evaporative-cooling crystallizers the loaded liquor has a higher temperature than the crystallizer which is operated at reduced pressure. As a result, solvent flashes instantly and, thereby concentrating the solute in the mixture and decreasing its temperature (Seidel, 2007).

Crystallization from solutions is most frequently used method in the wastewater treatment industry for the separation and recovery of salts in wastewaters. For instance, solute crystallization is widely used to recover sodium sulfate by reducing the temperature of industrial wastewater with saline levels. In addition, it has successfully recovered ammonium sulfate from high saline and high ammonia-nitrogen wastewater. Moreover, organic compounds have been also managed to crystallize from industrial wastewaters. Lu *et al*. reports obtained recovery results of poly-phenols from olive mill wastewaters. The study found that poly-phenols yield from the solution was high and the level of impurities was negligible (Lu *et al*., 2017).

5.1 Cooling crystallization

Cooling crystallization is both a separation and purification process which is generally executed in batch mode in the pharmaceutical, food and fine chemicals industries. Therefore, according to Myerson, batch cooling crystallization is certainly one of the most common forms of crystallization (Myerson, 2002). Almost always the products are high value-added which compensates the lack of continuous

process. Moreover, batch cooling crystallization is a straight forward process where a high temperature, concentrated solution consisting of a solute dissolved in a solvent is delivered into a container equipped with a stirrer and afterwards cooled down. The solution is called mother liquor and the container is called crystallizer. The temperature inside the crystallizer is controlled by pumping cooling agent trough jackets and in several cases with a coil to maximize the cooling surface area (Forgione *et al*. 2015, Myerson, 2002). The yield and economy of the crystallizer are influenced by the initial temperature and concentration of the feed solution. Furthermore, used cooling agent, for instance cooling water or glycerin solution, has an effect on yield and economics (Myerson, 2002). When the solution is cooled, the equilibrium concentration of the solution is reduced and fraction of the solute is moved from the liquid phase to the solid crystalline phase. Therefore, there is no longer a clear solution inside the crystallizer, but two-phase fluid slurry comprised of the solution and the solid crystals. Hence, the concentration of the solute in the liquid phase declines. On the other hand, the concentration of the solute increases in the solid crystals (Forgione *et al*. 2015).

Universally, cooling crystallization is applied for solutions in which solubility of solute is strongly influenced by temperature. Multiple chemical compounds solubility increases with the increase of temperature which is called direct solubility. Accordingly, the production of crystals can be accomplished by cooling the solution under suitable conditions. As another traditional crystallization method, cooling crystallization is additionally often applied in a plethora of fields (Lu *et al*., 2017).

Cooling crystallization can be split into three main categories: crystallization from solutions, freeze crystallization (freeze concentration), and eutectic freeze crystallization (EFC). The principle of these methods can be clarified by an ordinary phase diagram of a binary aqueous solution, which is shown in figure 8. It is apparent from figure 8 that the initial concentration of the solution has a direct effect on the cooling crystallization product. For example, if the initial concentration of the solution is higher than the eutectic concentration C_E, the solute will crystallize first. However, ice will crystallize first if the initial concentration of solution is

lower than C_E. Yet, very seldom the initial concentration of the solution is precisely at the eutectic concentration and both ice and the solute will crystallize simultaneously (Lu *et al*., 2017).

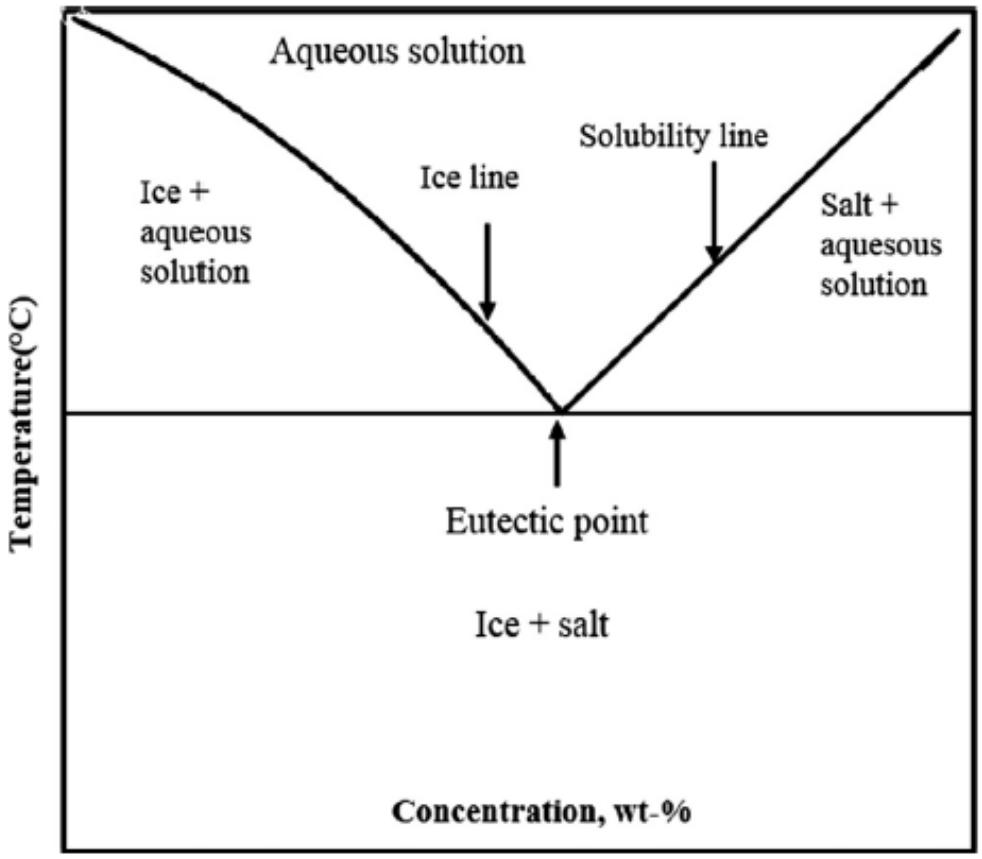

Figure 8. Binary phase diagram for a solution containing solute X in water (Hasan *et al.*, 2017).

According to Myerson, cooling is possibly the most frequent method of creating supersaturation. In addition, it is suitable for aqueous or nonaqueous liquids, in which the solute solubility is a strong function of temperature. In batch cooling crystallization the cooling is continued until the temperature difference between the solution and the cooling medium is minimal. As shown in figure 9, initially the temperature of the solution is vastly different from the cooling surface. Therefore, the solution is quickly brought to maximum supersaturation level due to this enormous subcooling. In addition, the disproportionate subcooling continues for a substantial part of the batch process. Subsequently, extensive nucleation of the solute can take place more than once. This phenomenon is called renucleation.

Nevertheless, the growth rate of nuclei subjected to maximum supersaturation is high which may cause dendritic growth and occlusions. Moreover, Myerson points out, crystallizing solute rapidly covers the cooling areas which is harmful to the heat transfer efficiency and may decrease the supersaturation rate. Furthermore, as the process proceeds, a considerable surface area of the crystal population generated earlier is able to utilize the excessive supersaturation level. As a result, the spontaneous formation of nuclei stops. The growth rate of the crystals generated from the spontaneous nucleation and secondary nuclei which are created due to the contact secondary nucleation may be slower. As the temperature difference between the solution and the cooling medium decreases, the growth rate of the crystal population decelerates rapidly (Myerson, 2002).

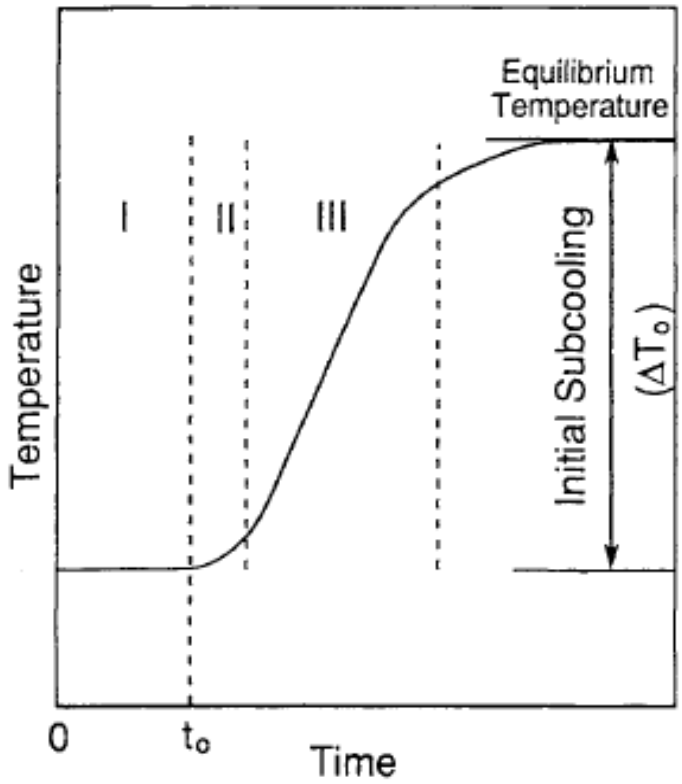

Figure 9. Temperature-time response curve (Myerson, 2002).

5.2 Freeze crystallization

Crystallization by freezing, more commonly known as freeze crystallization (FC) or as freeze concentration, refers to the generation of crystals of the solvent rather

than the solute, e.g. ice crystals from an aqueous solution, by removing heat. The product of FC is either high purity solvent crystals, e.g. water desalination, or the concentrated mother solution, for instance concentration of fruit juices. FC can only occur if the solution is undercooled below its freezing temperature, which provides the thermodynamic driving force for ice crystallization. After the crystals are formed they are separated, washed, and lastly melted to produce nearly pure solvent. On the other hand, ice crystallization will not take place, if the temperature is within the metastable zone, unless ice seeds are loaded into the solution. According to Hasan *et al.* ice crystallization from the aqueous solution emerges in an incremental concentration of the dissolved solid up to a precise supersaturation level is reached. After this supersaturation level, the dissolved solutes begin to crystallize out of the solution. Concurrent crystallization of solute and ice is known as eutectic freeze crystallization (EFC), which is discussed in detail below (chapter 5.3). The initial concentration of the solution dictates whether ice or dissolved solids start to crystallize, as shown in figure 8. Hasan *et al*. claim that previous research shows that one specific salt can be selectively crystallized under appropriate conditions from solution which includes multiple salts with seeding (Hasan *et al*., 2017; Arpe *et al*. 2012).

Freeze crystallization is theoretically applicable to numerous solutions and solvents. Still, in practice, it has only been widely applied in the wastewater industry, in which the ice is produced by cooling the wastewater below its freezing point. As a result, the produced ice has an exceptionally high purity as impurities are rejected from the crystal matrix as it forms. Hence, FC has huge potential for purification and recovery in wastewater treatment. Freeze crystallization can be divided into two categories: suspension freeze crystallization (SFC) and progressive freeze crystallization (PFC). The basic principle of both SFC and PFC methods is shown in figure 10. From these two methods SFC can be described as conventional, in which ice crystals crystallize out from the concentrated mother liquor and grow by the Ostwald ripening mechanism. The separation of these crystals, however, is quite complicated due to their small size. According to Hasan *et al*. there is not any industrial application of suspension freeze crystallization in wastewater treatment. However, PFC has also sparked intrigue in the wastewater treatment industry due

to its separation concept. In PFC, an intact ice layer forms and grows in the crystallizer. Therefore, the separation of the ice crystals from the mother liquor is extremely simple. Moreover, the operation intricacy, device design, and separation cost of PFC is considerably lower than SFC (Lu *et al*., 2017; Arpe *et al*. 2012).

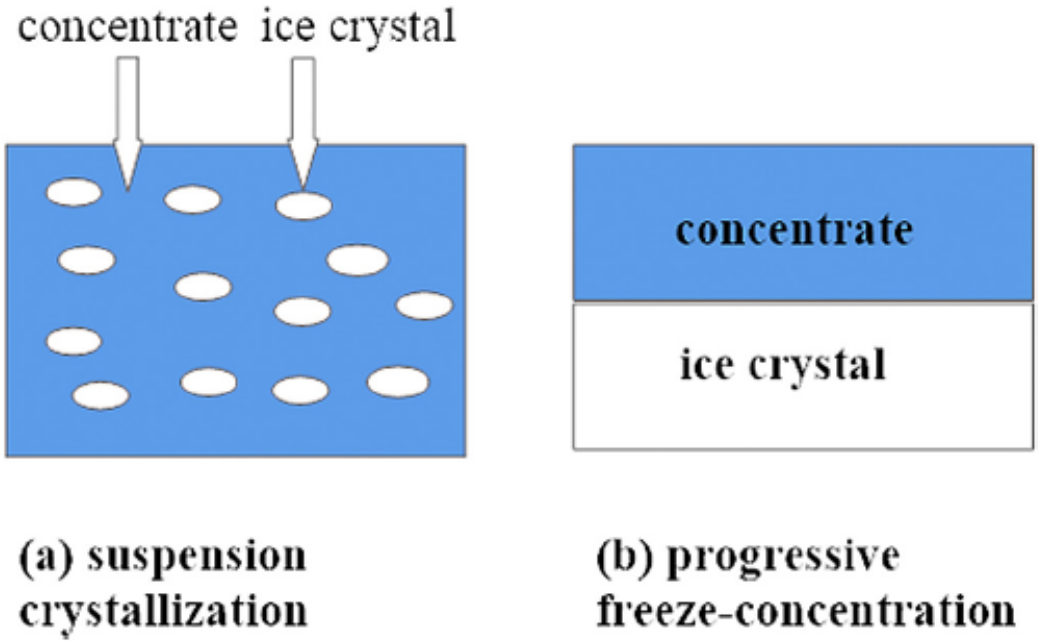

Figure 10. Schematic diagram of suspension freeze crystallization (a) and progressive freeze concentration (b) (Lu et al., 2017).

Despite the lack of any industrial applications of PFC in wastewater treatment there have been many efforts devoted to that. Numerous different wastewaters have been studied, for instance, organic and inorganic synthetic solutions, one-pollutant synthetic solution, complex mixtures, industrial and municipal wastewaters. Furthermore, various types of experimental devices for wastewater treatment have been investigated. One of adapted apparatus, as a freeze concentration technique, is the rotating evaporator, in which a balloon flask was fixed onto an evaporator at an angle of 45° and submerged in a cooling liquid. Ice crystals progressively form on the inner surface of the balloon flask. Separation of the ice layer from the liquid can be made easier by adding ice seeds to the solution. This is also known as heterogeneous crystallization. Moreover, using ice seeds the solution could be cooled to lower temperature without spontaneous nucleation. Lu *et al*. claim that it is not uncommon to achieve separation efficiency up to 100% using PFC in

wastewater treatment. In addition, Lu *et al*. concluded that PFC is widely applicable to wastewater treatment because all soluble pollutants were separated in the liquid phase. (Lu *et al*., 2017)

Freeze crystallization has several advantages for wastewater treatment. For example, there is no need for wastewater pretreatment, product ice is very pure, energy efficiency is high, biological fouling cannot take place, separation factor is high, and the produced ice can be used as a heat sink, etc. Despite all of the advantages of FC listed above, it has not been extensively applied in industries yet due to its drawbacks. The most important drawback of FC in wastewater treatment is high capital costs, which are two or three times higher than the cost of competitive systems (evaporation and distillation). Besides, device design and low treatment capacities are other disadvantages of freeze crystallization (Lu *et al*., 2017).

According to Mullin, large-scale freeze crystallization has been utilized in the petrochemical industry since the 1950s when the first continuous column crystallizers were built. The motivation of using freezing over evaporation for the separation of water from solutions is the potential for decreasing energy consumption due to differences in enthalpy. For instance, the enthalpy of crystallization of ice is 334 kJ kg^{-1} which is roughly 15% of the enthalpy of vaporization of water (2260 kJ kg^{-1}). The cost savings of using FC over evaporation, however, decrease in practice due to other additional separation steps. Besides, phase-change enthalpy does not take into consideration the energy recycle methods, which are generally employed in evaporation (Mullin, 2001; Arpe *et al*. 2012).

In fact, at the moment, FC is most widely applied in the food industry because flavor components, which can be preserved in the freeze crystallized product, are normally lost during evaporation process. Especially fruit juices and coffee extracts etc. are concentrated by using indirect-contact freeze processes, in which solution is crystallized in the surface of a heat exchanger. Hitherto, the ice slurry is washed and product crystals are recovered. However, in spite of earlier enthusiasm,

industrial applications in desalination, effluent treatment, solvent recovery etc., have not yet appeared (Mullin, 2001; Arpe *et al*. 2012).

Crystallization of a solvent out of a melt at its freezing temperature is known as freeze crystallization. For example, crystallization of ice from aqueous solution at its freezing point can be categorized as freeze crystallization of water or ice crystallization. As shown in figure 10, there are two main methods for generating ice crystals from aqueous solutions: suspension crystallization and progressive-freeze crystallization which is also known as layer crystallization. Both of these methods include ice nuclei formation from the mother solution, followed by their growth. Suspension freeze crystallization operates by cooling the mother liquor in an agitated vessel by pumping cooling agent through the jacket and in some cases cooling coils. As a result, ice crystals are formed in the suspension. The crystals are removed from cooling surface by scrapers in order to keep the heat transfer rate from reducing. The disadvantages of SFC are high investment and maintenance costs. On the other hand, in PFC the ice crystals form a single layer on the cooling surface which is easy to remove from the mother liquor and wash. In the case of fast crystallization rate, however, product quality often decreases due to impurities trapped inside the ice, therefore, hindering the practical implementation of this method (Hasan *et al*., 2017).

Freeze crystallization is applicable for several fields associated with solute concentration, separation, and purification processes. FC has not been utilized widely outside the food industry, despite high product quality, good separation properties and low energy consumption, due to high capital investment and maintenance cost. Besides, the ice layer formation on the cooling surface thwarts the heat exchange rate, as the thermal conductivity of ice is extremely low compared, for instance, to stainless steel which is commonly used as a surface wall material (Hasan *et al*., 2017).

5.3 Eutectic freeze crystallization

Eutectic freeze crystallization (EFC) is a derivative of freeze crystallization, in which both ice and salt are crystallized simultaneously with high purity levels by operating at the eutectic temperature (figure 8). A major advantage of EFC is that the separation of ice and salt from the mother liquor happens naturally due to their significant density differences, as ice floats to the top of the column as salt sinks to the bottom. This eliminates one separation step in the process. On the other hand, like freeze crystallization, the major drawback of EFC is the reduction of production rates due to ice scale forming on the cooling surfaces which significantly reduces the heat transfer capacity. To make matters worse, according to Hasan *et al*. scaling during EFC is discovered to be more drastic than that incurred by either ice or salt separately (Hasan *et al*., 2017; Lu *et al*., 2017).

High investment cost due to the use of scrapes to discard ice-fouling limits the applications of any EFC the same way as in FC. Besides, the use of scrapes makes scale-up and maintenance problematic. Therefore, it is very important to cause the start of ice-scaling for any FC/EFC on cooling surface, as the heat transfer between the mother liquor and the cooling agent is hindered onward (Hasan *et al*., 2017).

Lu *et al*. reported that $MgSO_4 \cdot 12\ H_2O$ and $Na_2CO_3 \cdot 10\ H_2O$ were recovered successfully from separate wastewaters using EFC. Besides, both the ice and salts had good filtration properties. The average size of the disk-shaped ice crystals was 300 µm and 600 µm for $MgSO_4 \cdot 12\ H_2O$ crystals. The eutectic temperatures were reported at – 3.9 °C for magnesium sulfate industrial wastewater and – 3.8 °C for an industrial Na_2CO_3- $NaHCO_3$-H_2O wastewater. Lu *et al*. used a scaled-up version of the SCWC-2 prototype in order to achieve the high production rates of ice and $Na_2CO_3 \cdot 10\ H_2O$ crystals from the wastewater samples. Still, the SCWC-2 prototype was easily scaled up by adding one heat exchanger on top of another heat exchanger. Both of these heat exchangers consist of two vertical concentric cylinders which are scraped from all sides. The schematic of the scaled up SCWC-2 prototype is shown in figure 11 (Lu *et al*., 2017).

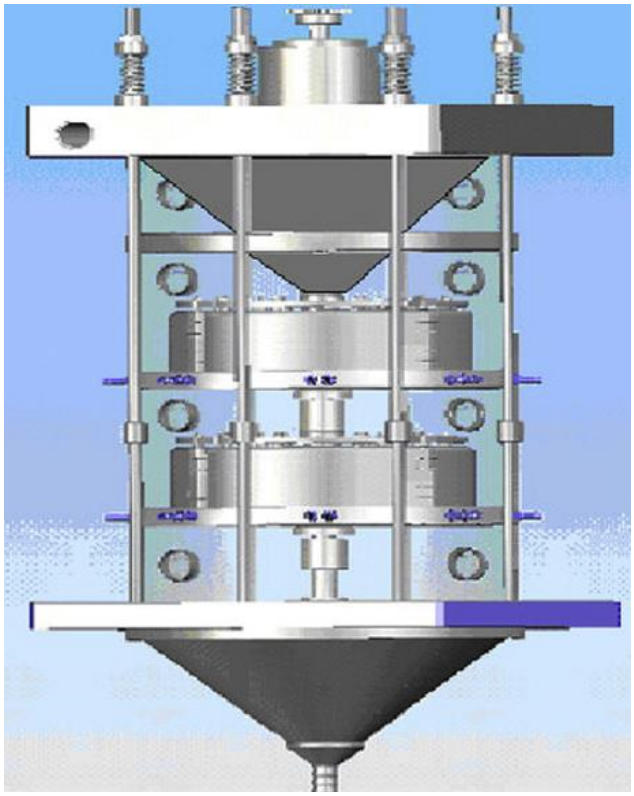

Figure 11. Scaled-up version of the SCWC-2 with two heat exchanger modules for eutectic freeze crystallization (Lu et al., 2017)

As in freeze crystallization, in EFC the energy requirements are drastically lower compared to separation by evaporation, since heat fusion of ice (6.01 kJ/mol) is one-sixth of water evaporation heat (40.65 kJ/mol). Lu *et al*. claims that eutectic freeze crystallization has been found to have considerably lower energy consumption than that of triple-effect evaporative crystallization (EC). Hence, the operating costs savings of EFC over EC was reported at 80% for complex hypersaline brines containing NaCl and Na_2SO_4. The energy consumption reductions of EFC compared with traditional triple-effect EC were less than that of complex hypersaline brines, but still significant: about 30% for $NaNO_3$ and 65% for $CuSO_4$ (Lu *et al*., 2017). On the other hand, EFC requires, as relatively new technology, much higher investment costs and is more mechanically complicated than conventional EC. As a result, EFC has not been widely utilized in the wastewater treatment industry (Lu *et al*., 2017). A summary of EFC related research is represented in table I.

Table I Summary of EFC related research

Type of wastewater	Comments and findings
Industrial solution[a)]	Ice and Na_2CO_3 was produced at high production rates. Improved separation and ice scaling removal. Residence times: 2.7 h (ice) and 4.0 h (Na_2CO_3).
Na_2CO_3-$NaHCO_3$-H_2O system[b)]	High purity $Na_2CO_3{\cdot}10H_2O$ was produced at −3.8°C. At −4.0°C $NaHCO_3$ started to crystallize resulting in poor product purity and filtration properties.
Na_2CO_3-$NaHCO_3$-H_2O system[c)]	Only anhydrous $NaHCO_3$ and $Na_2CO_3{\cdot}10H_2O$ were present in equilibrium with ice crystals in the ternary system. Crystal sizes: 5-10 µm ($NaHCO_3$) which agglomerated into 100-300 µm particles and 100-500 µm ($Na_2CO_3{\cdot}10H_2O$).
Industrial brine[d)]	Operating costs: 169 $/day (EFC) and 930 $/day (EC). Capital costs: 574673 $/day (EFC) and 318255 $/day (EC).
Synthetic Na_2SO_4 solution[e)]	At high level of temperature driving force ($\Delta T>6.0°C$) agitation has a significant effect on induction time. At low level ($\Delta T<2.0°C$) the agitation has insignificant effect on induction time.
Synthetic Na_2SO_4-brine system[f)]	100% pure $Na_2SO_4{\cdot}10H_2O$ and ice crystals containing <20 ppm impurities were produced from synthetic RO retentate stream.
Synthetic Na_2SO_4-brine system[g)]	Impurities in the system raised the eutectic temperature significantly. $Na_2SO_4{\cdot}10H_2O$ crystals formed before ice crystals.
Process streams of $CuSO_4$ and $NaNO_3$[h)]	Energy consumption reduction compared to evaporation are: ~30% ($NaNO_3$) and ~65% ($CuSO_4$)

a) Rodriquez Pascual *et al*., 2010. b) Van Spronsen *et al*., 2010.
c) Rodriquez Pascual *et al*., 2010. d) Lu *et al*., 2017
e) Hasan *et al*., 2017 f) Reddy *et al*., 2010
g) Lewis *et al*., 2010 h) van der Ham *et al*., 1998.

6 Cooling crystallization methods for carbonate solutions

Cooling crystallization of industrial green liquor has been in investigated by Covey *et al*. Their aim was to separate sodium carbonate from green liquor and use it in split-sulfidity kraft pulping. According to Covey *et al*., solubility of sodium carbonate at low temperatures is similar between industrial green liquor and synthetic mixtures. However, the dynamics of the crystallization are more complicated than equilibrium tests suggest. In addition, numerous metastable conditions are present in cooled liquor. Covey *et al*. report that below 15°C, crystals form rapidly and the measured solubility is comparable to equilibrium values found for synthetic solutions. On the other hand, above 15°C, although crystals are formed, the solubility of sodium carbonate is significantly higher than the equilibrium would suggest (Covey *et al.*. 1999)

Sodium carbonate has considerably lower solubility at low temperatures than at high temperatures which enables its separation by cooling crystallization. According to Covey *et al*., high yield of sodium carbonate heptahydrate or decahydrate can be obtained from green liquor, especially from highly concentrated green liquor, if the cooling is adequate. Although the energy requirements are considerably less compared to evaporating process, refrigerant utilization is less convenient compared to heat (Covey *et al.*. 1999).

Covey *et al*. report that first crystals formed at 20°C if equilibrium was reached fast and generation of metastable zones was avoided. Sodium carbonate solubility in concentrated green liquor as a function of temperature is presented in figure 12. Figure 13 shows the concentration of the sulfide, hydroxide, and carbonate in the solution as its temperature decreases. It is visible from figure 13 that carbonate concentration sharply decreases around 15°C as nucleation and crystallization becomes accelerated. As a result, formed sodium carbonate crystals are hydrated which remove water from the mother liquor, and therefore increases the concentration of the remaining species. In addition, this increases the amount of crystallization of sodium carbonate at any given temperature (Covey *et al.*. 1999).

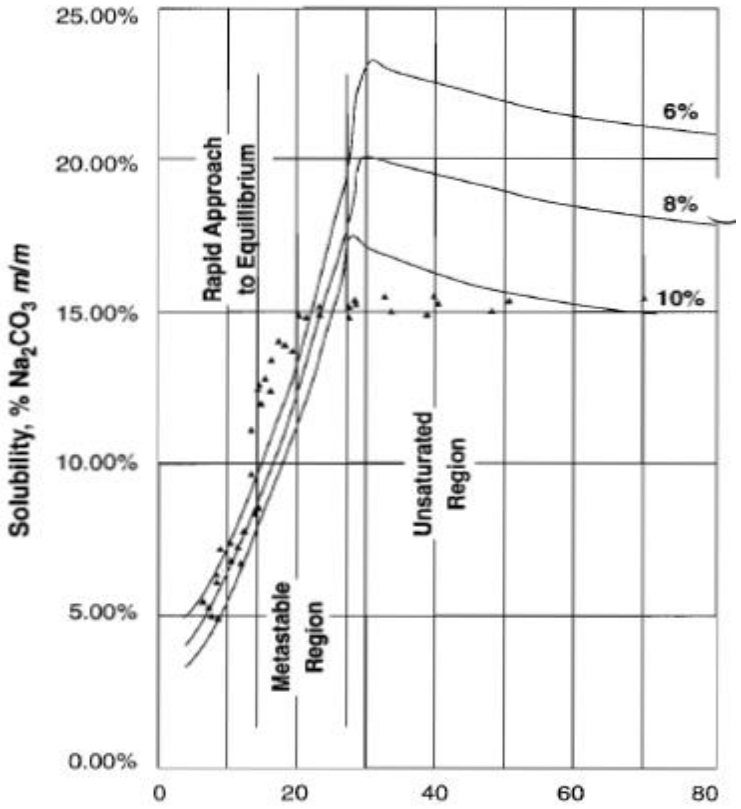

Figure 12. Measured concentration of sodium carbonate in concentrated green liquor at temperature for 15 minutes (solid lines are equilibrium curves at various sodium sulfide concentrations) (Covey *et al.*. 1999)

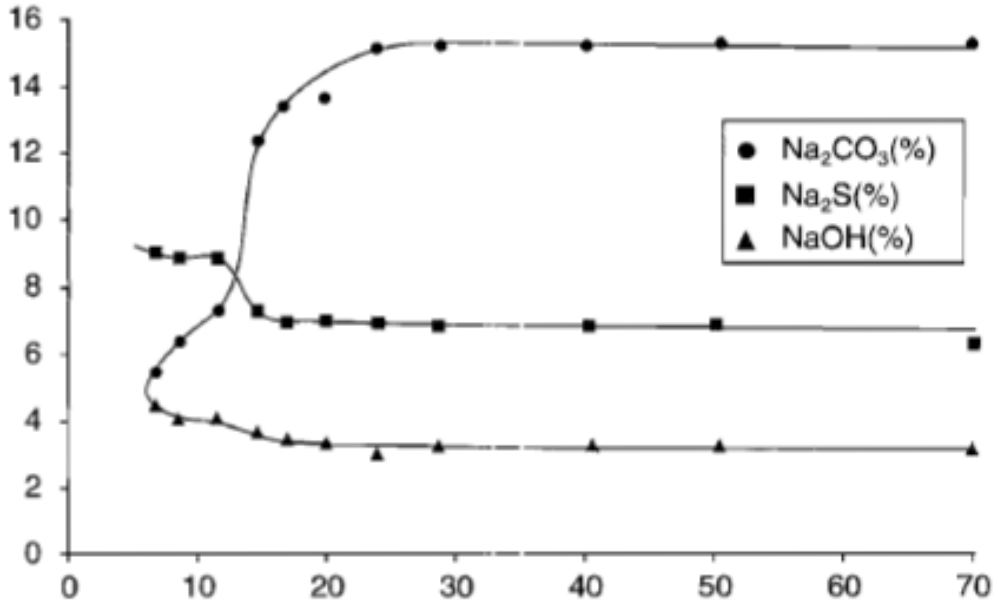

Figure 13. The concentration of sodium carbonate, sulfide and hydroxide in cooled concentrated green liquor. (Covey *et al.*. 1999)

Jaretun and Aly have suggested a process for the removal of chloride and potassium from green liquor by cooling crystallization which is shown in figure 14. As shown in figure 14, the process contains evaporation, crystallization, and filtration stages. More importantly, according to Jaretun and Aly, both sodium carbonate and sodium bicarbonate crystallized at low temperature in the crystallizer. The potassium and chloride retained in the remaining solution. Last step in the process is the filtration of precipitated crystals where the solution is fed into the purge stream (Jaretun and Aly, 2000).

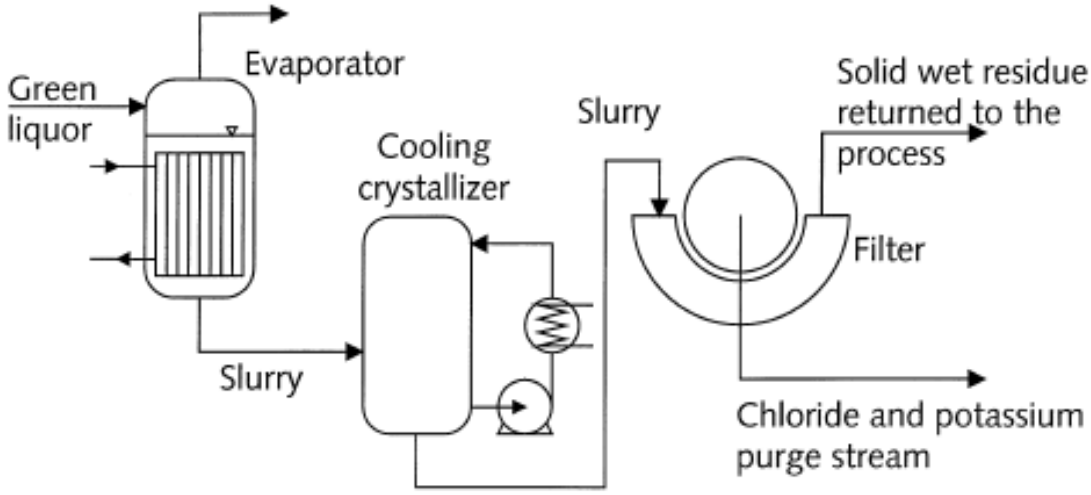

Figure 14. Suggested process for the removal of chloride and potassium through green liquor cooling crystallization (Jaretun and Aly, 2000).

6.1 Cooling crystallizers

Generally, only the crystallizer temperature is controlled in an industrial batch crystallizer. The temperature of the crystallizer is controlled by varying the cooling agent flowrate in the jacket and, if installed, coils. Various different cooling crystallizers will defined in the following discussion (Forgione *et al*. 2015).

6.1.1 Non-agitated vessels

The unstirred tank is the most uncomplicated type of cooling crystallizer, in which hot liquor is loaded into the open vessel and allowed to cool. Generally, cooling

takes place over several days, mostly by natural convection. Metal bars can be suspended in the solution in order to grow large crystals on their surface, thereby reducing the amount of crystals that sinks to the bottom of the crystallizer. The product is extracted manually (Mullin, 2001).

Due to slow cooling rate the produced crystals are generally large and interlocked. Moreover, retention of mother liquor is bound to happen. Therefore, the dried crystals have impurities, thereby lowering the product quality. Furthermore, crystal size distribution of the product is wide due to the uncontrolled nature of the process. Generally, labour costs are high in this method. On the other hand, capital, operating, and maintenance costs are low making this method economical for small batches. Still, the production rate of this type of equipment is low and space requirements are high (Mullin, 2001).

6.1.2 Agitated vessels

The crystal size distribution can be made narrower by installing an agitator to the open-tank crystallizer. In addition, this generally produces smaller crystals at reduced batch times. The purity of the final product, also, is usually higher because the crystals contain less mother liquor after filtration and more adequate washing is possible. Mixing inside the crystallizer can be enhanced by installing vertical baffles. However, they ought to stop below the liquor level to prevent excessive encrustation. According to Mullin, water jackets are generally preferred to coils for cooling intents and, where possible, the crystallizer surface walls should be smooth and crevice-free (Mullin, 2001).

An agitated cooling crystallizer has a much higher productivity rate than a simple tank crystallizer, but it has higher operational costs. The final product is, still, collected by hand which raises the labour costs rather high. There are numerous different design options for tank crystallizers from shallow pans to large tanks (Mullin, 2001).

Efficient mixing inside the vessel and high heat transfer rates between liquor and cooling surfaces can be achieved by using external circulation, as seen in figure 15. The vessel can be equipped with an internal agitator. Due to high liquor velocities in the tubes, small temperature differences between liquor and cooling agent are sufficient for cooling purposes. Besides, encrustation on the cooling surfaces can be reduced significantly and the equipment is available in batch or continuous mode (Mullin, 2001).

The large cooling crystallizer with fitted agitator shown in figure 15 dispenses the spent liquor from the top. Produced crystals are prevented from entering this stream by a conical section which decelerates the liquor velocity. Near the bottom of the crystallizer an agitator circulates the crystal slurry through the growth zone (Mullin, 2001).

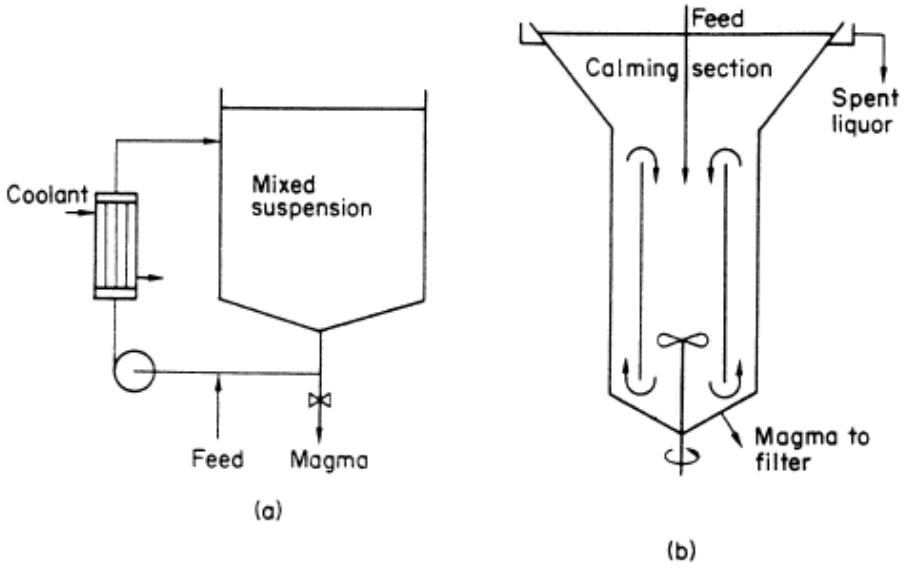

Figure 15. Agitated tank crystallizers: (a) external circulation through a heat exchanger, (b) internal circulation with a draft tube (Mullin, 2001).

6.1.3 Wolff-Bock crystallizer

The first continuous crystallizer in chemical industry was Wolff-Bock unit in the beginning of 1900s. It was generally known as the crystallizing cradle or rocking crystallizer. The schematic of this type of crystallizer is shown in figure 16 and its

main component is a long shallow gutter rocked on supporting rollers. Feed stream is located at one end of the crystallizer and produced crystals are discharged at the other end, continuously. In order to prevent massive longitudinal overflow of the liquor, diagonal baffles can be fitted inside the gutter. As a result, the mother liquor flows from side to side along the gutter. Residence time of the mother liquor is controlled via the slope of the gutter, especially towards the end (Mullin, 2001).

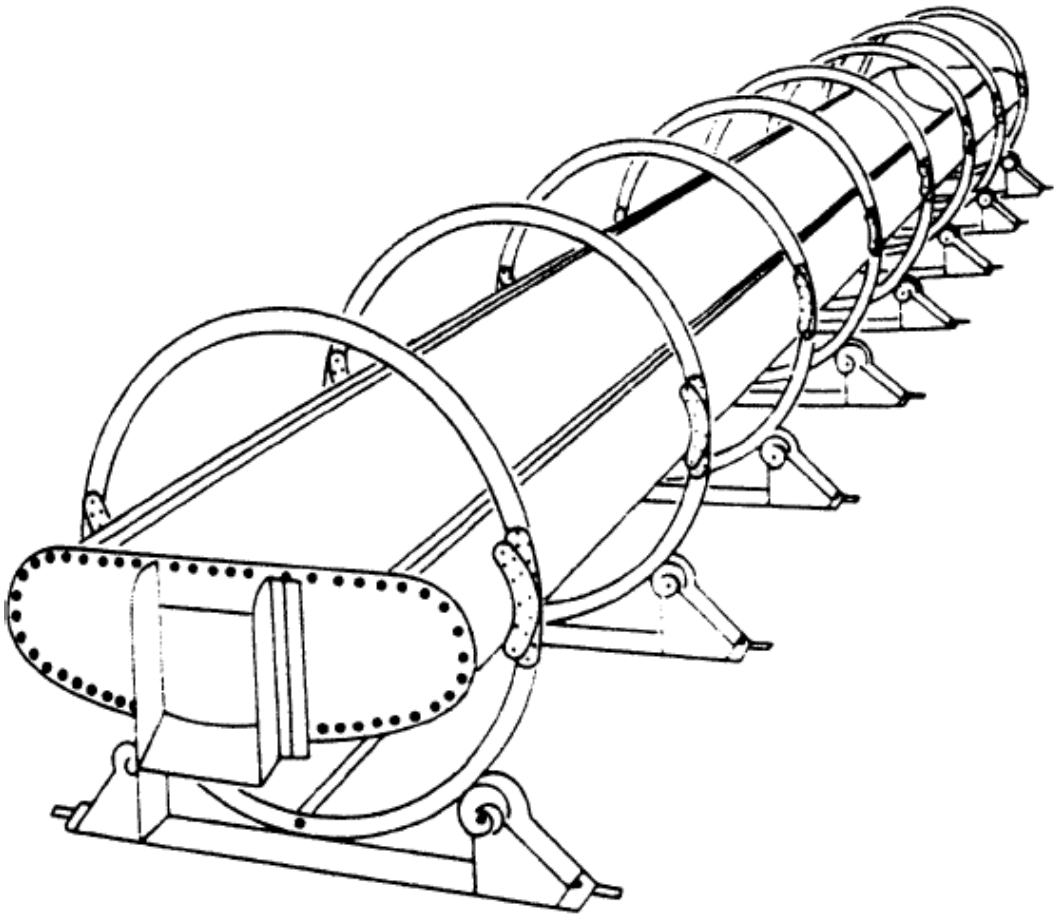

Figure 16. Wolff-Bock crystallizer (Mullin, 2001).

6.2 Freeze crystallizers

Freeze crystallizers can be classified into two main groups: direct freeze crystallizers and indirect freeze crystallizers. In direct freeze crystallizers, the utilized cooling liquid is combined directly with the mother solution. In indirect freeze crystallizers, however, the cooled solution goes through a heat exchanger. Secondary refrigerant freeze and vacuum freeze crystallizers are included in direct

freeze processes, while the indirect freeze crystallizers include progressive freeze-concentration, suspension crystallization, and external freeze crystallizers (Randall, 2015).

Mullin notes that, one of the biggest engineering challenges of the 21st century is the production of fresh water from seawater. Desalination by crystallization has been studied over the years. Moreover, the pursued freeze processes, at the time, were vacuum flash freezing, immiscible refrigerant freezing and hydrate freezing (Mullin, 2001). Still, all freeze separation processes rely on the generation of high purity solvent crystals from mother solution. This grants single-stage equipment for eutectic systems, as described in section 5.3. Generally, multistage solid-solution operations are avoided. Freeze crystallizers can be categorized into several groups based on the used refrigeration system. For example, vacuum flash freezing, direct and indirect freezing, and cryogenic freezing (Arpe *et al*. 2012).

Vacuum flash freezing takes advantage of the cooling effect of vaporization, where a high vacuum is utilized to vaporize a fraction of water. This decreases the temperature of the solution, causing ice crystallization to happen. Scale formation on the heat-transfer surfaces is avoided, because traditional heat exchangers are not necessary in these processes. The solution is sprayed into a container which is operated at reduced pressure. As a result, fraction of the water vapour flashes off and the remaining salt solution partially freezes. The resulting ice-brine slurry is filtered, and the ice crystals are washed and remelted. According to Mullin, units based on this principle have been operated at a commercial scale. However, Arpe *et al*. claims that vacuum freezing has not achieved commercial success despite it being attractive for aqueous systems due to massive enthalpy differences between ice crystallization and water evaporation (Mullin, 2001; Arpe *et al*. 2012; Randall, 2015)

The hydrate processes work because certain species can generate inclusion compounds with water which are also known as hydrates. These hydrates are separated from the mother liquid and decomposed to recover the hydrating agent.

Mullin states that propane is one of the most promising hydrating agents. The major advantage of this method is that it operates near ambient temperature (10-15°C). Furthermore, the energy consumption is minimized. On the other hand, the produced crystals usually have both poor filtration and washing properties due to the crystals light, feathery nature (Mullin, 2001).

In indirect-contact freeze crystallizers the solution is crystallized inside a scraped-surface heat exchanger which is fitted with internal blades and an external jacket. A typical scheme is presented in figure 17. These have been discarded as a process of desalinating seawater. However, the direct contact between the cooling agent and mother solution is an extremely promising technique, and has been investigated extensively for desalination purposes. Also known as secondary refrigerant freeze process, direct freezing utilizes a volatile liquid, for example butane or propane, which is mixed into the mother solution. The vapour pressure of the crystallizer is operated below that of the cooling liquid, and therefore evaporating the refrigerant, thus reducing the temperature of the solution. For example, direct contact crystallization between liquid n-butane and seawater has been broadly investigated. A schematic layout of desalination of seawater with liquid n-butane is presented in figure 18, in which precooled seawater is continuously fed into the crystallizer where it is mixed with liquid n-butane. As a result, n-butane vaporizes which generates ice crystals due to the transfer of latent heat. Hitherto, the ice-brine slurry is washed with fresh water. The resulting pure ice crystals are remelted. Vigorous boiling action of the butane means there is usually no need for agitation in the crystallizer (Mullin, 2001; Arpe *et al*. 2012; Randall, 2015).

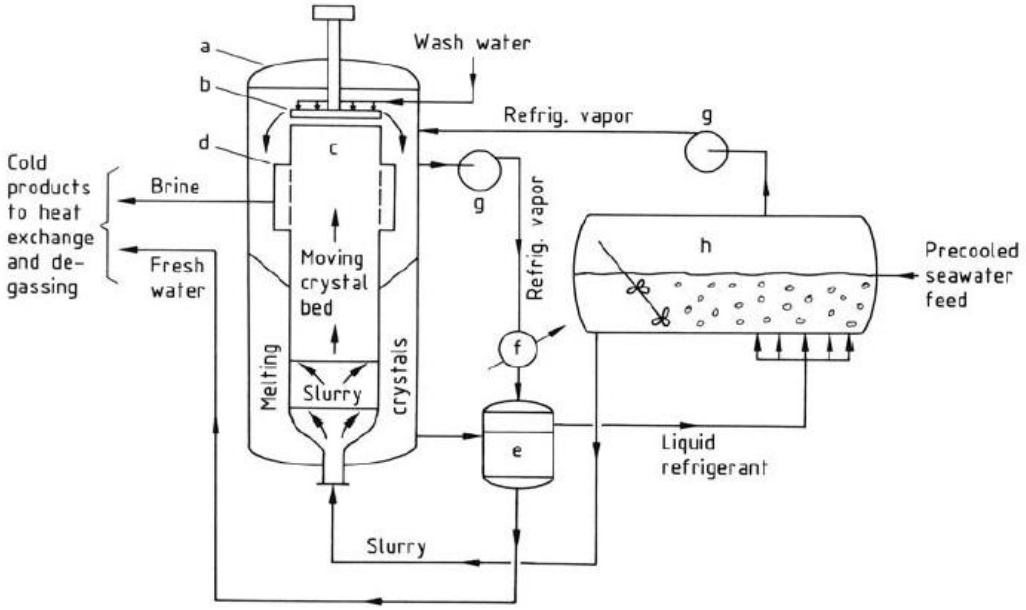

Figure 17. Desalination of seawater by freeze crystallization a) Washer-melter; b) Scraper; c) Wash column; d) Screens; e) Decanter; f) Heat exchanger; g) Compressor; h) Crystallizer (Arpe et al. 2012)

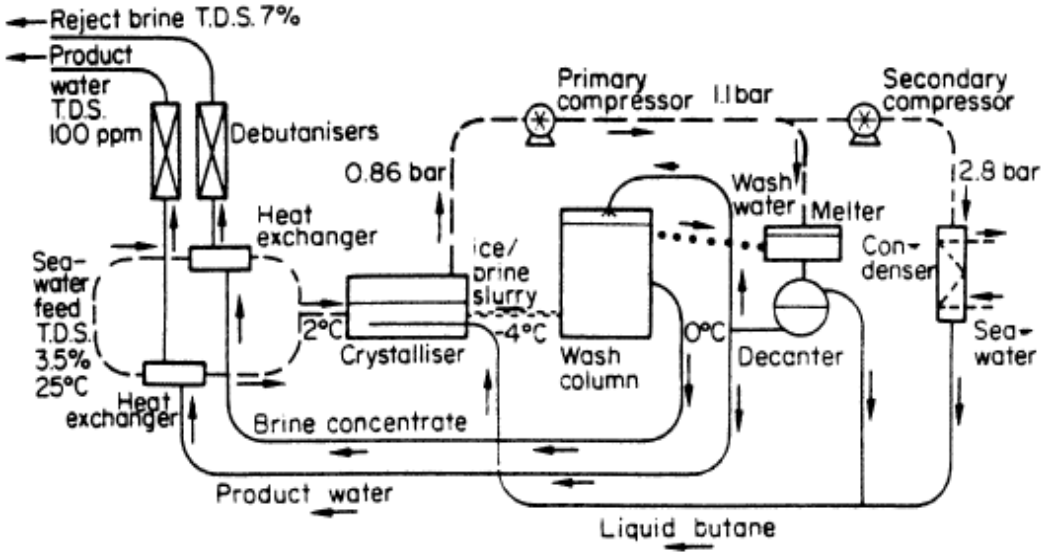

Figure 18. Immiscible refrigerant (n-butane) freeze desalination process (Mullin, 2001).

The indirect freeze crystallizers can be categorized into two groups: internally cooled and externally cooled. Internally cooled crystallizers include the nucleation and growth of a layer of ice on the heat exchanger surface. On the other hand, the nucleation and growth of suspension of ice crystals in mother solution is considered internally cooled crystallization. Externally cooled crystallizers circulate the

solution through a heat exchanger which is external to the crystallizer vessel (See figure 15) (Randall, 2015). Although indirect-contact freeze crystallizer have been abandoned as a method for desalinating seawater does not mean that they do not have any use. For instance, indirect-contact freeze crystallizers are used widely in food industry, because they retain volatile flavor components that are normally lost during conventional evaporation process. In indirect-contact freeze processes the mother solution is crystallized in a scraped-surface heat exchanger. Subsequently, the resulting ice-slurry is separated and washed. The wash column is the main component in this process. A Grenco system that utilizes indirect-contact freeze crystallization is shown in figure 19 (Mullin, 2001).

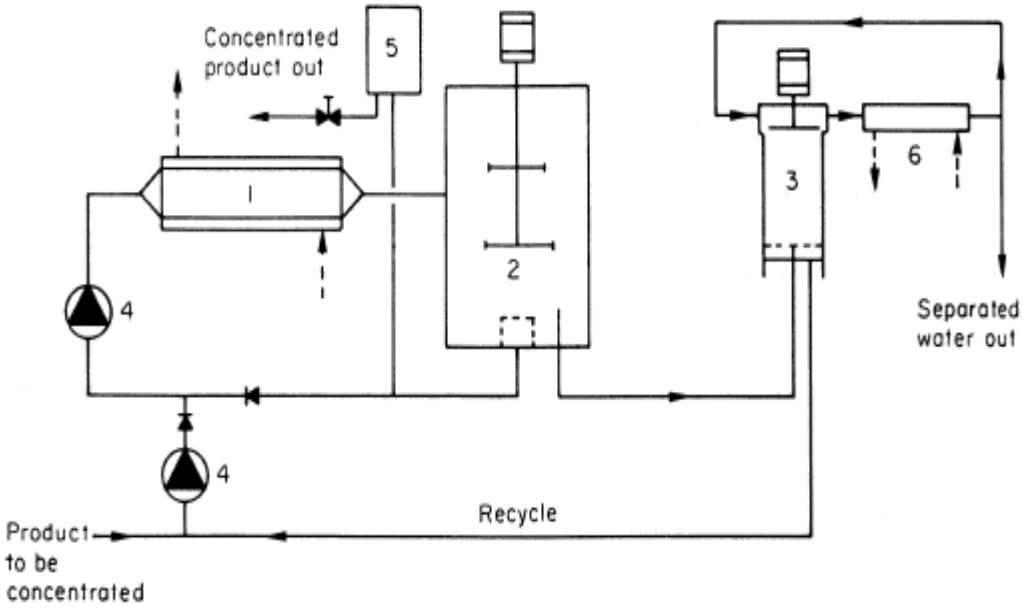

Figure 19. Grenco freeze concentration process (single stage). 1, scraped surface heat exchanger; 2, agitated recrystallizer; 3, wash column with bottom perforated piston and top ice scraper; 4, circulating pumps; 5, concentrated product expansion vessel; 6, ice melter (Mullin, 2001).

Conventional industrial food freezers utilize cold air as the cooling medium due to its low cost and low risk of food contamination. The cold air reduces the food temperature below its freezing temperature. Generally, the temperature of the air is between −40°C and −20°C and the velocity varies from 1 m/s to 6 m/s. Both the temperature and velocity of the cooling medium depend on the type, shape, and size of the processed food product. In rapid-freeze processes the temperature of the cooling medium is at very low temperature (even under −80°C). As a result, water

inside the food forms very small ice crystals, and therefore avoids damaging the food cell membrane which can occur in conventional freezing temperature (−40°C/−20°C). The cooling medium utilized in rapid-freeze processes in usually a cryogenic fluid, i.e. liquid nitrogen (Biglia *et al.*, 2016).

7 Recausticizing process

The recausticizing reaction is an important part in the production of white liquor. Although this reaction has been used for ages to produce NaOH, it is not fully understood despite many investigations (Theliander, 1992). Recausticizing is a part of the chemical recovery in kraft pulping process. A schematic of the kraft pulping process is shown in figure 20. Two consecutive reactions occur at the same time in recausticizing process: slaking and causticizing, as shown in equations (7.1) and (7.2). The second reaction is generally called causticizing reaction which produces $CaCO_3$ as a by-product of NaOH. Both take place in the solid phase of the heterogeneous system of lime and green liquor. Recausticizing process starts with the mixing of green liquor with calcium oxide, CaO, where calcium oxide slakes with water producing calcium hydroxide, $Ca(OH)_2$, as shown in equation (7.1). This proceeds to react with Na_2CO_3 found in green liquor to form NaOH and $CaCO_3$, as shown in equation (7.2) (Konno, 2002; Gullichsen and Fogelholm, 2000).

$$CaO(s) + H_2O(l) \rightarrow Ca(OH)_2(s) + 65\ kJ/mol \quad (7.1)$$

The slaking of lime is vigorously exothermic reaction which takes place very quickly at raised temperatures (~80 °C). The causticizing reaction occurs simultaneously with slaking. The duration of the slaking reaction varies between 10 and 30 minutes to complete depending on the purity of lime. The reaction rate is strongly influenced by solution temperature. For instance, at the normal operating temperature (~100 °C) the reaction rate is significantly faster than below 70 °C. However, in practice, all the lime which is adept of slaking will react with water (Gullichsen and Fogelholm, 2000).

$$Ca(OH)_2(s) + CO_3^{2-}(aq) \rightleftharpoons 2OH^-(aq) + CaCO_3(s) \quad (7.2)$$

As shown in equation (7.2), the causticizing reaction is an equilibrium reaction. Still, the reaction does not have any considerable consequence on the heat balance. Both generated calcium hydroxide and calcium carbonate are insoluble and react in the heterogeneous mixture as solids. In practice, some reactants will be present in the system after the equilibrium of the causticizing reaction is reached. Equilibrium composition is influenced by the total liquor strength, i.e., a boost in the liquor concentration will move the equilibrium to the reactant side. Likewise, in dilute liquors, the equilibrium will move to the product side. As a result, the causticizing efficiency increases (Gullichsen and Fogelholm, 2000).

Heretofore, the main focus of the causticizing reaction has been on the production of NaOH. According to Konno, the number of papers regarding crystallization of $CaCO_3$ is extremely few and far between. To make matters worse, studying is made difficult because the causticizing reaction takes place in very high alkaline systems. In addition, the concentration of NaOH in the mother liquor increases as the reaction proceeds, therefore, complicating the studies even further (Konno, 2002)

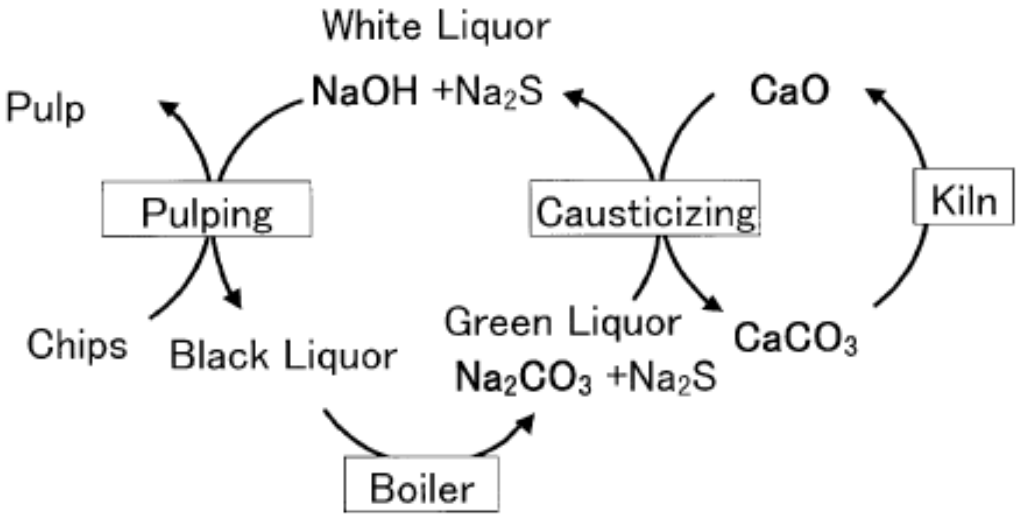

Figure 20. Schematic of kraft pulping process (Konno, 2002).

As seen in figure 20, the causticizing process converts Na_2CO_3 in green liquor to NaOH. Causticizing process includes the following unit operations: dissolving of

molten smelt to weak white liquor to generate green liquor, filtration of green liquor, mixing green liquor with CaO (lime) in reaction tanks to generate NaOH and $CaCO_3$ (lime mud), white liquor purification and filtration from lime mud, and lime mud washing. However, small quantities of unreacted carbon and nonprocess elements are present in the molten smelt from the recovery boiler. These impurities found in green liquor require separation for disposal. The separation can be achieved by settling or filtration. Furthermore, chemical losses can be reduced by washing the green liquor dregs (Gullichsen and Fogelholm, 2000).

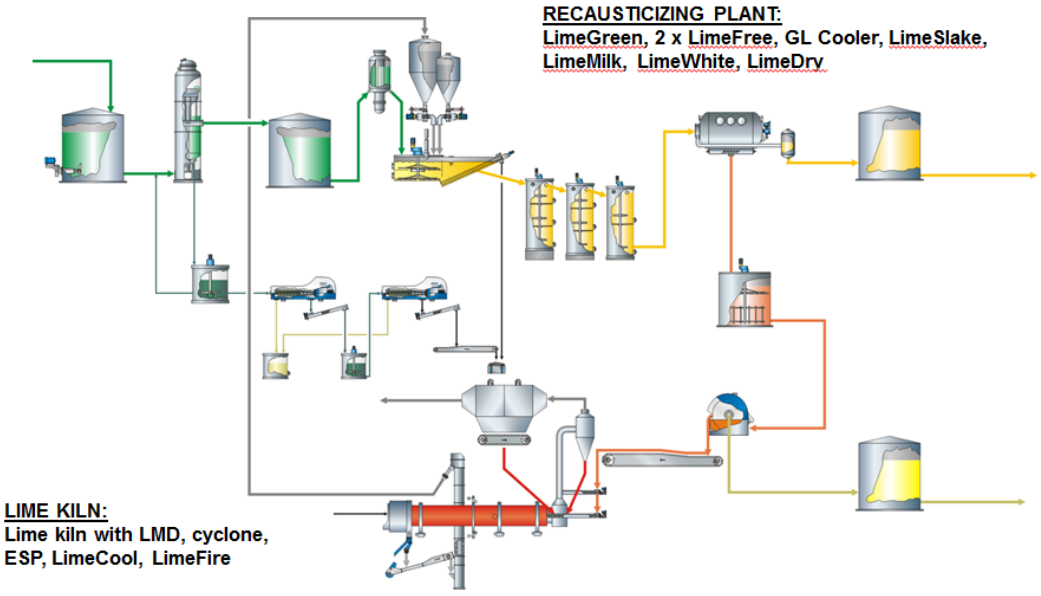

Figure 21 Recausticizing process (Andritz Oy, 2017)

As seen figure 21, the seven unit operations in recausticizing plant converting Na_2CO_3 in the green liquor to NaOH in the white liquor, are: separation of dregs from green liquor, lime slaking, recausticizing reaction (equation (7.2)), separation of white liquor from lime mud, washing of lime mud, drying of lime mud, and reburning of lime. During this process, Na_2CO_3 reacts with slaked lime ($Ca(OH)_2$) forming solid lime mud. The produced lime mud is filtered from the white liquor, dehydrated, incinerated, and recycled. The lime reburning process is a closed recovery system where fresh chemicals are added only to compensate chemical losses during the process. Moreover, accumulation of impurities and contaminations in the closed cycle is avoided by purging part of the lime regularly (Gullichsen and Fogelholm, 2000).

7.1 Green liquor

The molten smelt from a kraft recovery boiler (see figure 20) is dissolved in weak wash liquor from the recausticizing plant. This resulting mixture is called green liquor which is subsequently clarified. As described in previous chapter, the green liquor is converted to white liquor in a process called recausticizing. The regenerated, purified white liquor is recycled back to the cooking process (Gullichsen and Fogelholm, 2000).

Green liquor is formed when smelt from the dissolving tank is dissolved into weak white liquor, weak wash liquor, or water. It is important to notice that all of these streams contain impurities and alkali. Therefore, green liquor is an aqueous solution which consists of sodium sulfides, sulfates, carbonates, and traces of unburned char. Table II presents an analysis of green liquor and table III presents a typical green liquor composition (Gullichsen and Fogelholm, 2000).

Table II Typical green liquor composition (Gullichsen and Fogelholm, 2000).

Component	**Concentration, g Na_2O/L**
Na_2CO_3	80-100
Na_2S	40-50
Na_2SO_4	3-6
NaOH	5-20
Other dissolved	5-10
Suspended solids	0.6-1.5

Table III Typical green liquor analysis (Gullichsen and Fogelholm, 2000).

Location		**US**	**US**	**US**	**Finland**	**Finland**
Dry solids	%	18.9	18.5	21.8		
Suspended solids	mg/L	580	809	534	500	800
NaOH	g/L	15.5	17.8	18.8	11.7	14.1
Na_2S	g/L	30.8	32.5	42.7	46.8	49.2

Na_2CO_3	g/L	143.2	133.3	134.9	95.4	105.3
Na_2SO_3	g/L	2.19	2.09	1.41	0.2	0.9
$Na_2S_2O_3$	g/L	4.57	5.10	7.08	2.4	3.8
Na_2SO_4	g/L	3.28	4.50	8.79	6.5	3.1
Total alkali	g Na_2O/L	124.6	122.6	134.7	106	144.9
Active alkali	g Na_2O/L	36.5	39.6	48.5	46.8	50.0
Effective alkali	g Na_2O/L	24.3	26.7	31.5	27.7	30.5

7.2 White liquor

It is very important to have as pure white liquor as possible in order to produce pulp at a high yield and low energy consumption. The active ions in white liquor are OH^- and S^{2-}. In addition, white liquor contains ballast ions such as CO_3^{2-}, SO_4^{2-}, Cl^- etc. (Theliander, 1992). White liquor is very alkaline solution (pH~14), in which main active compounds are sodium hydroxide and sodium sulfide, Na_2S. In addition, small quantities of sodium carbonate, sodium sulfate, sodium chloride, sodium thiosulfate, and calcium carbonate plus various accumulated impurities and non-process elements. On the other hand, these supplementary reactants present in white liquor are practically inert from a cooking point of view in either as impurities in raw materials or as a result of poor chemical regenerating cycle (Gullichsen and Fogelholm, 2000).

Hydrolysed sodium hydroxide and sulfide are the active compounds in kraft pulping. Sodium carbonate is not important in that process. However, they all dissociate in water due to their strong electrolyte nature. The following equilibria are found in white liquor:

$$NaOH(l) + H_2O(l) \rightleftharpoons Na^+(aq) + OH^-(aq) + H_2O(l) \quad (7.3)$$

$$Na_2S(s) + H_2O(l) \rightleftharpoons 2Na^+(aq) + S^{2-}(aq) + H_2O(l) \quad (7.4)$$

$$S^{2-}(aq) + H_2O(l) \rightleftharpoons HS^-(aq) + OH^-(aq) \quad (7.5)$$

$$HS^-(aq) + H_2O(l) \rightleftharpoons H_2S(g) + OH^-(aq) \quad (7.6)$$

$$Na_2CO_3(s) + H_2O(l) \rightleftharpoons 2Na^+(aq) + CO_3^{2-}(aq) + H_2O(l) \quad (7.7)$$

$$CO_3^{2-}(aq) + H_2O(l) \rightleftharpoons HCO_3^-(aq) + OH^-(aq) \quad (7.8)$$

Usually, reactions (7.5), (7.6), and (7.7) are expected to proceed entirely to the right. Reaction (7.8) is irrelevant in the pH range of kraft pulping due to the formation of HS^-, whose formation depends strongly on pH and temperature. Besides, HS^- contains most of the sulfide sulfur during kraft cooking.

The composition of white liquor, according to Gullichsen and Fogelholm, is shown in table IV. Note that potassium has been excluded from the total mass concentration. The separation of lime mud from white liquor by filtering or sedimentation is not perfect. As a result, white liquor contains small amounts of lime mud particles which compose most of the total suspended solids in white liquor. Therefore, the purity of white liquor does not correlate with purity of the green liquor (Gullichsen and Fogelholm, 2000).

Table IV An example of white liquor composition (Gullichsen and Fogelholm, 2000).

Compound	**Concentration, g NaOH/L**	**Concentration, g Na_2O/L**	**As compound, g/L**
NaOH	95	73.6	95
Na_2S	40	31.8	39
Na_2CO_3	23	17.8	30.5
Na_2SO_4	4	3.1	7.1
$Na_2S_2O_3$	2	1.6	4.0
Na_2SO_3	0.5	0.4	0.8

Other compounds	-	-	-
Effective alkali	135	105.4	-
Active alkali	115	89.5	-
Total alkali	164.5	128.3	179.4

7.3 Cold alkali dissolution

Cold alkali dissolution of pre-treated cellulose in the presence of zinc and surfactants is a method which has been proposed for producing regenerated cellulose. Above described process has not been utilized in the pulping industry, and therefore the composition of this mixture is not certain. However, modelled composition of the involved streams in the crystallizer is presented in table V.

Table V Modelled composition of respective streams in the additional alkali purification stage

Stream/parameter	**Stream in**	**Stream out**	**Separated salt**
Total mass, t/t fibre	7.43	6.32	1.11
Suspended solids, %wt	0	0	Not modelled
Dissolved solids, %wt	22.8	20.3	Not modelled
NaOH, %wt	16.1	16.6	13.1
Na_2CO_3, %wt	5.34	2.27	22.80
ZnO, %wt	1.51	1.56	1.23
Additive, %wt	Not modelled	Not modelled	Not modelled
Water, %wt	77.2	79.7	63.0
Na_2CO_3: NaOH mass ratio	33.1%	13.6%	173%

8 Experimental part

8.1 Materials

Anhydrous Na_2CO_3 (>99.9%), CaO (97+ %), and ZnO (min. 99%) supplied by VWR was used to produce the synthetic liquor which simulated the liquor used in the cold alkali dissolution process. In addition, industrial green liquor obtained from UPM Kymi pulp mill located in Kuusanniemi, Finland was used in the crystallization experiments as well. Ethanol absolute (99.96%) and ultrapure water (ELGA PURELAB flex) with a conductivity of 0.055 $\mu S \cdot cm^{-1}$ was used in this study. All reagents were used as received.

8.2 Experimental setup and procedure

In this chapter the experimental setup and procedure are described for the experiments that were conducted in this thesis. These experiments included the production of the synthetic liquor, solubility of sodium to the synthetic liquor, and crystallization experiment with both synthetic liquor and industrial green liquor.

8.2.1 Production of synthetic liquor

The amounts of chemicals used to produce one batch of synthetic liquor are represented in table VI.

Table VI The weighed amounts of chemicals to produce one batch of synthetic liquor.

Chemical	Weighed amount
Anhydrous Na_2CO_3	1783.7 g
CaO	918.8 g
ZnO	117.4 g
H_2O	6000 g

6 L of pure water was firstly loaded into a metallic reactor. After this both the heat plate under the reactor and the impeller inside the reactor were turned on. Certain amount of Na_2CO_3 and ZnO were added into the reactor when the temperature of the water had reached 50°C. CaO was gradually added into the suspension in order to control the raise in temperature which occurs when CaO reacts with H_2O as described in equation (7.1). The suspension in the reactor was kept at 90°C for 2 h after finishing the addition of CaO. The speed of the impeller was kept at 600 rpm during the process. Subsequently, the solution was filtered hot using two 3 L suction flasks and Büchner funnels that were preheated to 90°C. WHATMAN GF/A glass fiber filters were used in the filtration process. The filtrate was left to cool down in the suction flasks which were covered with aluminum foil before it was transported into a plastic canister for storage. All of the synthetic liquor was filtered a second time before the crystallization experiments due to existence of solids in the liquor. Figure 22 shows the synthetic liquor in a glass bottle.

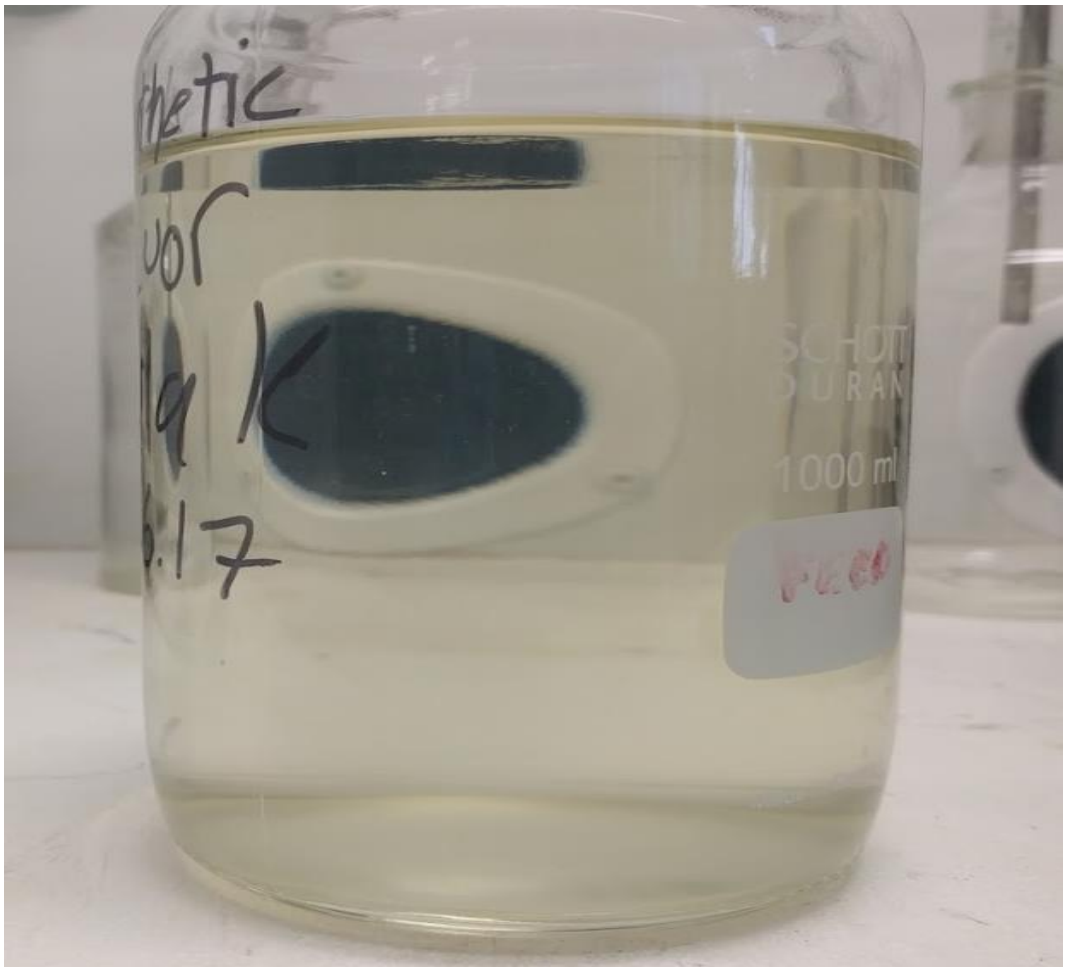

Figure 22 Synthetic liquor

8.2.2 Solubility experiment

200 ml of synthetic liquor was prepared into a jacketed glass reactor and a metallic reactor separately. Excess amount of anhydrous Na_2CO_3 powder was added into both reactors until the synthetic liquor was saturated with Na_2CO_3. Impeller speed was kept at 600 rpm for the duration of the experiment. Investigated temperatures were 20°C, 15°C, 10°C, 5°C, 0°C, -1°C, -2°C, -3°C and -4°C. The temperature of the solution was controlled by circulating a cooling agent through the jackets of the reactors with LAUDA T 2200 thermostat. The solutions were mixed for 24 hours at each temperature to achieve equilibrium state. Furthermore, the reactors were covered with aluminum foil during the experiment. The temperature of the solution was checked before sampling in order to be sure that the temperature had not changed during the past 24 hours. The temperatures were precisely correct with every sample. Samples were taken with syringes and syringe filters. The syringes, syringe filters and test tubes were precooled when sampling temperatures below 10°C. All the samples were stored in closed test tubes in a fridge. The experimental setup of solubility experiments is shown in figure 23.

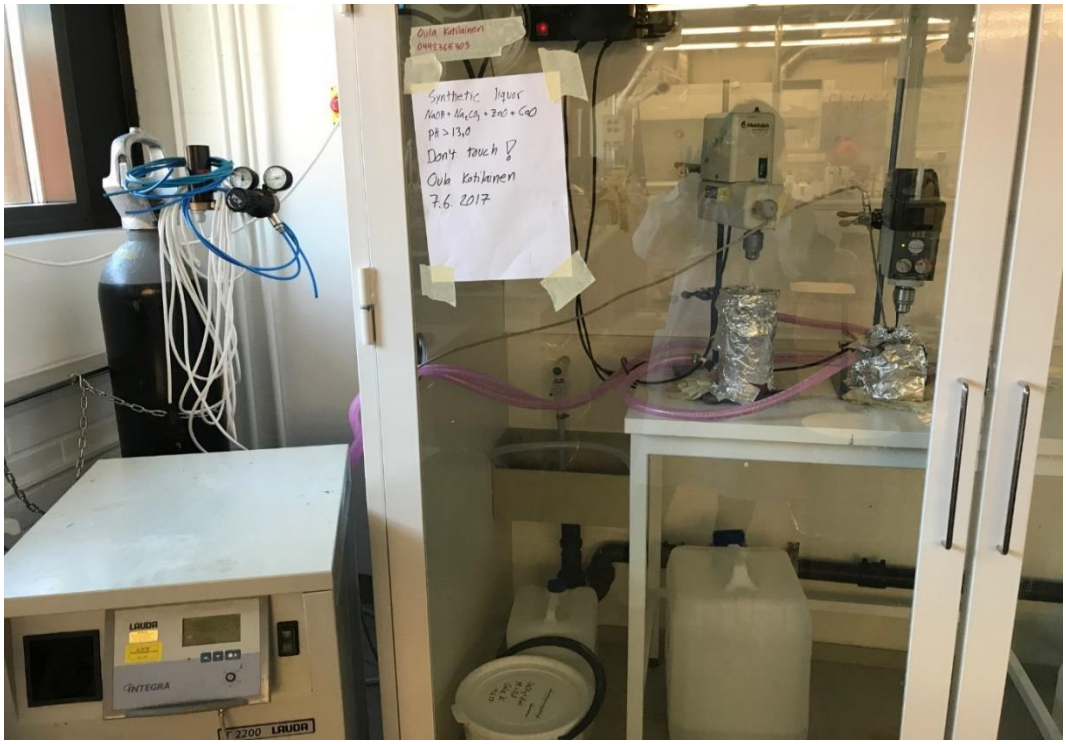

Figure 23 Experimental setup for solubility test

8.2.3 Crystallization experiment

1.5 liters of synthetic liquor or green liquor was prepared into a jacketed metallic reactor equipped with baffles. The cooling agent circulating in the jacket equipped with LAUDA PROLINE RP 855 thermostat was cooled to 20°C before the solution is loaded into the reactor. Subsequently, the reactor was closed and impeller was turned on. A thermal probe was immersed into the liquor to monitor its temperature changes. Simultaneously stopwatch was started to record the time. Impeller speed was kept at 550 rpm for the duration of the experiment. The impeller speed was measured using TRIFITEK TR-520 tachometer. The liquor was cooled to -5°C in six steps. Temperature of these steps were 20°C, 15°C, 10°C, 5°C, 0°C, and -5°C. Two different cooling rates were investigated: in the first cooling rate the temperature was changed every ten minutes and every twenty minutes in the second cooling rate. Therefore, in the first cooling the liquor was cooled in 60 minutes, and in 120 minutes in the second cooling rate, from the starting temperature of 20°C to the target temperature -5°C. The industrial green liquor had to be heated to dissolve all formed solids in the canister. Therefore, the green liquor was stored at an oven which was kept at 60°C. In addition, the green liquor was mixed before it was loaded into the reactor. After the crystallization time (60 minutes or 120 minutes) the crystals were separated from the mother liquor in 2 L suction flask and Büchner funnel. WHATMAN GF/A glass fiber filters were used in the filtration process. Moreover, the crystals were instantly washed with pure ethanol (absolute grade) in another 1 L suction flask in order to remove all mother liquor from the crystal surface. If the crystals were not washed instantly, they would start to dissolve to a slurry as shown in figure 24.

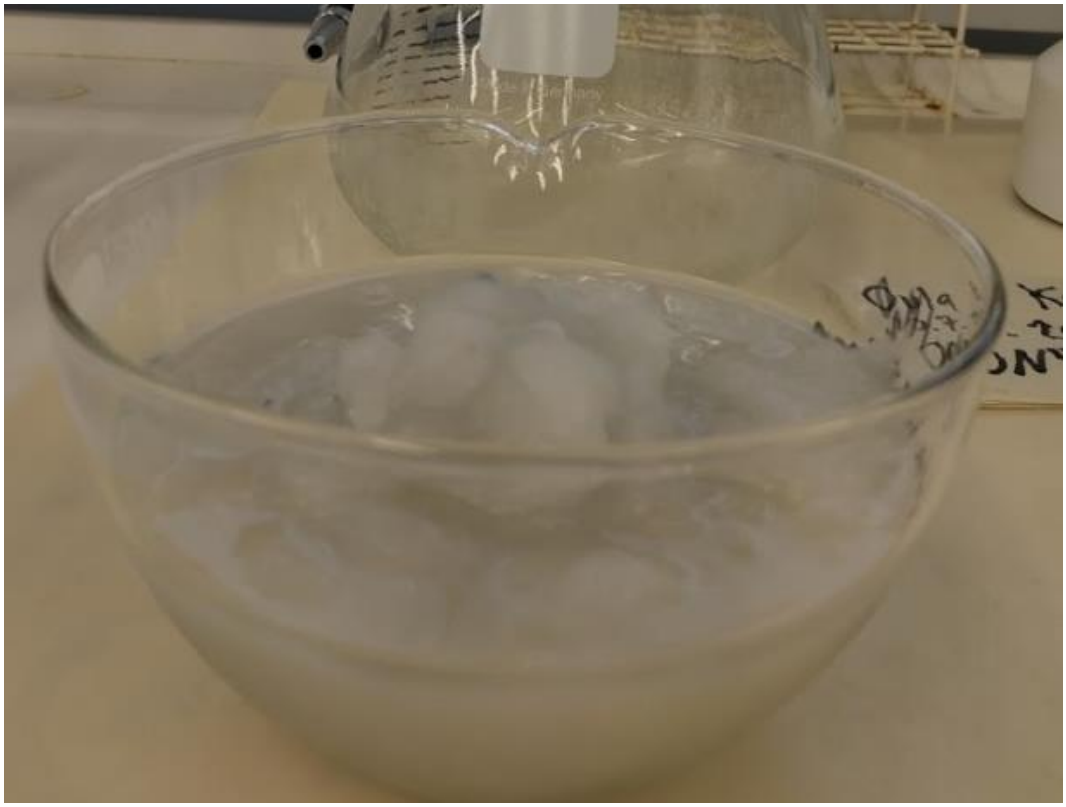

Figure 24 Partially dissolved crystals which were not washed instantly with ethanol after filtration.

During the separation of crystals from mother liquor and crystals washing process the flux was measured with a stopwatch. After the crystals had been washed they were put in a desiccator to dry. Also, the mother liquor filtrate was stored for further analysis but the washing filtrate was discarded. During the crystal washing process it was noted that some of the crystals looked like that they would dissolve in the ethanol and also a small amount of crystals would pass through the filter paper and end up in the filtrate. The crystals were transferred from the evaporation dishes to sealed plastic bags after 24 hours in the desiccator. The portion of the crystals that would be analyzed is stored in sealed plastic bags inside the desiccator. The experimental setup, for the crystallization experiment, is shown in figure 25.

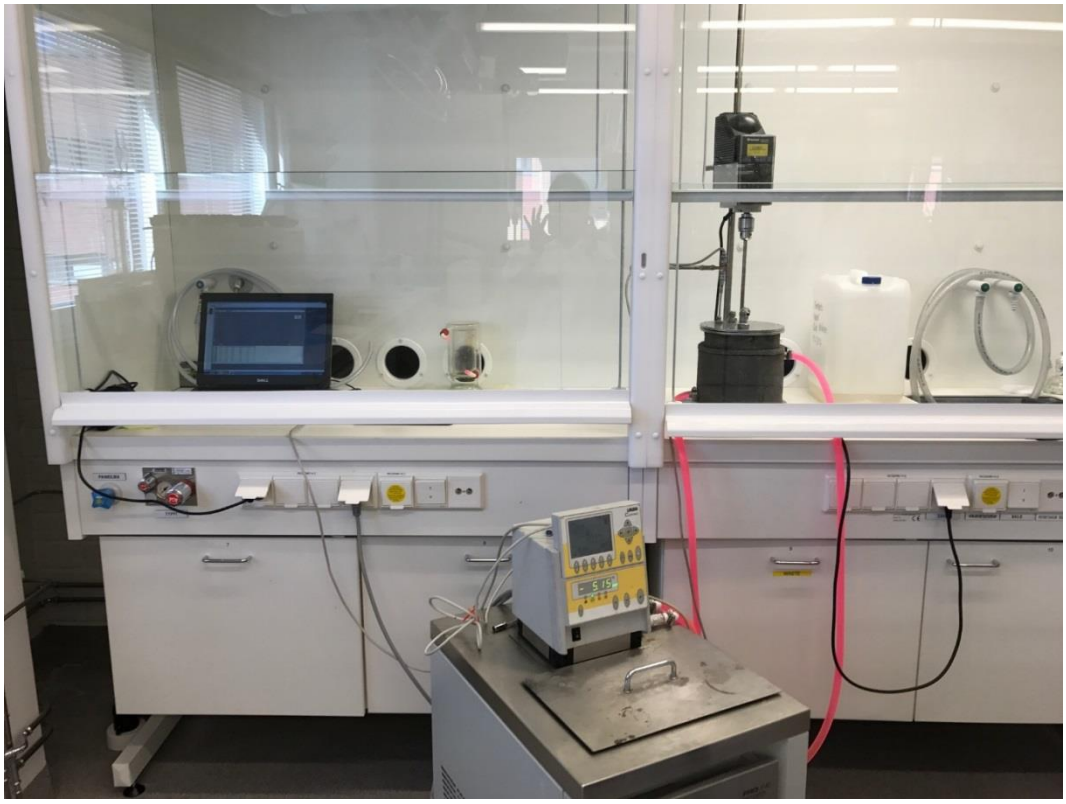

Figure 25 Experimental setup for crystallization experiment

8.3 Analytical methods

In this chapter the analytical methods and procedure are described for the experiments that were described above. Analytical methods included titration, atomic absorption spectroscopy (AAS), crystal size distribution, filtration resistance determination, scanning electron microscope (SEM), X-ray diffraction (XRD), inductively coupled plasma (ICP), and total water fraction measurement.

8.3.1 Titration

Every synthetic liquor batch was titrated after production to confirm that it would simulate the liquor expressed in table V (stream in). The titration setup consisted of: magnetic stirrer and plastic-coated stirring bar, pH-meter, and 50 ml burette. All of the carbonate from the samples was precipitated using $BaCl_2 \cdot 2H_2O$ (20 g/100 g H_2O). First the samples were titrated to pH=9.5 where the concentration of OH^- could be determined. After this the samples were titrated to pH=4.0 where the

concentration of CO_3^{2-} could be determined. Moreover, the dissolution of the solids in the samples implies that all of the carbonate was titrated. The samples were titrated by using 1.087 M HCl which was produced from 37% HCl. The produced HCl was analyzed by titrating sodium carbonate solution which was also prepared in the laboratory. Detailed information for the procedure can be found in the standard SFS-EN ISO 9963-1. Moreover, the filtrate from the crystallization experiment was titrated in order to investigate the decrease in the Na_2CO_3 concentration. Therefore, the causticizing degree can be calculated using the following equations (8.1-8.5):

$$DC = \frac{m(NaOH)}{m(NaOH)+0.755*m(Na_2CO_3)} * 100 \quad (8.1)$$

$$m(NaOH) = M(NaOH) * c(NaOH) \quad (8.2)$$

$$m(Na_2CO_3) = M(Na_2CO_3) * c(Na_2CO_3) \quad (8.3)$$

$$c(NaOH) = a * \frac{c(HCl)}{V(sample)} \quad (8.4)$$

$$c(Na_2CO_3) = \frac{a-b}{2} * \frac{c(HCl)}{V(sample)} \quad (8.5)$$

Where, *DC* = Degree of causticizing, %

m(NaOH) = Mass of NaOH in the liquor, g l^{-1}

m(Na_2CO_3) = Mass of Na_2CO_3 in the liquor, g l^{-1}

c(NaOH) = Concentration of NaOH in the liquor, mol l^{-1}

c(Na_2CO_3) = Concentration of Na_2CO_3 in the liquor, mol l^{-1}

M(NaOH) = Molar mass of NaOH (39.998), g mol^{-1}

M(Na_2CO_3) = Molar mass of Na_2CO_3 (105.99), g mol^{-1}

c(HCl) = Concentration of the HCL (1.087), mol l^{-1}

V(sample) = Volume of titrated sample (5), ml

a = Volume of the consumed HCl at pH=9.5, ml

b = Volume of the consumed HCl at pH=4.0, ml

In addition, the first two titration results were verified in a commercial laboratory in order to be sure that the titration analysis yields accurate results for the synthetic liquor.

8.3.2 Atomic absorption spectroscopy (AAS)

The samples from the solubility experiment were analyzed using AAS in order to investigate the supersaturated concentration of sodium as a function of temperature. The initial liquor samples were taken directly from the synthetic liquor batch. Furthermore, changes in the zinc concentration during the temperature decrease were investigated. The sodium samples were diluted 1000 times and the zinc samples 20000 times using pure water and all samples were stabilized using 0.1 M HNO_3. Moreover, the glass volumetric flasks were washed using acid. Besides, other laboratory equipment was made of plastic. These steps ensured that any species from the glass would not dissolve in the acidic sample and, therefore, affect the AAS results. Moreover, there is no similar risk when plastic laboratory equipment is used. The parameters of the AAS are represented in table VII.

Table VII Parameters used in the atomic absorption spectroscopy

Element	**Na**	**Zn**
Wavelength, [nm]	330.3	213.9
Flame type	Air-C_2H_2	Air-C_2H_2
Linearization fit	Linear fit	Linear fit
Calibration concentrations, [ppm]	50, 100, 200, 300, 400	0.2, 0.4, 0.6, 0.8, 1

8.3.3 Crystal size distribution (CSD)

In order to evaluate the crystal size distribution of the produced crystals, they were analyzed using a laser diffraction Malvern Mastersizer 3000 analyzer. Ethanol was used as background for the obtained crystals because they would dissolve into pure water. Therefore, the samples for CSD analysis were prepared by mixing crystals and ethanol. In addition, the crystal size distributions were analyzed 24 hours after

the samples were prepared. The stirrer speed was set to 3000 rpm in order to break apart the crystal agglomerates and determine the true crystal size. Several different stirrer speeds were tested in order to find a speed which was sufficient to break the agglomerates. Due to the agglomerate nature of the crystals, the results were obtained by using the Mastersizer's number method which shows the crystal size distribution more accurately than, in this case, the volumetric method.

8.3.4 Filterability studies

When every crystallization experiment had finished, the produced crystals were separated by filtration. The filtration resistance experiment setup consisted of a Büchner funnel, a 1 L suction flask, a 2 L suction flask, WHATMAN GF/A glass fiber filter, vacuum pump and a stopwatch. First a constant vacuum was applied and then the mixture of crystals and mother liquor was poured to the Büchner funnel. The time between volume units, in this case 100 ml, was written down. The pressure difference was 800 mbar. Filtering was continued until the cake surface was mostly dry. Subsequently, the vacuum was removed and the suction flask changed in order to obtain the mother liquor. Then absolute grade ethanol was poured on to the crystals and the vacuum was applied again. The time between volume units was recorded in the same way as with the mother liquor. Ethanol was poured until the liquid level was at the top of the Büchner funnel. This was done three times to insure that the crystals were sufficiently washed.

8.3.5 Scanning electron microscope (SEM)

To investigate the crystal morphology of the produced crystals and examine the possibility of zinc traces in the crystals, a morphological evaluation was conducted to the produced crystals by imaging with Hitachi SU3500 scanning electron microscope, at acceleration voltage of 5 kV and BSE-3D detector, equipped with optical head 50X, 100X, 200X, 500X and 2000X, respectively. Samples were prepared by placing a small amount of sample to two-sided carbon tape in which the pictures were taken. In addition, energy dispersive X-ray spectroscopy (EDS)

analysis was conducted with SEM. EDS is from Thermo Scientific which uses Ultra Dry SDD EDS detector and Pathfinder software.

8.3.6 X-ray diffraction (XRD)

In order to examine the composition of the obtained crystals, X-ray diffraction (XRD) was employed with a Bruker D8 Advance diffractometer using Cu Kα radiation at 40 mA and 40 kV, step size of 0.02° 2θ, range of 10-80° 2θ, and counting time of 0.5s per step. In addition, the mineral identification was executed by DiffracPlus EVA software which is made by Bruker.

8.3.7 Inductively coupled plasma mass spectrometry (ICP-MS)

To explore the elements in liquors and obtained crystals, they were detected by inductively coupled plasma mass spectrometry (ICP-MS) on Agilent 7900 ICP-MS. The obtained data were processed with the ICP-MS MassHunter software. Samples were prepared using analytical balance and micropipette. First, the empty sample containers were weighed. After this, a sample was pipetted into the container which was weighed a second time. Pure water was added into the container and it was weighed one more time. These prepared samples were diluted one more time before they were placed in autosampler of the ICP-MS. In addition, the densities of the liquid samples were measured using Anton Paar DMA 4500.

8.3.8 Total water fraction measurement

To verify the precise crystal forms (i.e., Na_2CO_3, $Na_2CO_3 \cdot 1H_2O$, $Na_2CO_3 \cdot 7H_2O$ or $Na_2CO_3 \cdot 10H_2O$) of produced crystals, total water fraction was determined. A small sample of ~1.5 grams was weighed in a watch glass. Then, the crystal samples were kept inside a desiccator, at room temperature, until constant weight was achieved. This drying took over two weeks. Therefore, it can be assumed that any water attached to the crystal surface was completely evaporated. The dried crystals and watch glasses were weighed together and then put into an oven at 110°C. According

to literature (Ye *et al*., 2013; Perry, 1995; Lewis, 1998), the hydrous sodium carbonate crystals are converted completely into anhydrous sodium carbonate above 109°C. The crystals were in the oven for six days. After that, the crystals were moved and cooled down in a desiccator and then the total amount of crystals were measured. It was assumed that all of the water of hydration was evaporated and anhydrous sodium carbonate was produced. Thus, the total water fraction can be calculated using equation (8.6):

$$TWF = \frac{m(beginning) - m(final)}{m(beginning) - m(container)} * 100 \quad (8.6)$$

Where, *TWF* = total water fraction, %

m(beginning) = initial mass of dried crystals and container, g

m(final) = final mass of anhydrous Na_2CO_3 and container, g

m(container) = mass of the container, g

9 Results and discussion

9.1 Chemical equilibrium simulations

In this thesis the equilibrium liquid and solid compounds upon cooling was estimated using OLI Studio Stream Analyzer software by OLI Systems, Inc. In addition, cooling of the partially regenerated alkali stream was simulated by means of temperature survey at constant pressure and input composition. The temperature range for the simulations was assumed to be between 100°C and −15°C. In the simulations Mixed Solvent Electrolyte (MSE) databank was used because it provided relevant parameters for the solid phase under −2°C, unlike the Aqueous Databanks (AQ), which is shown in figure 28. The raw output from the causticizing process simulation is shown in figure 26.

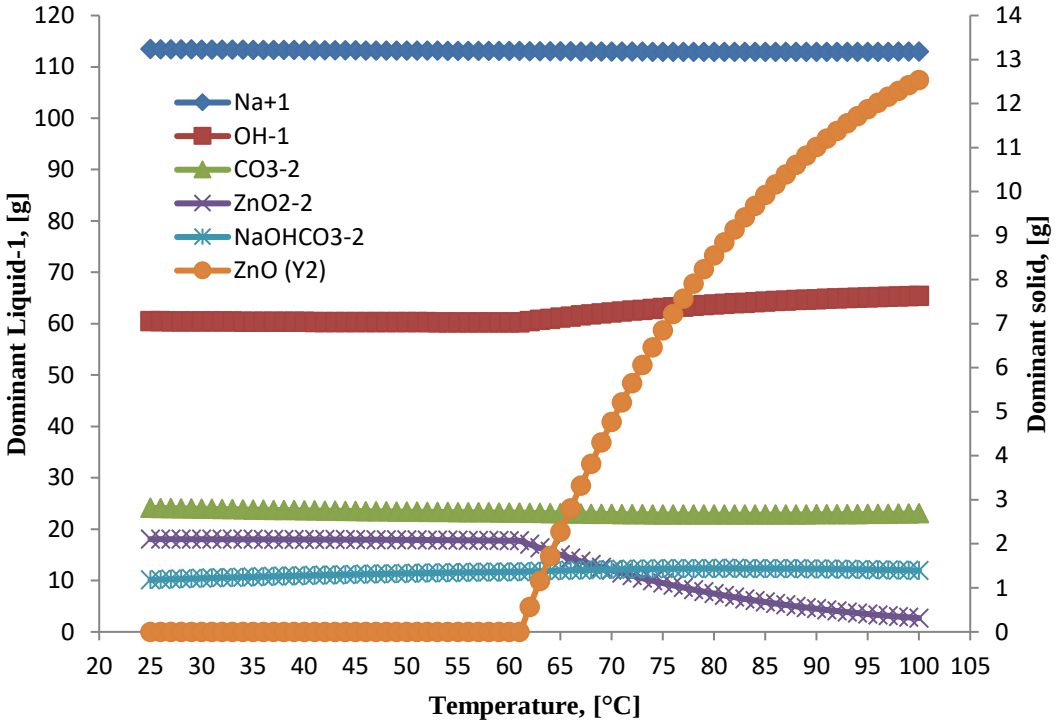

Figure 26 Raw output from the synthetic liquor recausticizing process simulation using OLI Studio Stream Analyzer software, MSE Databanks.

It is visible from figure 26 that ZnO starts to precipitate slightly above 60°C and at 90°C, 11 g from total of 15 g is in solid form. Therefore, this simulation suggests that under normal causticizing temperature only around 4 g could be dissolved in the synthetic liquor. The results from the simulated cooling crystallization are shown in figure 27.

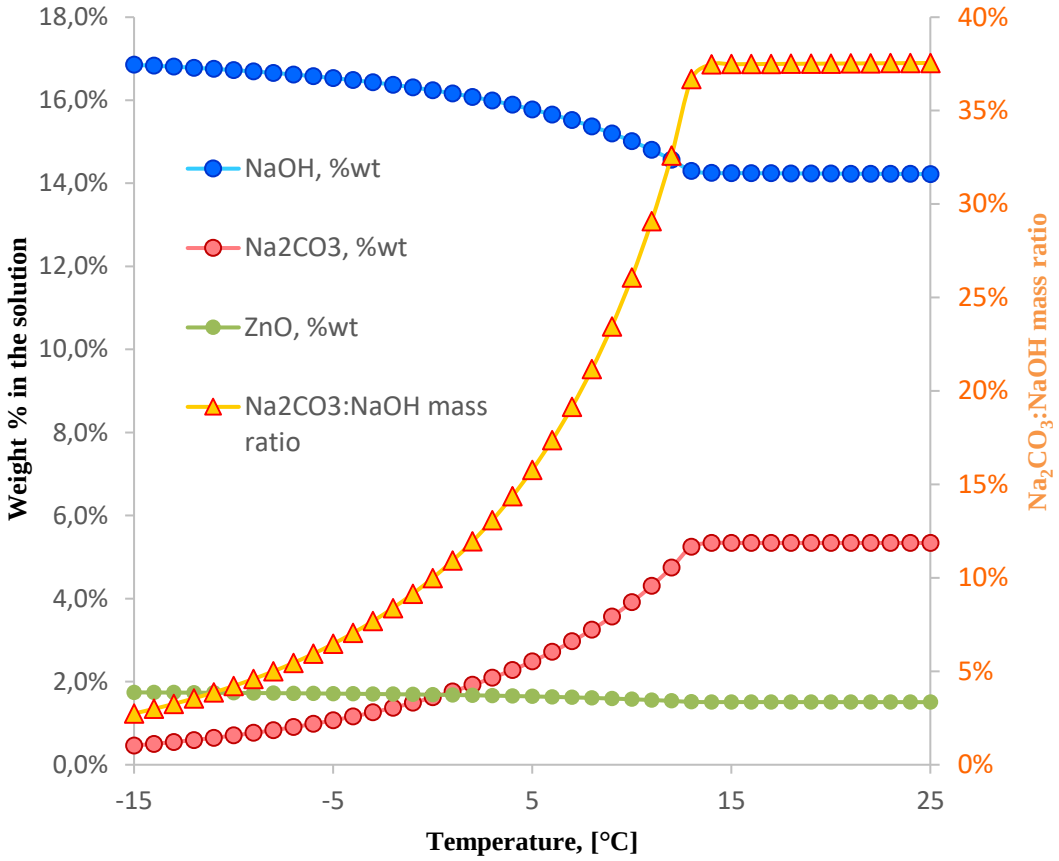

Figure 27 Chemical equilibrium calculation results for the simulated cooling crystallization process of synthetic liquor using OLI Studio Stream Analyzer software, MSE databanks.

According to the simulated results presented in figure 27 it appears that the desired Na_2CO_3:NaOH ratio (13.6%) is achieved at 3°C, which is relatively low degree of cooling. The desired Na_2CO_3:NaOH ratio is a precondition from another part of the process. At −5°C the Na_2CO_3:NaOH is 6.5% according to figure 27.

Figure 28 shows the amount of solids produced during crystallization of the synthetic liquor. It is visible from figure 28 that the AQ Databanks does not show any reliable results below −2°C.

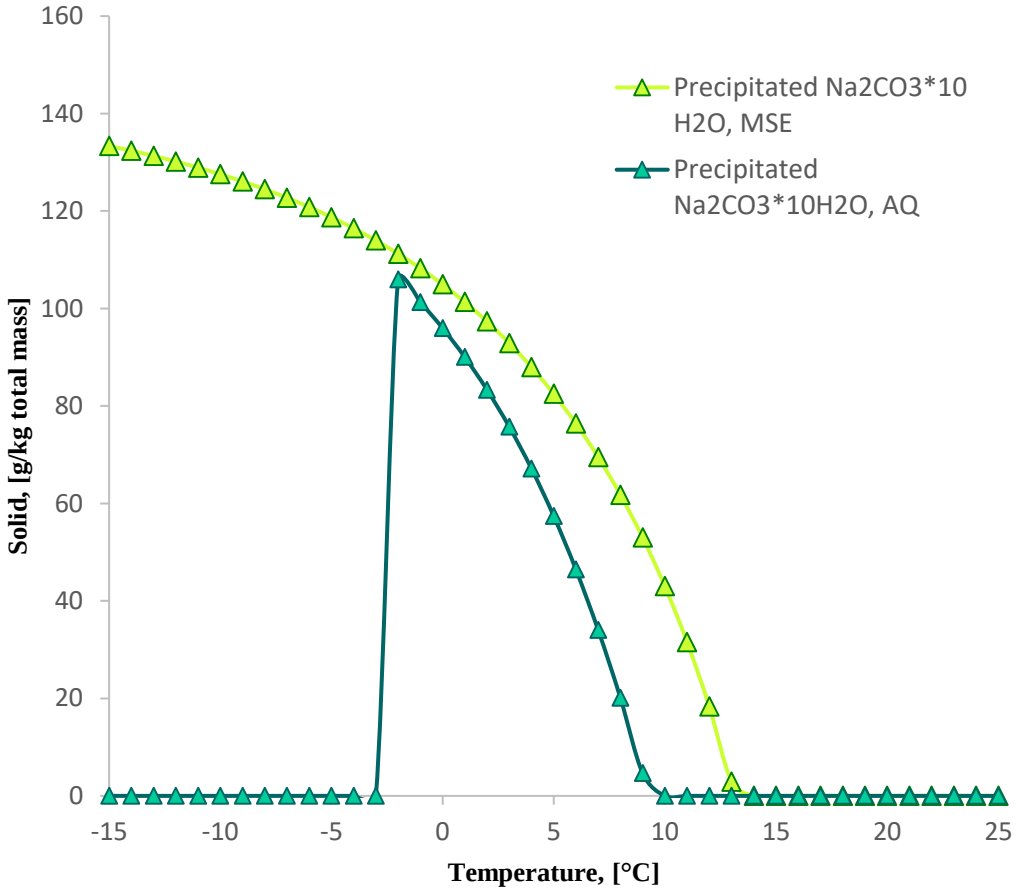

Figure 28 Amount of solid phase formed in the simulated cooling crystallization process of synthetic liquor using OLI Studio Stream Analyzer software, AQ and MSE databanks.

It can be observed from figure 28 that both the AQ and MSE databanks give the same equilibrium solid which is $Na_2CO_3 \cdot 10H_2O$. Moreover, the amount of solids formed at −5°C is ~120 g/kg total mass. The densities of the simulated system are presented in figure 29.

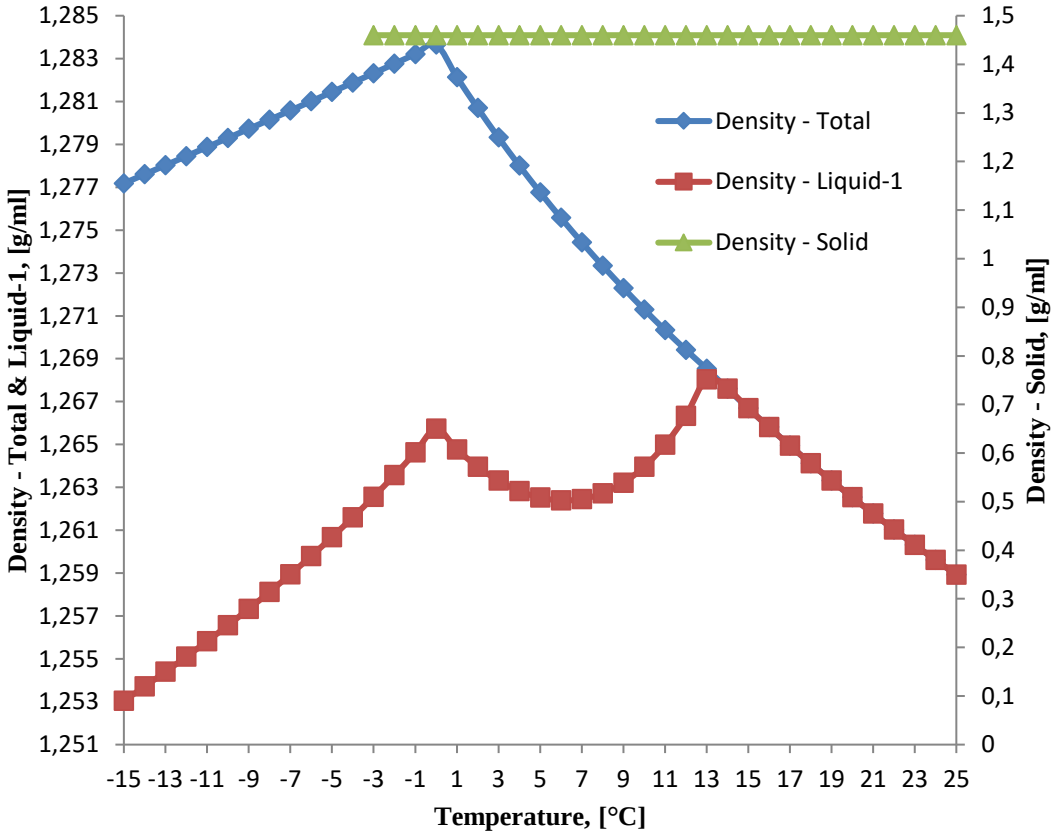

Figure 29 Densities of the simulated cooling crystallization process of synthetic liquor using OLI Studio Stream Analyzer software, MSE databanks.

9.2 Solubility of Na species in synthetic liquor

In order to investigate the effect of temperature to the solubility of species containing sodium to the synthetic liquor, the synthetic liquor was saturated with Na_2CO_3 and its temperature was lowered during nine days from 20 °C to -4°C. The results from this experiment are represented in figure 30.

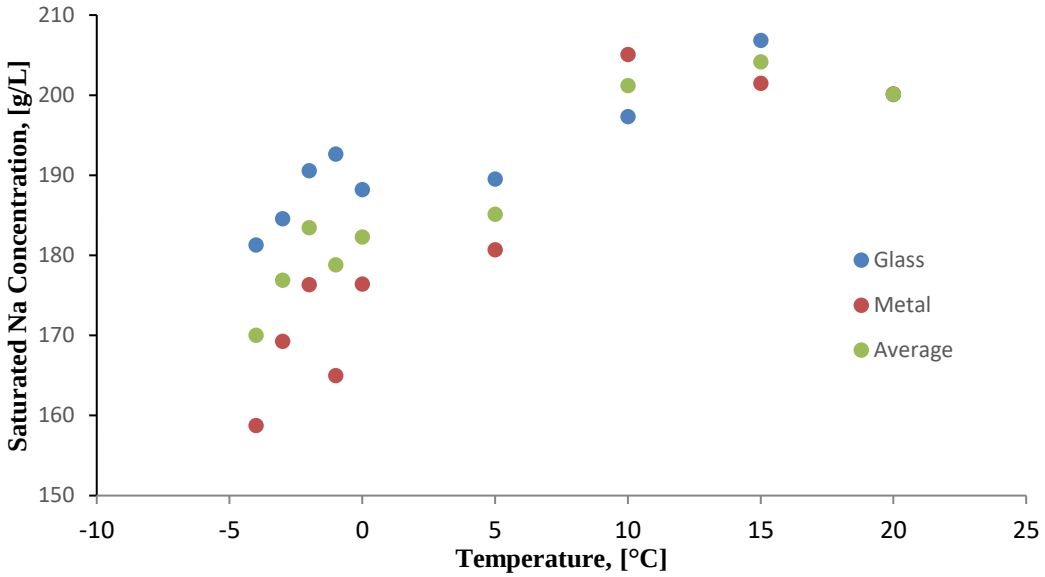

Figure 30 Na concentration in the synthetic liquor in glass and metal reactor. Impeller speed=600 rpm.

The results in figure 30 suggest that the concentration of sodium, in the synthetic liquor, decreases as the temperature decreases. However, it is clear from figure 30 that there is a significant effect to the sodium concentration between the glass and metal reactor. This effect may be produced by the differences in the mixing rates and heat transfer between metal and glass. It was observed during the subzero temperatures of the experiment that a layer of ice produced around the metal reactor. This ice, however, did not touch the liquid inside the metal reactor. Besides, another possible explanation would be different crystals forming in the reactors. For example, some metastable hydrates might have higher solubility than their more stable equivalents. In addition, the interactions between sodium and silicon in the glass reactor might explain the differences between the reactors. However, the concentrations needed to yield any significant effect would cause heavy etching of the glass material which would be clearly visible and, in this case, no significant etching of the glass reactor was observed.

In addition, the concentration of the zinc was analyzed from the original synthetic liquor and from samples at 0°C and -4°C. The results from these analyses are represented in figure 31.

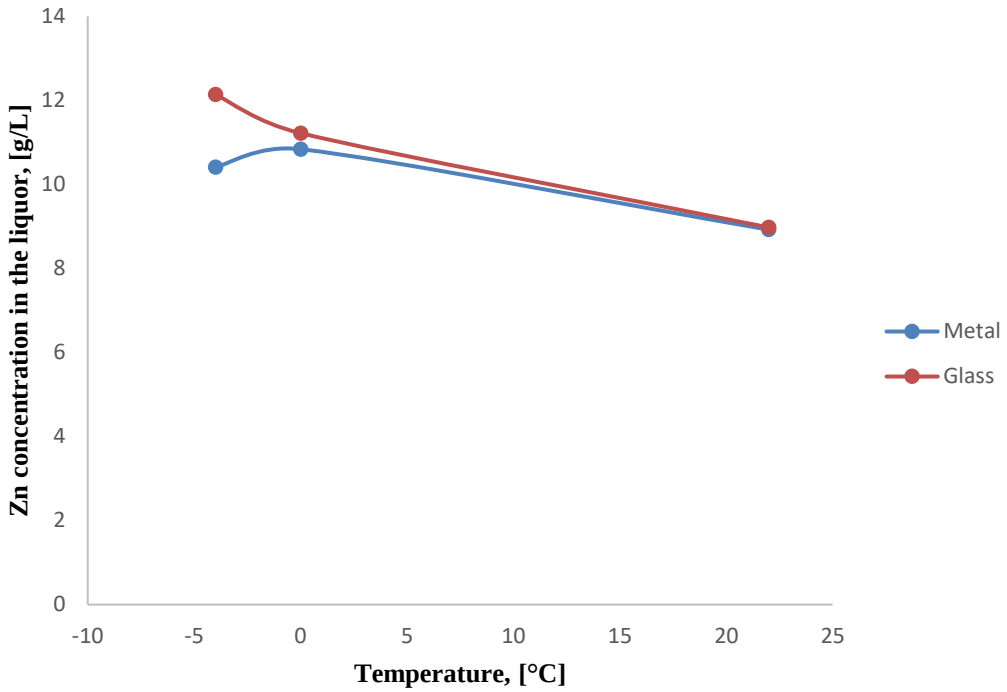

Figure 31 Zn concentration in the synthetic liquor in glass and metal reactor. Impeller speed=600 rpm.

Results shown in figure 31 indicate that as the temperature decreases the concentration of zinc increases. This result can be explained using the results from figure 30. The zinc does not precipitate in the reactor and, therefore, as the concentration of Na decreases the concentration of Zn increases in the remaining liquid phase. It is visible from figure 31 that the reactor material does not have as significant effect to the zinc concentration as it has on the Na concentration. Only at −4°C there is a noticeable difference between the samples from different reactors. When the zinc concentration of the first batch of synthetic liquor was analyzed it was in close agreement with the simulated results shown in figure 26, which was ~4.0 g/l for the simulated system and ~3.7 g/l for the AAS analysis. However, the recipe for the following synthetic liquor batches was modified in order to make the synthetic liquor match the liquor used in the simulation as close as possible by increasing the amounts of chemicals used in production of synthetic liquor (see table VI in chapter 8.2.1). This change resulted in a higher concentration of NaOH in the produced liquor. The increased concentration of NaOH caused problems with the filtration. In this case when the liquor was filtered, using a normal filter paper, it destroyed the filter paper. In order to save the produced liquor it was filtered using a very small filter paper which was made from glass fiber. Therefore, the filtration

took several hours which meant that the liquor had time cool down. This may explain the significant differences between the measured Zn concentrations (figure 31) and simulated Zn concentrations (figure 26), where the amount of dissolved zinc in the liquor is more than double than what the equilibrium simulation predicts. Besides, the simulated results shown in figure 26 suggest that the concentration of Zn increases as the temperature of the liquor decreases, as in this case. Furthermore, according to the simulated results in order to have 9 g/l of zinc in the liquor the temperature has to be 73°C which is completely plausible in this case.

9.3 Cooling rate effect on mother liquor

The typical temperature profiles of both cooling rates are represented in figures 32 and 33.

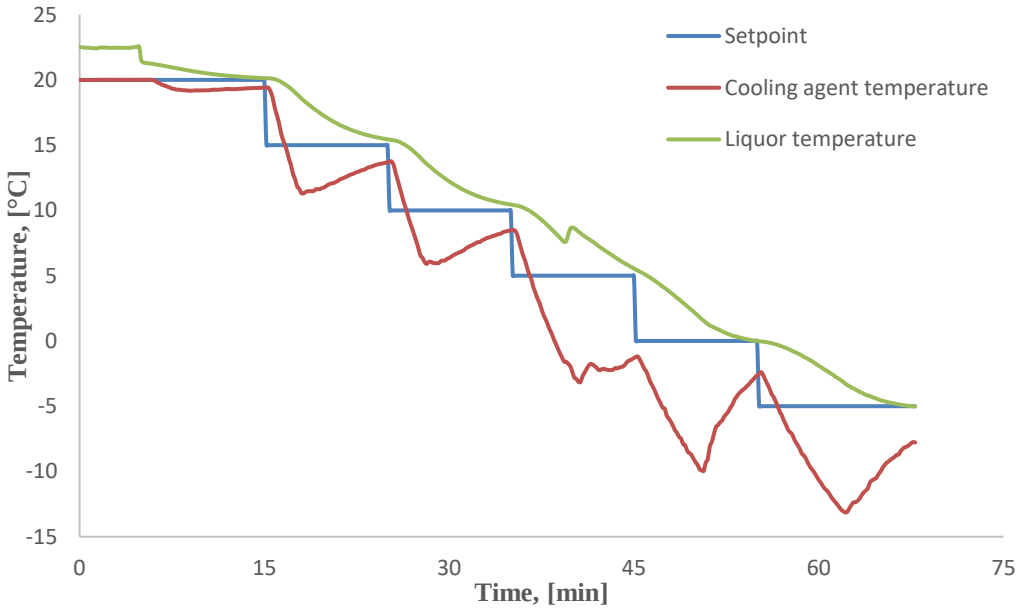

Figure 32 Typical temperature profile when liquor temperature is decreased with cooling rate 1

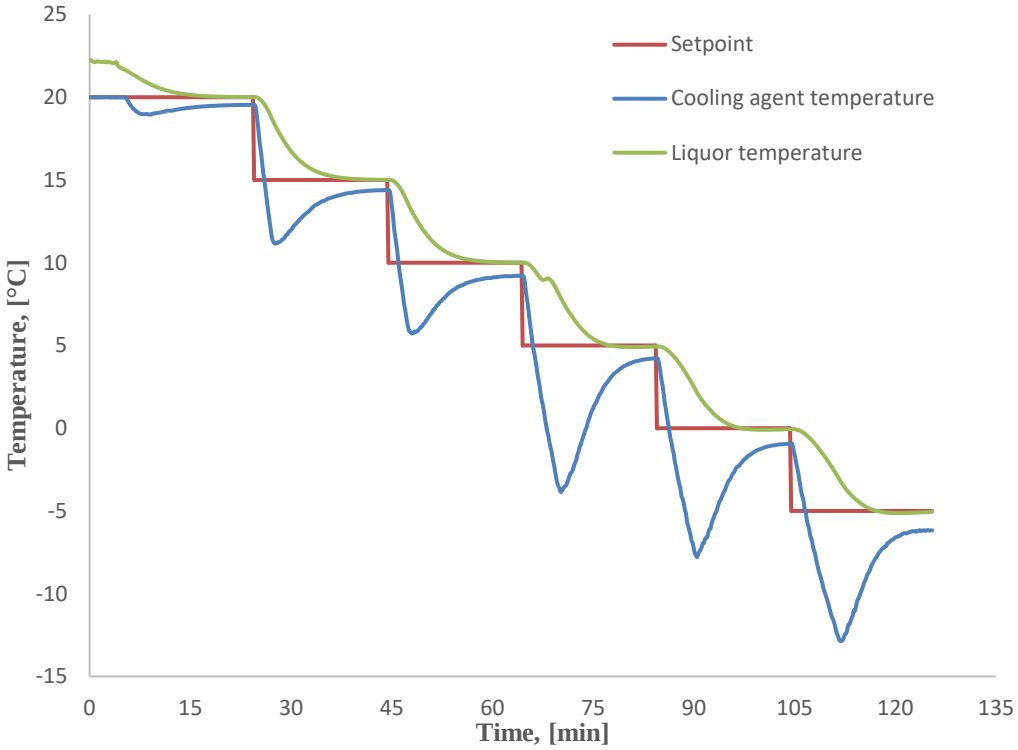

Figure 33 Typical temperature profile when liquor temperature is decreased with cooling rate 2

It is visible from figures 32 and 33 that liquor temperature increases around 8°C, which is caused by crystallization. After the crystallization experiment was over, it was observed visually that the crystals had formed a layer over the reactor wall. However, there was no significant crystal layer over the impeller or baffles in the reactor. Furthermore, the amount of crystals was vastly greater with green liquor than with synthetic liquor. For example, synthetic liquor yielded ~230 g of crystals from 1.5 l. The amount of crystals was ~530 g from 1.5 l of green liquor. The amount of obtained crystals from synthetic liquor is in agreement with the simulation results shown in figure 28 (120 g/kg total mass vs. 124 g/kg total mass).

Table VIII shows the titration results (averages from two parallel titrations) for the synthetic liquor, before the crystallization and after crystallization with both cooling rates.

Table VIII Titration results from the produced synthetic liquor before crystallization and after crystallization with both cooling rates. CR is an abbreviation from cooling rate.

	Batch 12.6	**Batch 12.6 CR 1**	**Batch 12.6 CR 2**	**Batch 14.6**	**Batch 14.6 CR 1**	**Batch 14.6 CR 2**	**Batch 15.6**	**Batch 15.6 CR 1**	**Batch 15.6 CR 2**
First turning point	pH=9.59	pH=9.45	pH=9.30	pH=9.45	pH=9.58	pH=9.48	pH=9.79	pH=8.83	pH=9.03
HCl consumption at the first turning point, [ml]	21.2	24.1	23.95	21.88	24.43	24.05	21.85	25.1	24.475
Second turning point	pH=4.08	pH=4.18	pH=4.05	pH=4.23	pH=4.07	pH=3.91	pH=4.16	pH=4.13	pH=4.28
Total HCl consumption, [ml]	28.85	27.9	27.78	29.73	28.1	27.68	29.63	28.63	27.93
m(NaOH), [g/l]	184.35	209.56	208.26	190.22	212.39	209.13	190.00	218.26	212.82
m(Na_2CO_3), [g/l]	88.14	43.78	44.07	90.44	42.34	41.76	89.58	40.61	39.75
Degree of causticizing, [%]	73.48	86.38	86.23	73.59	86.92	86.90	73.75	86.68	87.64
Na_2CO_3:NaOH mass ratio, [%]	47.8	20.9	21.1	47.5	19.9	20.0	47.1	18.6	18.7

It is visible from table VIII that crystallization of synthetic liquor reduces the concentration of Na_2CO_3 significantly (from ~90 g/l to ~40 g/l). However, there is no significant difference to the Na_2CO_3 concentration between the two different cooling rates. Despite the substantial decline in Na_2CO_3 concentration in the synthetic liquor during the crystallization, the Na_2CO_3:NaOH mass ratio is not at the desired level which is described in table V (13.6%). On the other hand, the Na_2CO_3:NaOH mass ratio can be lowered by keeping the crystals at −5°C for longer period of time. This was confirmed in test crystallization where synthetic liquor was cooled to −5°C as fast as the heat exchanger could manage and then kept there for ~50 minutes. In this case, the Na_2CO_3:NaOH mass ratio was 16.2%. However, the results from the experiments are not in agreement with the simulated results, in which the Na_2CO_3:NaOH mass ratio is predicted to be 6.5% at −5°C. This result may be explained by differences in liquor's retention time at −5°C. In the experiments the liquor was filtered instantly after it reached the target temperature of −5°C and starting to warm up the liquor. Therefore, the liquor is not subjected to the target temperature no more than a few minutes and if the simulation assumes the equilibrium value of Na_2CO_3:NaOH mass ratio in −5°C then the difference can be explained as it was noticed above that a longer period of time decreases the Na_2CO_3:NaOH mass ratio of synthetic liquor. Furthermore, the synthetic liquor's color turned from light yellow (see figure 22) to transparent during the crystallization experiment. The same change was observed also with green liquor. This color change is visible from figure 33.

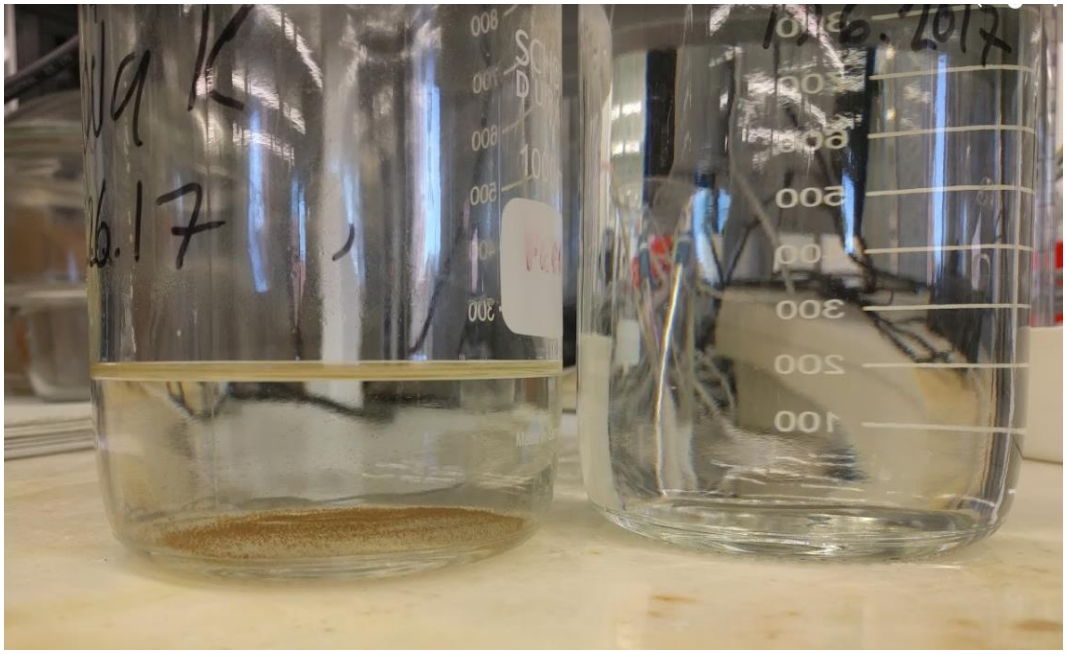

Figure 33 Synthetic liquor before (left) and after (right) the crystallization

The results from the density measurements for both synthetic and green liquor samples are represented in table IX.

Table IX Density results from all of the liquors.

Sample	Density, [g/ml]
Batch 12.6 original	1.2372
Batch 14.6 original	1.2372
Batch 15.6 original	1.2387
Batch 12.6 cooling rate 1	1.2163
Batch 12.6 cooling rate 2	1.2153
Batch 14.6 cooling rate 1	1.2156
Batch 14.6 cooling rate 2	1.2157
Batch 15.6 cooling rate 1	1.2147
Batch 15.6 cooling rate 2	1.2169
Green liquor original	1.1866
Green liquor cooling rate 1	1.1025
Green liquor cooling rate 2	1.1035
Green liquor cooling rate 1 repeat 1	1.1034
Green liquor cooling rate 2 repeat 1	1.1047

Green liquor cooling rate 1 repeat 2	1.1039
Green liquor cooling rate 2 repeat 2	1.1035

It can be observed from table IX that the densities of synthetic liquor are significantly higher than the densities of green liquors. This result can be explained by the amount of dissolved solids in the liquors, which is higher in synthetic liquor. Besides, the densities, in every case, decrease after the crystallization which is explained by removal of solids from the liquor during filtration after crystallization. In addition, the density results for synthetic liquor shown in table IX are in close agreement with the simulated results shown in figure 29 (~1.26 g/ml vs ~1.22 g/ml).

The ICP results from synthetic liquor, green liquor, and the dissolved crystals are represented in tables X-XII.

Table X ICP results for synthetic liquor. Numbers in the table represent the batch date and CR is an abbreviation from cooling rate.

Sample name	**Dilution**	**Na conc. in the sample, [ppb]**	**Na conc. in the liquor, [g/l]**	**Cl conc. in the liquor, [g/l]**	**Zn conc. in the liquor, [g/l]**
12.6 original	100421	1354.6	136.04	0	1.47
14.6 original	103415	1330.3	137.57	2.33	1.94
15.6 original	99894	1399.2	139.77	1.86	1.26
12.6 CR 1	99452	1254.2	124.73	2.76	1.40
12.6 CR 2	101180	1240.7	125.54	5.28	1.33
14.6 CR 1	106044	1183.0	125.45	3.45	1.34

14.6 CR 2	106023	1207.7	128.05	5.42	1.55
15.6 CR 1	98719	1297.1	128.05	1.98	2.31
15.6 CR 2	99066	1303.1	129.09	3.19	2.65

It is visible from table X that the concentration of Na decreases in the synthetic liquor during crystallization. This result can be explained by the removal of solids from the liquor during filtration after crystallization. In addition, cooling rate does not have any significant effect on the Na concentration, when original batch is compared to its two cooling rates, after the crystallization. However, the results for Zn concentrations are not as easy to explain as Na concentrations. According to table X the zinc concentration does decrease during crystallization. On the other hand, in the 15.6 batch the concentration of Zn doubles during the crystallization. Therefore, there is not any trend for Zn concentration. Moreover, the zinc concentrations are not in agreement with AAS results (figure 31). This result may be explained by sampling and the massive dilution (100000X). Besides, the liquors are not homogeneous and, therefore, the sampling has an effect to the results. In order to obtain reliable results, sampling and chemical analyses have to be repeated until the results are statistically reliable and the reproducibility are verified. Then, obtained average values of those results can be used for the final conclusions. Furthermore, ICP results showed that there were significant amounts of Cl in the liquor which was unexpected, because Cl was not added into the liquor in any stage. This result may be explained by the corrosion of the metallic materials (reactors and impeller) during the experiment or traces from washing which could release chlorine into the liquor. For example, the impeller was washed using diluted HCl, because washing with soap and water was insufficient. This would explain why there is no amount of Cl in the sample which was done chronically first (12.6 original). Moreover, significant etching of both the crystallization reactor and impeller was observed during the experiment. The results from ICP analyses for green liquor are shown in table XI.

Table XI ICP results for green liquor. CR is an abbreviation from cooling rate, rep from repeat and GL from green liquor in table XIII.

Sample name	Dilution	Na conc. in the sample, [ppb]	Na conc. in the liquor, [g/l]	Cl conc. in the sample, [ppb]	Cl conc. in the liquor, [g/l]
GL original	99978	926.6	92.64	57.4	5.74
GL CR 1	107783	424.9	45.80	34.3	3.70
GL CR 2	102977	459.8	47.35	20.7	2.13
GL CR 1 rep 1	100770	464.4	46.80	8.7	0.88
GL CR rep 1	99599	476.3	47.43	42.1	4.19
GL CR 1 rep 2	99391	476.1	47.32	49.8	4.95
GL CR 2 rep 2	104592	454.0	47.49	85.1	8.90

The results shown in table XI indicate that the Na concentration decreases almost 50% during the crystallization. Furthermore, the cooling rate does not have any significant impact on the Na concentration. In addition, the second major element found in the green liquor was Cl like it was in synthetic liquor. The concentration of Cl behaves in the same manner as the concentration of Na which means that it decreases during the crystallization. The results from ICP analyses for obtained crystals are shown in table XII.

Table XII ICP results for obtained crystals. Numbers in the table represent the batch date and CR is an abbreviation from cooling rate, rep from repeat, and GL from green liquor in table XIV.

Sample name	Dilution	Na conc. in the sample, [ppb]	Na conc. in crystals, [g/l]	Cl conc. in the sample, [ppb]	Cl conc. in crystals, [g/l]
12.6 CR 1	1389162	394.7	548.35	60.7	84.39
12.6 CR 2	1143820	348.9	399.04	85.2	97.45
14.6 CR 1	1054665	337.0	355.46	35.7	37.62
14.6 CR 2	1105252	302.6	334.45	3.9	4.30
15.6 CR 1	1232738	282.3	348.00	36.7	45.21
15.6 CR 2	1049835	358.0	375.85	55.1	57.79
GL CR 1	1195938	647.9	774.90	78.1	93.37
GL CR 2	1198979	249.3	298.85	142.3	170.54
GL CR 1 rep 1	871210	776.6	676.56	85.3	74.34
GL CR rep 1	1120487	266.4	298.54	78.6	88.03
GL CR 1 rep 2	1406597	206.3	290.19	125.6	176.69
GL CR 2 rep 2	1235828	286.1	353.62	98.0	121.13

The results from table XII show that the crystals are predominantly made of sodium. Moreover, the crystals seem to contain significant amounts of chlorine. However, this result is not in agreement with any other analysis conducted in this thesis and,

therefore, should be treated with extreme prejudice. Moreover, a semi quantitative analysis was performed to all samples in order to find if there were any other impurities in the samples. The semi quantitative analysis did not find any additional elements in the samples, but the fully quantitative results show that there are trace amounts of arsenic, mercury, lead, and bismuth in all of the samples. It should be noted that there was minor difference between the standards done before and after the analyses. In addition, the big dilution will erase the small quantities of impurities.

9.4 Cooling rate effect on crystals

The results from three different filtration trials are represented in figure 34.

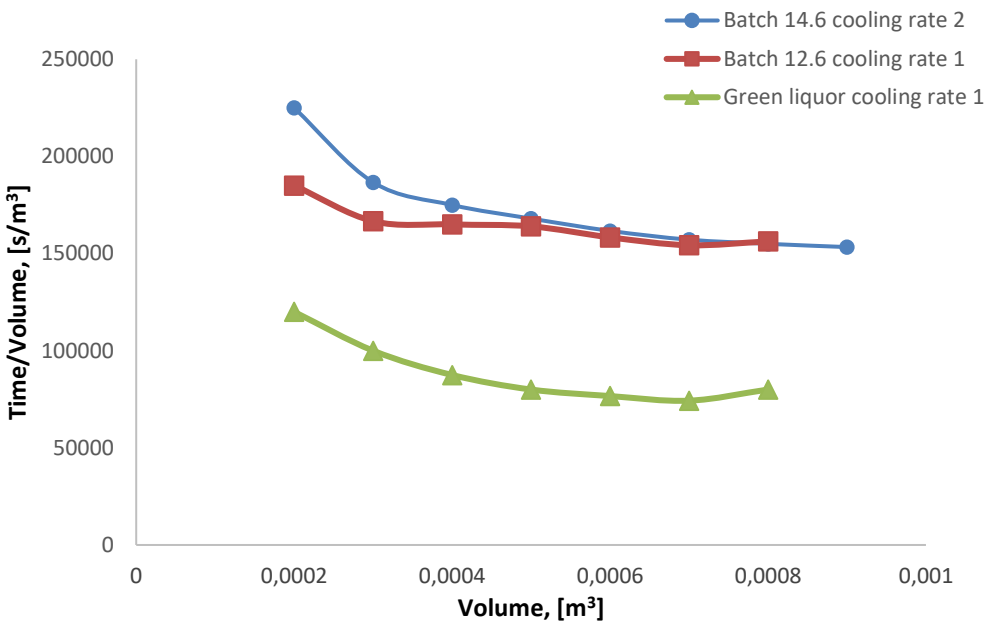

Figure 34 Liquor filtration resistance results when ΔP=0.8 bar and T=-5.0°C

Figure 34 shows that the filtration resistance decreases as the filtration cake grows. The first and last points are left out from every result in order to make the trends more linear. Despite of this it is clear that the trends are not linear. Both the decrease in filtration resistance as the cake grows and nonlinear results suggests that the samples are compressible. This trend has been observed with every crystal batch. This result may be explained by the increase in temperature of the crystals and

significant amounts mother liquor left in contact with the crystals. In addition, it was noticed that some black spots had appeared into the filter paper during the filtration experiment. These black spots shown in figure 35 may be explained by impurities in the liquor.

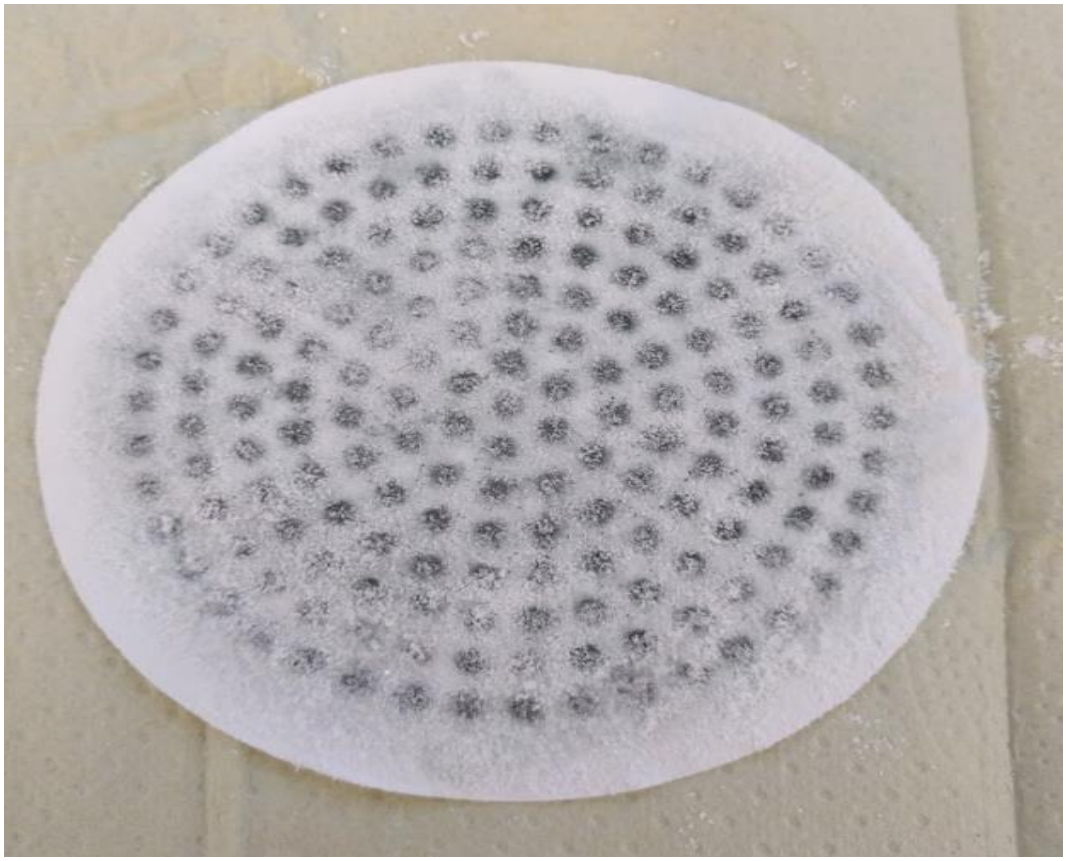

Figure 35 Filter paper after filtration of crystals produced from green liquor

It is visible from figure 35 that the black spots are in line with holes in the Büchner funnel.

Figures 36-40 show the XRD patterns of the obtained crystals from both synthetic and green liquor with two different cooling rates. CR in figures indicates cooling rate and GL means green liquor. Identifying XRD peaks were taken from literature (Ye *et al*., 2013; Harabor *et al*., 2013).

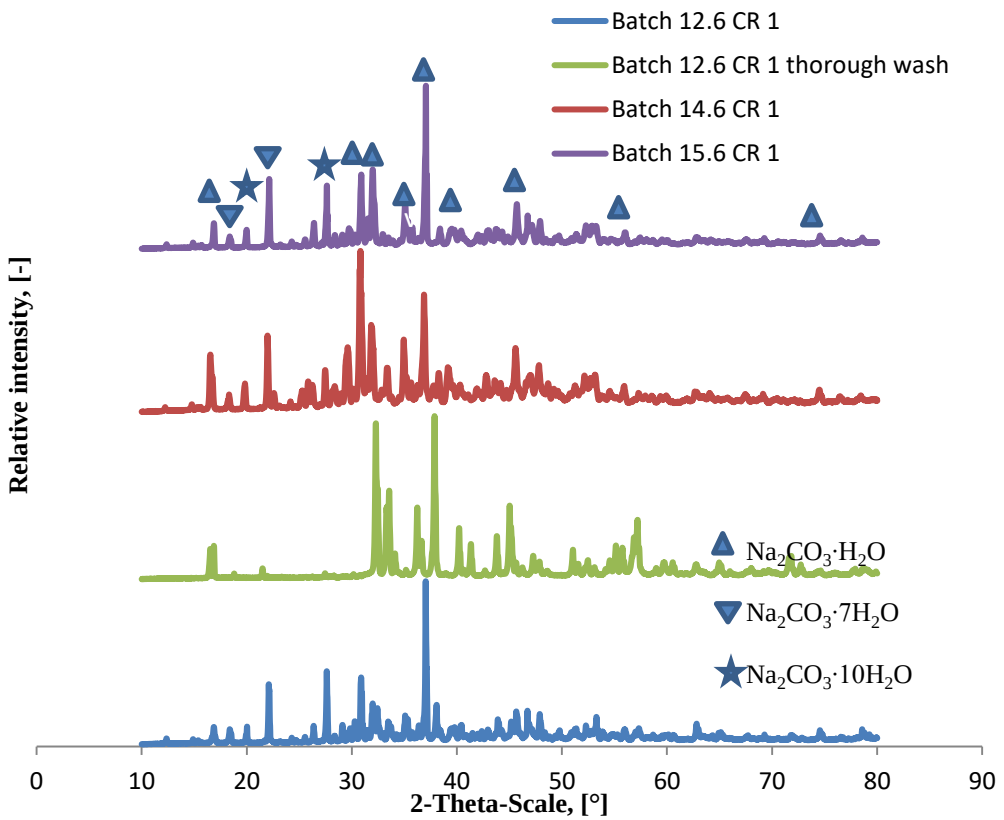

Figure 36 XRD patterns of crystals obtained from synthetic liquor with cooling rate 1

It can be observed from figure 36 that there is some difference between the samples. Especially, the difference is significant between batch 12.6 CR 1 and 12.6 CR 1 thorough wash which suggest that the ethanol wash has major influence on the crystal form. In addition, the results suggest that the crystals before ethanol wash are a combination of Na_2CO_3 hydrate, i.e., $Na_2CO_3 \cdot 1H_2O$, $Na_2CO_3 \cdot 7H_2O$, and $Na_2CO_3 \cdot 10H_2O$, but after the washing step the crystals are monohydrate. This result can be verified by the total water fraction measurements (see table XV). Besides, more thorough washing results in almost pure monohydrate crystals. This phenomenon was visually observed in the laboratory during the washing stage. The color of the crystals changed from transparent to white. The reason may be that the covalent bond between sodium carbonate and one crystallization water (monohydrate) is far greater that between seven or ten crystallization waters. Therefore, ethanol can take every crystallization water from sodium carbonate expect one. The XRD patterns of the crystals from synthetic liquor batches with cooling rate 2 are shown in figure 37.

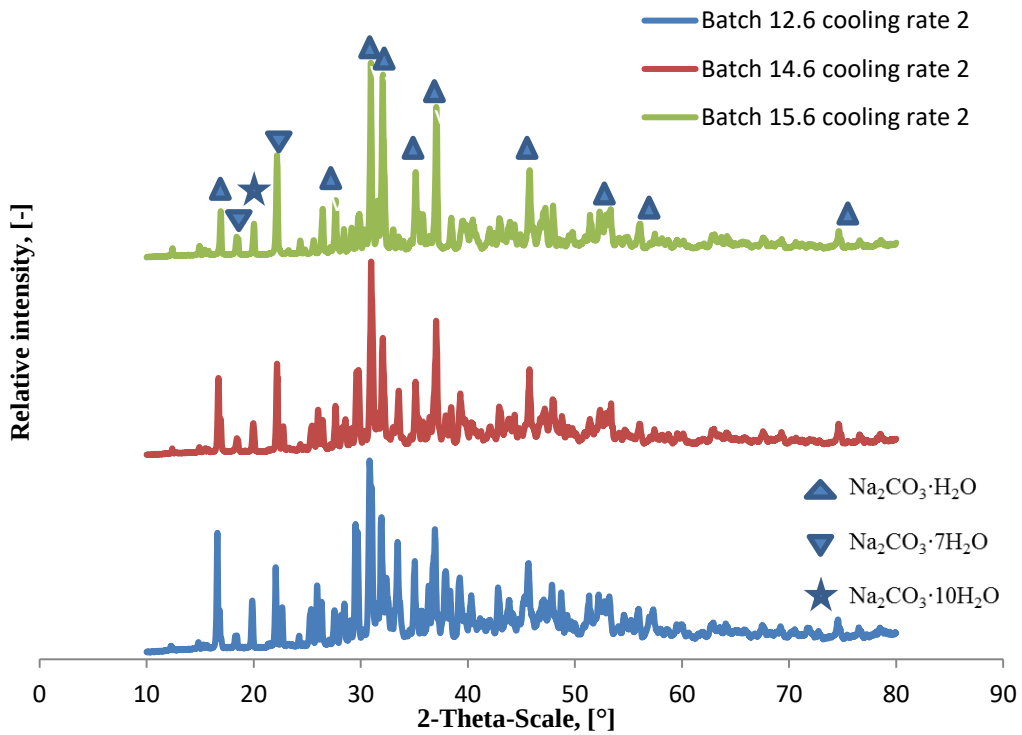

Figure 37 XRD patterns of crystals obtained from synthetic liquor with cooling rate 2

The results from figure 37 differ from the results shown in figure 36. For example, there are a lot more peaks in figure 37 than in 36. However, the main identifying peaks in figure 37 are the same between samples. Besides, as described above, the ethanol washing has a major effect to the crystals. The results depicted in figure 37 suggest that the crystals are a mixture of sodium carbonate hydrates which indicate that there is little or no difference between synthetic liquor batches. The XRD patterns of the crystals obtained from green liquor with cooling rate 1 are shown in figure 38.

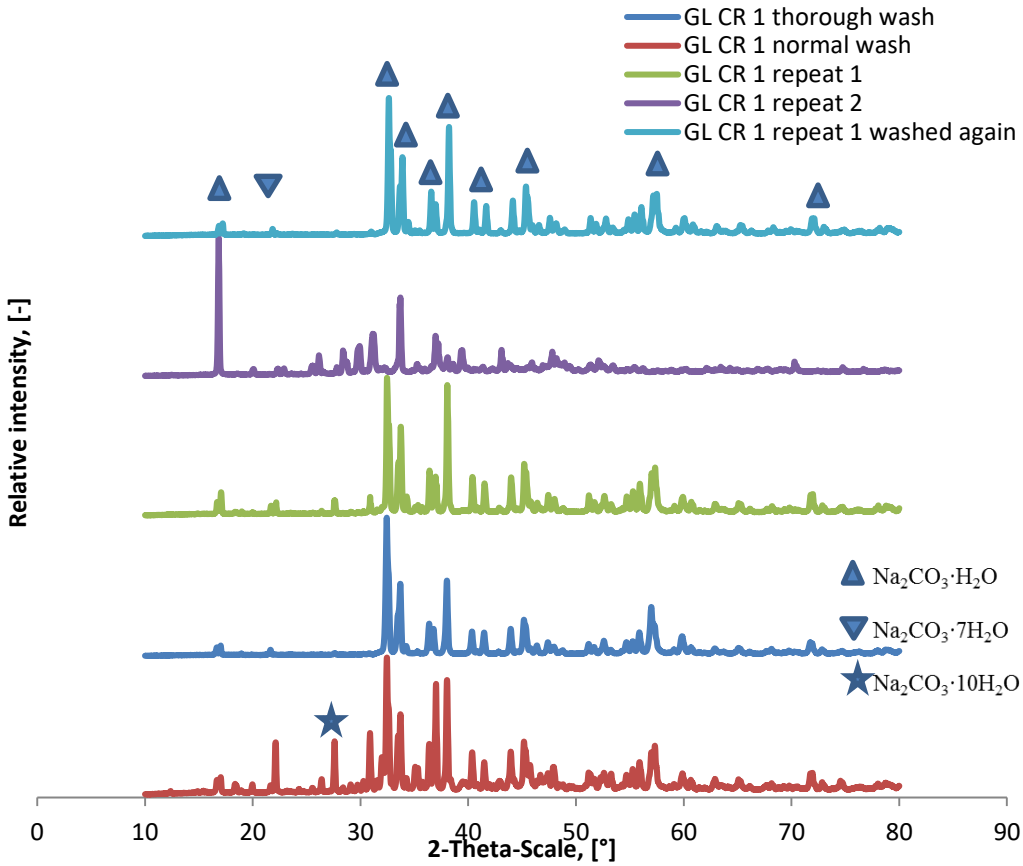

Figure 38 XRD patterns of crystals obtained from green liquor with cooling rate 1

It can be seen from figure 38 that the obtained crystals from green liquor are sodium carbonate hydrates as with synthetic liquor. Furthermore, the ethanol washing has the same effect on the crystals formed from green liquor as it has on the synthetic liquor crystals. Moreover, the XRD patterns do not differ significantly between the crystals which are washed the same way, i.e., GL CR 1 normal wash, GL CR 1 repeat 1, and GL CR 1 repeat 2. All of the produced crystals were obtained from the first green liquor crystallization experiment (GL CR 1 normal wash). However, due to the large amount of the crystals (~530 g) the ethanol washing was insufficient which can be seen from figure 38. For this reason, only part of the obtained crystals, from the following experiments with green liquor, were washed and stored. It can be observed that number of peaks, in GL CR 1 normal wash, is significantly greater than in GL CR 1 repeat 1. This difference can be explained by the ethanol washing efficiency and the amount of crystals which were washed. The XRD patterns of the crystals obtained from green liquor with cooling rate 2 are shown in figure 39.

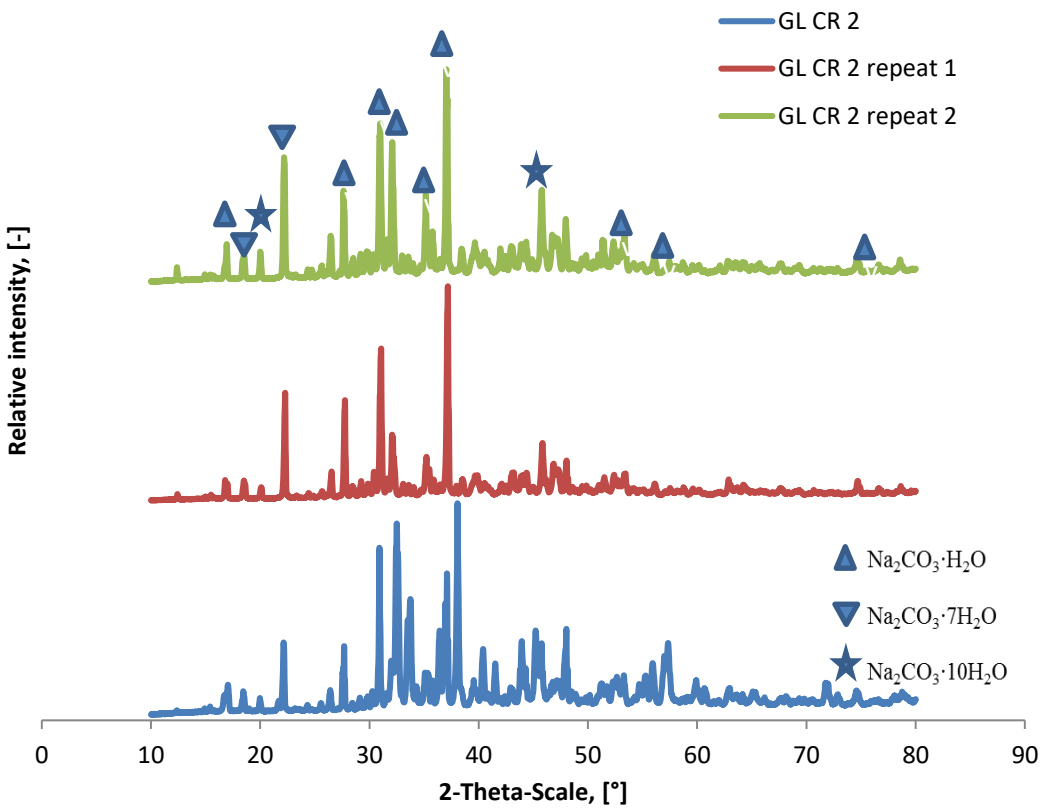

Figure 39 XRD patterns of crystals obtained from green liquor with cooling rate 2

The results from figure 39 are in line with results from figures 36 to 38 which means that the produced crystals are a mixture of sodium carbonate hydrates. Cooling rates do not have significant impact on the crystals that obtained from green liquor. Ethanol washing has a big role on the composition of crystals that obtained from both synthetic and green liquor. There are more XRD patterns with the cooling rate 2 than cooling rate 1 from both synthetic and green liquors. In order to demonstrate the effect of ethanol washing to the crystal XRD patterns, all of the thoroughly washed samples are represented in figure 40.

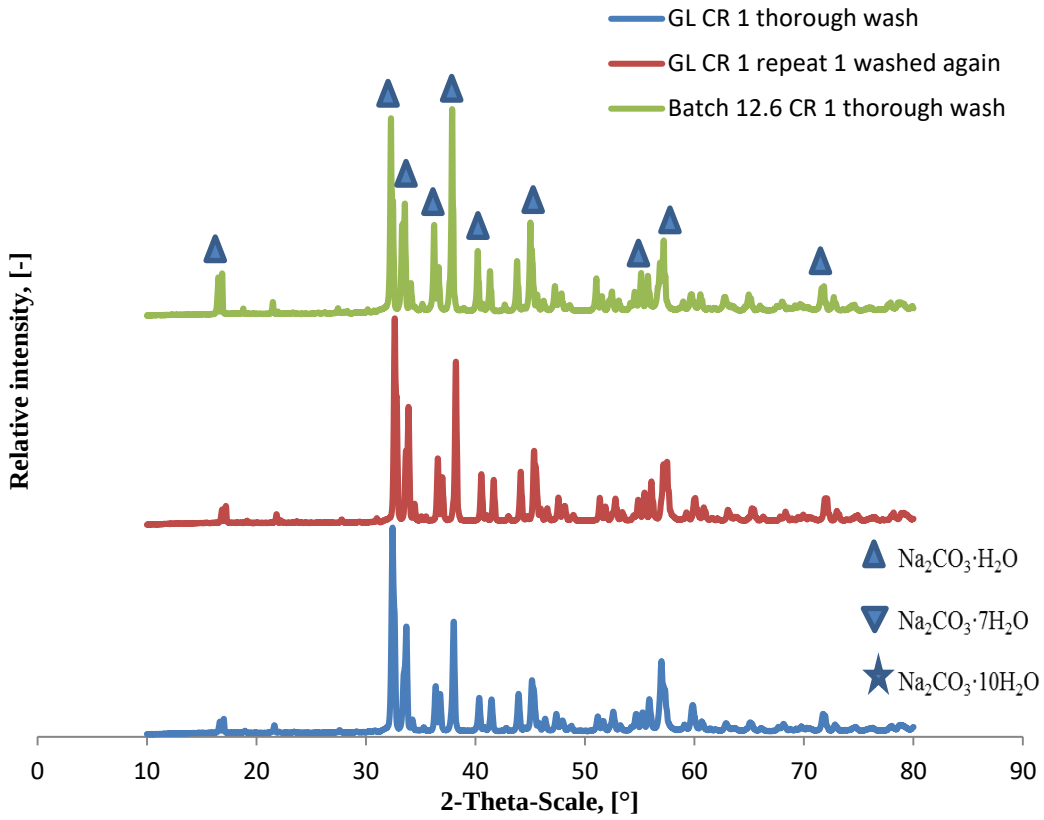

Figure 40 XRD patterns of thoroughly washed crystals obtained from green liquor and synthetic liquor with cooling rate 1

It is visible from figure 40 that when the produced crystals are washed thoroughly with ethanol, very pure sodium carbonate monohydrate crystals are obtained. As seen from figure 40, the XRD patterns are almost identical with three different crystallization experiments. In addition, results are the same with synthetic liquor and industrial green liquor. Furthermore, this ethanol washing can be done several days later and still high purity $Na_2CO_3 \cdot 1H_2O$ will be obtained, as seen from GL CR 1 repeat 1 washed again in figure 40. In this case, the stored crystals were still moist and part of the crystals were washed again, thoroughly, and dried in a desiccator. As seen from results depicted in figure 40, it does not matter if the crystals are washed immediately or even many days later. However, most of the mother liquor has to be washed from the crystal surface, otherwise the crystals will dissolve completely. Besides, if even small amounts of liquor left in the crystals, the sample will partially dissolve the crystals turning them into a paste. Thoroughly washed, normally washed, and partially dissolved crystals are shown in figure 41.

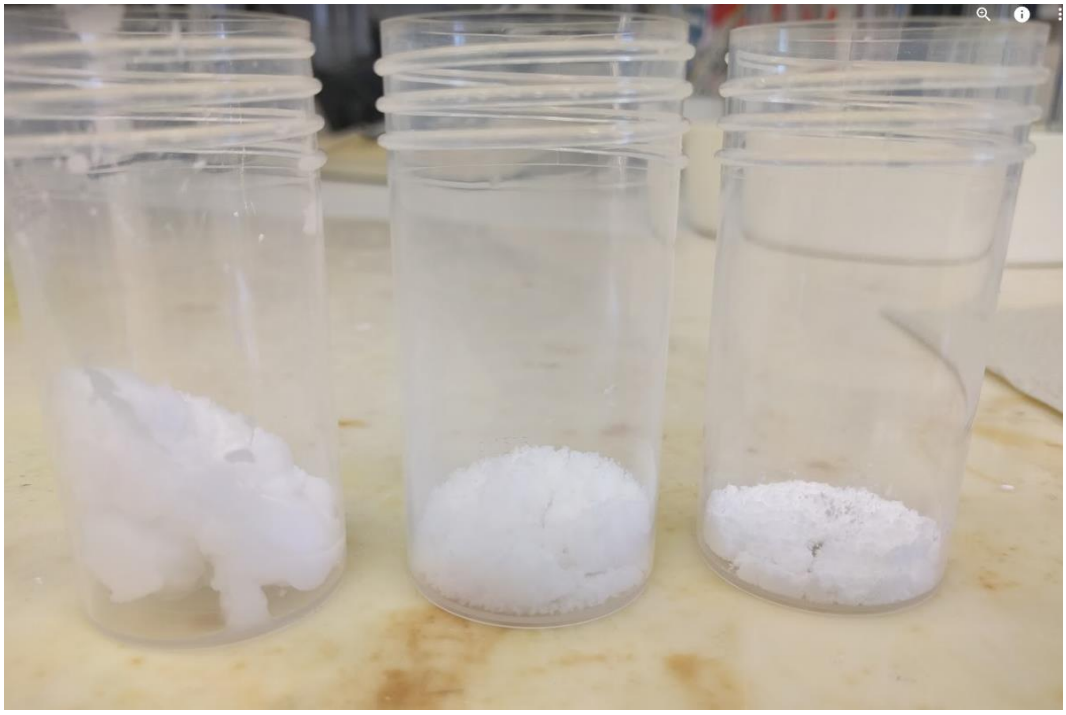

Figure 41 Partially dissolved crystals (left), normally washed crystals (middle), and thoroughly washed crystals (right)

Table XIII shows the total water fraction calculated using equation (8.6) in the washed and dried crystals for each experiment. Furthermore, in order to investigate the change in the sodium carbonate hydrate form, the total water fraction results from the obtained crystals after 24 hours of drying are represented in table XIII.

Table XIII Total water fraction results from the obtained crystals. CR is an abbreviation from cooling rate, rep from repeat, and GL from green liquor in table XIII

Sample	**Total water fraction (dried 216 h), [%]**	**Total water fraction (dried 24 h), [%]**
$Na_2CO_3 \cdot H_2O$ (Theoretical value)	14.51	14.51
$Na_2CO_3 \cdot 7H_2O$ (Theoretical value)	54.31	54.31
$Na_2CO_3 \cdot 10H_2O$ (Theoretical value)	62.94	62.94
Batch 12.6 CR 1	14.62	52.98
Batch 12.6 CR 2	15.27	58.79
Batch 14.6 CR 1	14.90	60.97
Batch 14.6 CR 2	14.87	62.37

Batch 15.6 CR 1	14.60	59.60
Batch 15.6 CR 2	15.05	58.67
GL CR 1	14.64	20.04
GL CR 2	14.78	67.49
GL CR 1 rep 1	14.77	64.59
GL CR 2 rep 1	14.83	61.22
GL CR 1 rep 2	14.55	67.96
GL CR 1 rep 2	14.93	66.13

It can be observed from table XIII that either cooling rate or liquor (synthetic or green) have no influence on the water fraction of the crystals. The results also show that all of the water fractions are not significantly different from each other. In addition, the values are slightly different from the theoretical value of $Na_2CO_3 \cdot H_2O$ (14.51%), which also confirms that the crystals are a mixture of sodium carbonate hydrates, but mostly monohydrate. Besides, the results represented in table XIII suggest that the crystals changes from sodium carbonate decahydrate to monohydrate during the drying. This result differs from the literature where it was stated that sodium carbonate decahydrate loses water at or above its melting point, 32.5-34.5°C (Perry, 1995; Lewis, 1998). The crystals were dried in a desiccator at room temperature. In addition, the desiccator was kept out of direct sunlight in order to keep its temperature from rising.

The crystal size distributions of all the samples are shown in figure 42. Each curve shown in figure 42 is an average result from five duplicate measurements. CR is an abbreviation from cooling rate, rep from repeat, SL from synthetic liquor and GL from green liquor in figure 42.

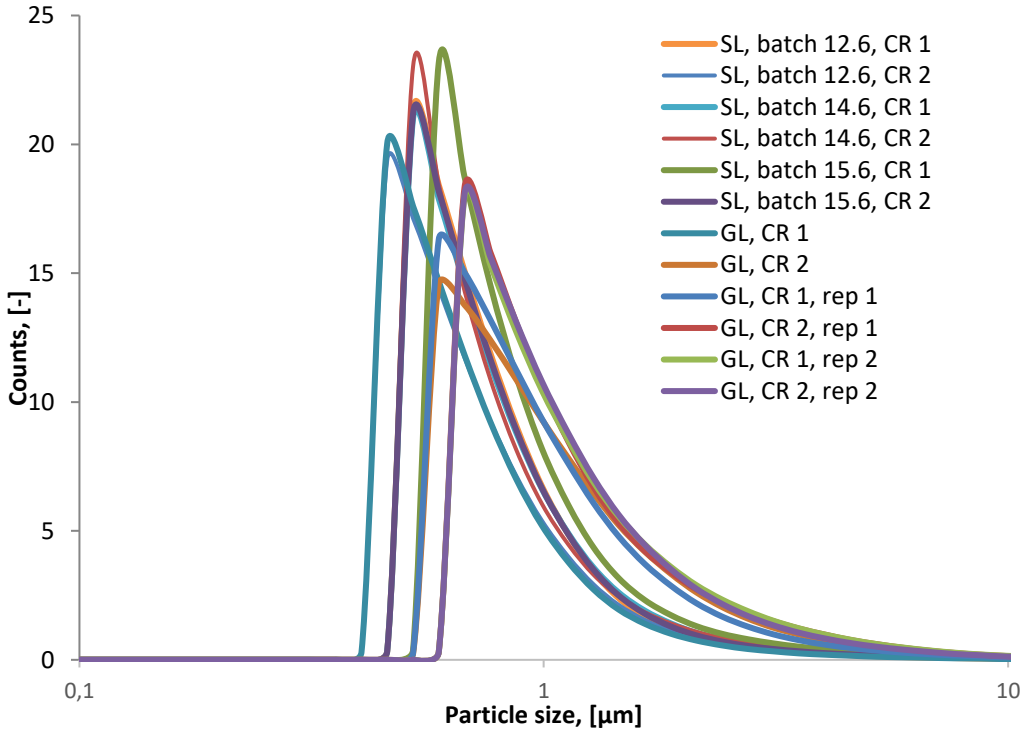

Figure 42 Crystal size distributions of the obtained crystals

Figure 42 shows that there is little or no difference between all of the samples and, therefore, neither the cooling rate nor liquor (synthetic or green) has any significant effect on the crystal size distribution of the obtained crystals. It is clear from figure 42 that the Dx(50) is below 1.0 µm in most cases. This result can be confirmed by SEM-pictures (see appendix 1). However, without effective mixing (3000 rpm) the crystals will agglomerate into larger crystals. This phenomenon was observed visually in the laboratory.

The morphology of the obtained crystals with synthetic liquor and green liquor is shown in figures 43 to 55 (see appendix 1). Figures 43 to 49 represent the morphology of synthetic liquor batch 12.6 with both cooling rates and also thoroughly washed crystals. Figures 50 to 55 show the morphology of green liquor crystals with cooling rate 1 and thoroughly washed crystals. Furthermore, energy dispersive X-ray spectroscopy (EDS) analysis was conducted with SEM.

The SEM images of figures 43 to 55 show some differences between the two cooling rates, as far as the crystal morphology is concerned. However, there is a remarkable difference between the thoroughly washed crystals and normally washed crystals. It is clear from figures 43 to 45 that the thoroughly washed crystals form a 'rough' surface and individual crystals can be seen clearly (see figure 45). On the other hand, the crystals obtained with cooling rate 2 have in some part almost a smooth crystal surface (see figure 55). These damaged crystals may be explained by the insufficient washing because small amounts of mother liquor left in contact with the crystals. The crystals then dissolved partially into the mother liquor. Figures 43 to 55 show that the crystals are actually agglomerates of smaller crystals, which confirms the results obtained from the crystals size distribution (see figure 42). The results from EDS analysis for crystals produced from synthetic liquor are shown in table XIV. In tables XIV and XV CR is an abbreviation of cooling rate, GL is green liquor, N is normal and T is thorough. 12.6 indicate the batch date.

Table XIV The results from EDS analysis for crystals produced from synthetic liquor

Element	**12.6 CR 1 T wash**	**12.6 CR 1 T wash; white**	**12.6 CR 1 N wash**	**12.6 CR 1 N wash; white**	**12.6 CR 2 N wash**
C, [m-%]	17.2	14.5	14.0	9.9	17.1
O, [m-%]	48.3	40.6	43.9	37.6	42.0
Na, [m-%]	31.9	21.9	39.6	0	40.8
Zn, [m-%]	2.6	23.0	2.5	52.4	0
Al, [m-%]	0	0	0	0	0.2

EDS results, shown in table XIV, suggest that the white material on the crystal surface is zinc. However, the EDS analysis also shows that the white material contains sodium but that may be explained by the small amount of the white material on top of the crystal surface. This means that the EDS show the material under the white material. In addition, the samples were prepared on carbon tape and thus, have an effect on the carbon concentration. Besides, the carbon tape explains the trace amounts of aluminum found in batch 12.6 cooling rate 2 normal wash. The

results from EDS analysis for crystals produced from green liquor are shown in table XV.

Table XV The results from EDS analysis for crystals produced from green liquor

Element	GL CR 1 T wash	GL CR 1 N wash	GL CR 2 N wash
C, [m-%]	15.0	16.6	15.4
O, [m-%]	48.8	45.6	49.4
Na, [m-%]	35.9	37.3	34.7
S, [m-%]	0.2	0.4	0.3
K, [m-%]	0.1	0.1	0.2

It can be observed from tables XIV and XV that there is no significant difference either between the cooling rates or ethanol washing to the EDS results. Furthermore, there is little or no difference between the crystals produced from synthetic liquor and green liquor, apart from the zinc with synthetic liquor. The zinc in the synthetic liquor can be explained easily, because it was one of the main species used in the production of synthetic liquor. Besides, table XV shows that the crystals obtained from green liquor have only trace amounts of impurities which is in agreement with the ICP results.

According to the results obtained from morphology of the crystals (figures 43 to 55), the XRD patterns (figures 36 to 40) and the total water fraction (table XIII), it can be concluded that the crystals consisted mostly $Na_2CO_3 \cdot H_2O$ after thorough ethanol wash. The purity level on the thoroughly washed crystals is high. However, the results show that ethanol washing affects the composition of sodium carbonate hydrates form significantly.

10 Conclusions

This Master's thesis contains a literature review and an experimental part. Cooling crystallization and brief introduction to recausticizing process are discussed in the literature review. In addition, batch cooling crystallization has been applied for the crystallization of sodium carbonate from both synthetic liquor and industrial green liquor in order to purify liquor beyond normal causticizing process. Furthermore, the cooling process was simulated using OLI Studio Stream Analyzer software.

The experiments conducted in this thesis included the production of synthetic liquor, solubility measurements of sodium to synthetic liquor and cooling crystallization of synthetic liquor and green liquor. The effect of cooling rate on the mother liquor, obtained crystals, and the XRD patterns, morphology, crystal size distribution and Na_2CO_3 purity were determined. It was found that the cooling rate did not have significant effect on above investigated parameters. Moreover, the cooling rate had little or no effect to the Na_2CO_3:NaOH mass ratio which was surprising. The results from filtration experiment showed that the crystals, from every experiment, are compressible which was unexpected. This phenomenon may be explained by the mother liquor left in the filter cake and by rise in temperature during the filtration, which causes the crystals to start to dissolve. Furthermore, the crystal purity is not dependent on the cooling rate. However, ethanol washing was found to have significant effect on the sodium carbonate hydrate form. The thoroughly washed crystals, from both synthetic and green liquor, were confirmed to be $Na_2CO_3 \cdot H_2O$ by XRD examination and total water fraction measurements. In addition, the crystal size distribution and SEM images show that the average crystal size, in every produced crystal batch, is roughly 1 µm. However, titration results indicate that the studied two cooling rates (20% and 18.6% Na_2CO_3:NaOH mass ratio) were not sufficient to purify the synthetic liquor to the desired level (13.6% Na_2CO_3:NaOH mass ratio). On the other hand, titration results from test crystallization indicate that the retention time at the target temperature of −5°C affects the liquor purity level.

Therefore, it was concluded that the cooling crystallization provides a plausible technology to produce Na_2CO_3 crystals with high purity in view of purification of synthetic liquor and green liquor.

11 Future work

In order to estimate the retention time of liquor in the continuous process, more laboratory experiments ought to be conducted. In this experiment the effect of time in the end temperature to the liquor's Na_2CO_3:NaOH mass ratio is investigated and cooling rate is kept constant.

12 References

Biglia, A., Comba, L., Fabrizio, E., Gay, P., Aimonino, D.R., Case studies in food freezing at very low temperature. *Energy Procedia* **101**(2016), pp. 305-312.

Chen, A., Xu, D., Chen, X., Zhang, W., Liu, X., Measurements of zinc oxide solubility in sodium hydroxide solution from 25 to 100°C. *Transactions of Nonferrous Metals Society of China* **22**(2012), pp. 1513-1516.

Covey, G.H., Creasy, D.E., Elliot, A.D., Phan, H.Q., Crystallization of sodium carbonate from green liquor by cooling. *Appita Journal* **52**(1999), pp. 56-61.

Forgione, M., Birpoutsoukis, G., Bombois, X., Mesbah, A., Daudey, P.J., Van den Hof P.M.J., Batch-to-batch model improvement for cooling crystallization. *Control Engineering Practice* **41**(2015), pp. 72-82.

Gullichsen, J., Fogelholm, C-J., *Chemical pulping*, 1st ed., Gummerus Printing, Jyväskylä, 2000, pp. 10-32.

Harabor, A., Rotaru, P., Harabor, N.A., Two phases in a commercial anhydrous sodium carbonate by air contact. *Physics AUC* **23**(2013), pp.79-88.

Hasan, M., Filimonov, R., Chivavava, J., Sorvari, J., Louhi-Kultanen, M., Lewis, A.E., Ice growth on the cooling surface in a jacketed and stirred eutectic freeze crystallizer of aqueous Na_2SO_4 solutions. *Separation and Purification Technology* **175**(2017), pp. 512-526.

Hurst, M.O., Fortenberry, R.C., Factors affecting the solubility of ionic compounds. *Computational and Theoretical Chemistry* **1069**(2015), pp. 132-137.

Jaretun, A., Aly, G., Removal of Chloride and Potassium from Kraft Chemical Recovery Cycles. *Separation Science and Technology* **35**(2000), pp. 421-438.

Konno, H., Nanri, Y., Kitamura, M., Crystallization of aragonite in the causticizing reaction. *Powder Technology* **123**(2002), pp. 33-39.

Kirk-Othmer Encyclopedia of Chemical Technology, Vol 27, Seidel A., 5th ed., John Wiley & Sons, 2007, pp. 1-27.

Lewis, A.E., Nathoo, J., Thomsen, K., Kramer, H.J., Witkamp, G.J., Reddy, S.T., Randall, D.G., Design of a Eutectic Freeze Crystallization process for multicomponent waste water stream. *Chemical Engineering Research and Design* **88**(2010), pp. 1290-1296.

Lewis, R.A., *Lewis' dictionary of toxicology*, 1st ed., CRC press, 1998, p. 954

Lu, H., Wang, J., Wang, T., Wang, N., Bao, Y., Hao, H., Crystallization techniques in wastewater treatment: An overview of applications. *Chemosphere* **173**(2017), pp. 474-484.

Marion, G.M., Carbonate mineral solubility at low temperatures in the Na-K-Mg-Ca-H-Cl-SO_4-OH-HCO_3-CO_3-CO_2-H_2O system. *Geochimica et Cosmochimica Acta* **65**(2001), pp. 1883-1896.

Mullin, J. W., *Crystallization*, 4th ed., Butterworth-Heinemann, 2001, pp. 27-119.

Myerson, A.S., *Handbook of Industrial Crystallization*, 2nd ed., Butterworth-Heinemann, 2002, pp. 16-83.

Perry, D. L., *Handbook of inorganic compounds*, 1st ed., CRC press, 1995, p. 359

Randall, D.G., Nathoo, J., A succinct review of the treatment of Reverse Osmosis brines using Freeze crystallization. *Journal of Water Process Engineering* **8**(2015), pp. 186-194.

Reddy, S.T., Lewis, A.E., Witkamp, G.J., Kramer, H.J.M., Van Spronsen, J., Recovery of $Na_2SO_4 \cdot 10H_2O$ from a reverse osmosis retentate by eutectic freeze crystallization technology. *Chemical Engineering Research and Design* **88**(2010), pp. 1153-1157.

Rodriquez Pascual, M., Cenceli, F.E., Trambitas, D.O., Evers, H., Van Spronsen, J., Witkamp, G.J., A novel scraped cooled wall crystallizer Recovery of sodium carbonate and ice from an industrial aqueous solution by eutectic freeze crystallization. *Chemical Engineering Research and Design* **88**(2010), pp. 1252-1258.

Rodriquez Pascual, M., Trambitas, D., Saez Calvo, E., Kramer, H., Witkamp, G. J., Determination of the eutectic solubility lines of the ternary system $NaHCO_3$-Na_2CO_3-H_2O. *Chemical Engineering Research and Design* **88**(2010), pp. 1365-1371.

Theliander, H., On the equilibrium of the causticizing reaction. *Nordic Pulp and Paper Research Journal* **21**(1992), pp. 81-88.

Ullmann's encyclopedia of industrial chemistry, Vol 8, Arpe H-J., Gerhartz W., Elvers B., ed. 5th ed., Wiley-VCH Verlag Gmbh & Co. KGaA, Weinheim, 2012, pp. 582-628.

van der Ham, F., Witkamp, G.J., de Graauw, J., van Rosmalen, G.M., Eutectic freeze crystallization: Application to process streams and waste water purification. *Chemical Engineering and Processing* **37**(1998), pp. 207-213.

Van Spronsen, J., Rodriquez Pascual, M., Cenceli, F.E., Trambitas, D.O., Evers, H., Witkamp, G.J., Eutectic freeze crystallization from the ternary Na_2CO_3-$NaHCO_3$-H_2O system A novel scraped wall crystallizer for the recovery of soda from an industrial aqueous stream. *Chemical Engineering Research and Design* **88**(2010), pp. 1259-1263.

Ye W., Lin J., Shen J., Luis P., Van der Bruggen B., Membrane Crystallization of Sodium Carbonate for Carbon Dioxide Recovery: Effect of Impurities on the Crystal Morphology. *Crystal Growth & Design* **13**(2013), pp.2362-2372.

The morphology of the obtained crystals with synthetic liquor and green liquor is shown in figures 43 to 55.

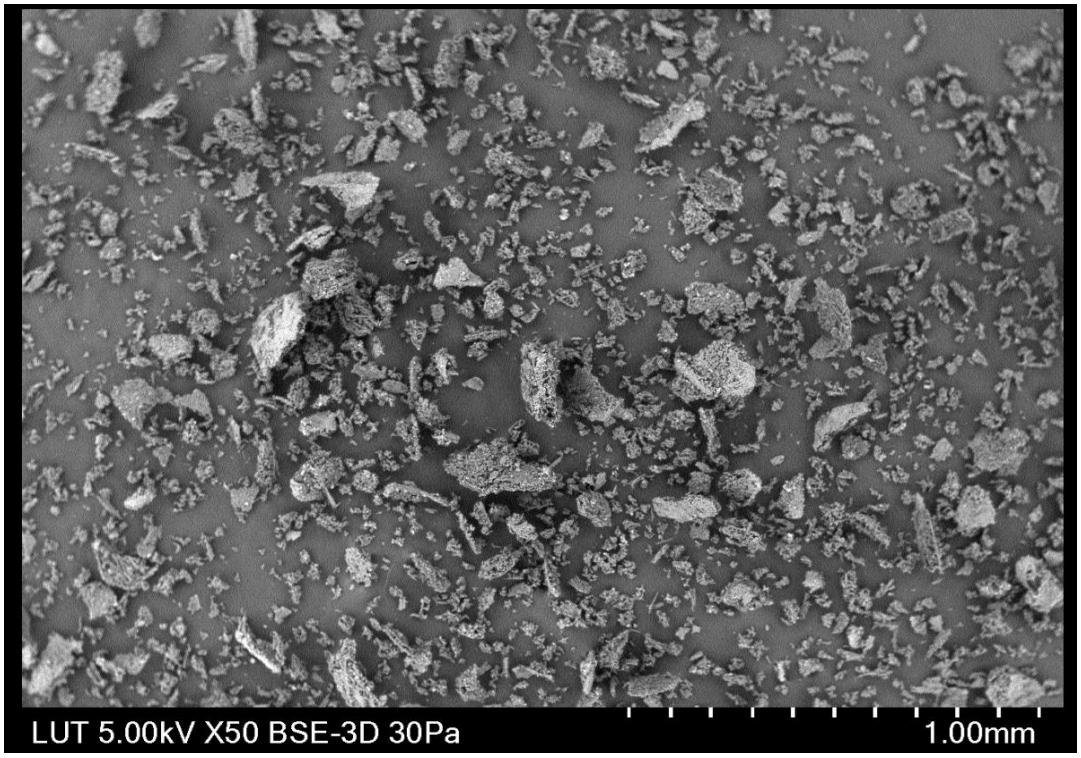

Figure 43. SEM pictures of the thoroughly washed crystals from batch 12.6 cooling rate 1

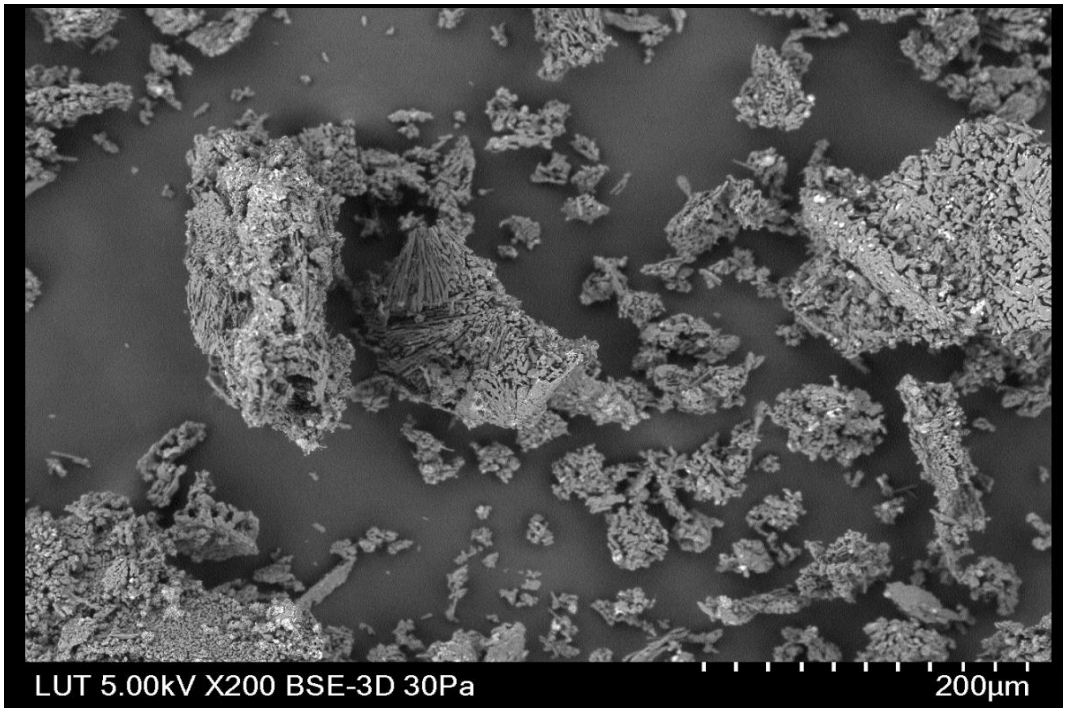

Figure 44. SEM pictures of the thoroughly washed crystals from batch 12.6 cooling rate 1

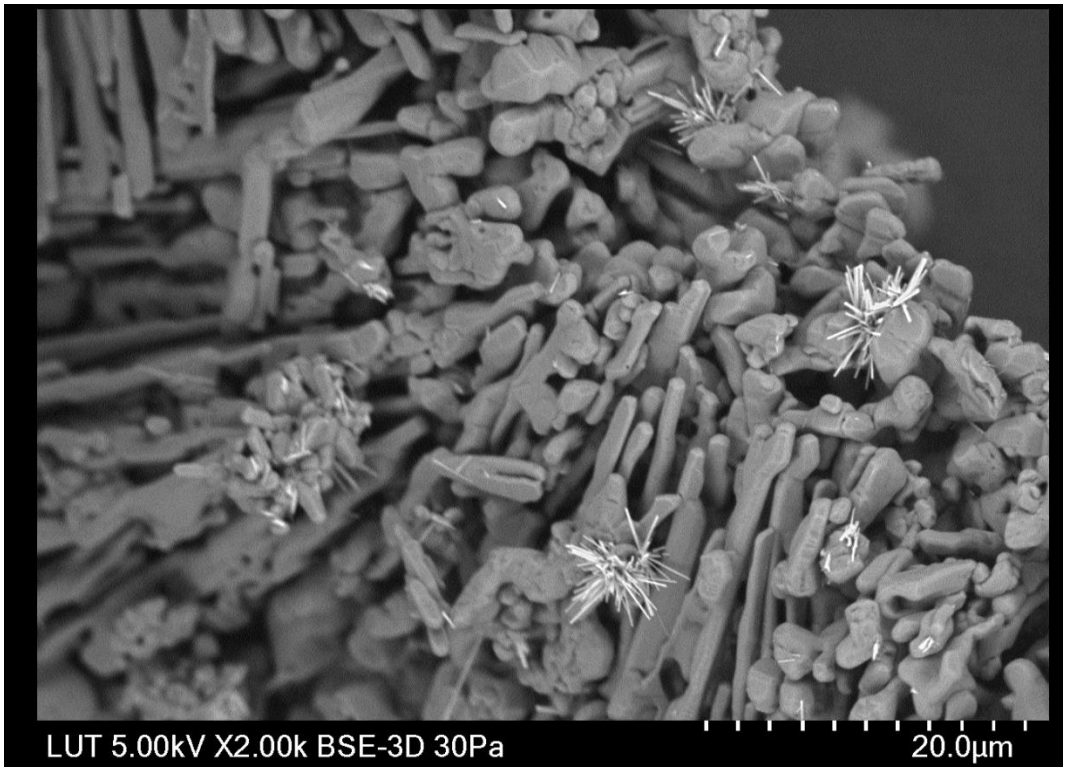

Figure 45 SEM pictures of the thoroughly washed crystals from batch 12.6 cooling rate 1

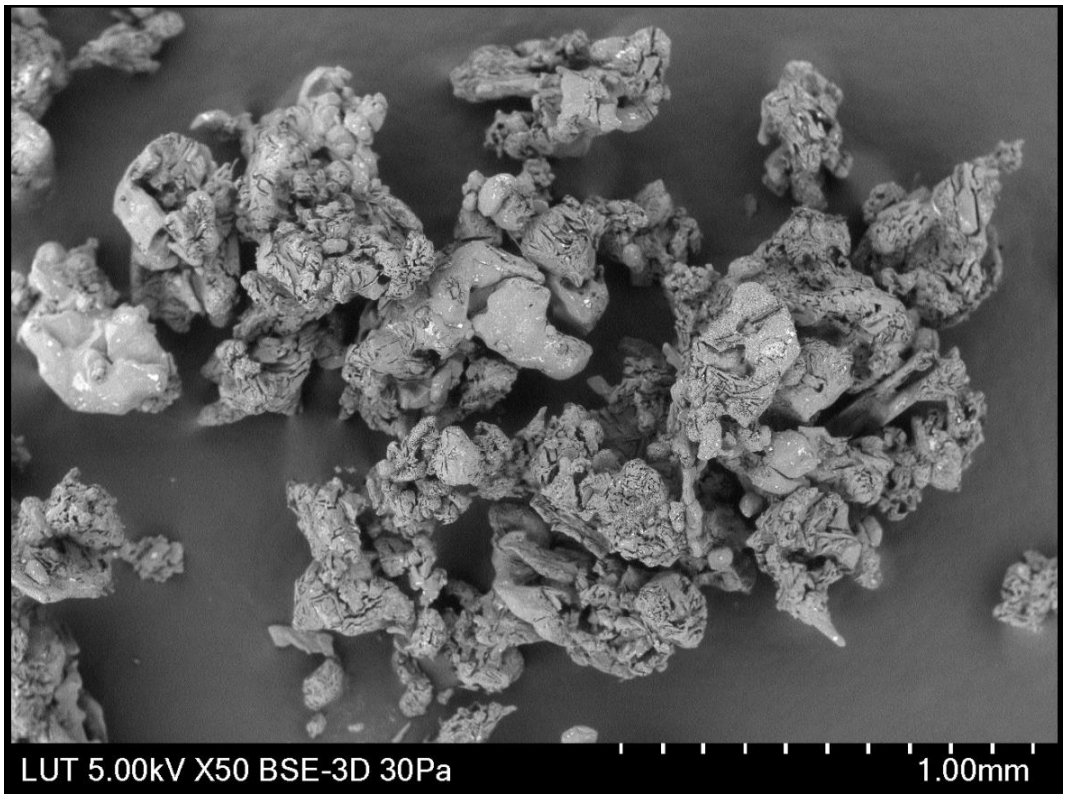

Figure 46 SEM pictures of the normally washed crystals from batch 12.6 cooling rate 1

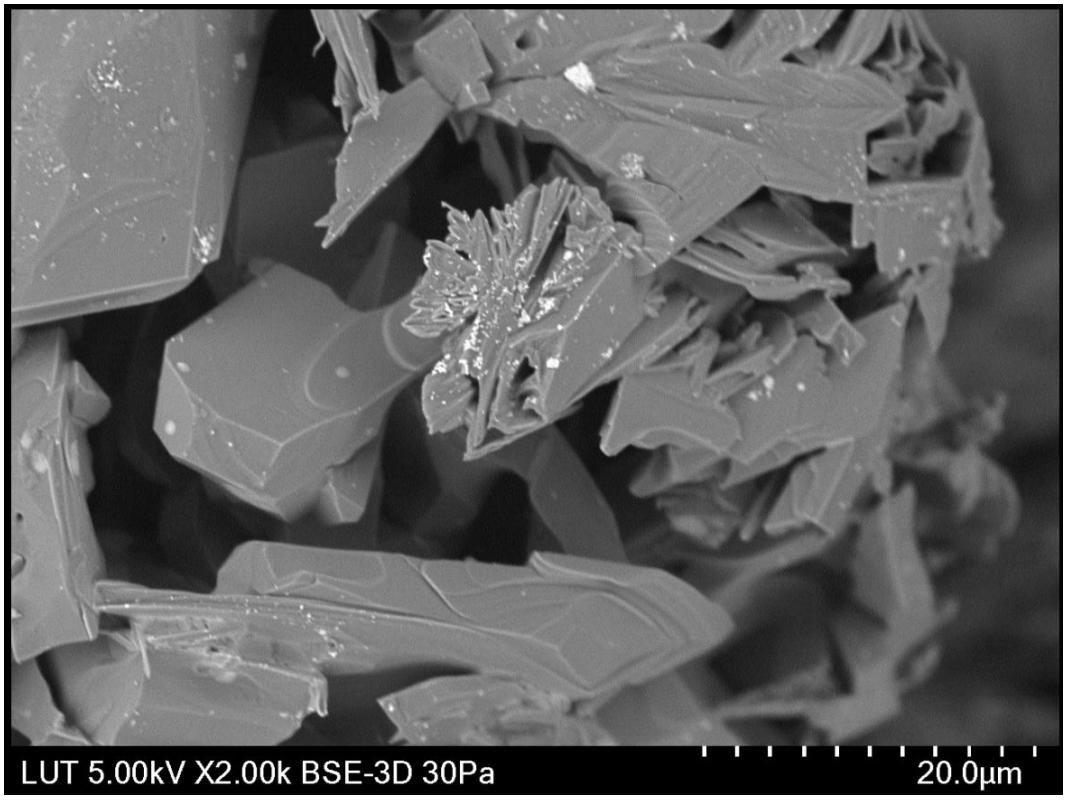

Figure 47 SEM pictures of the normally washed crystals from batch 12.6 cooling rate 1

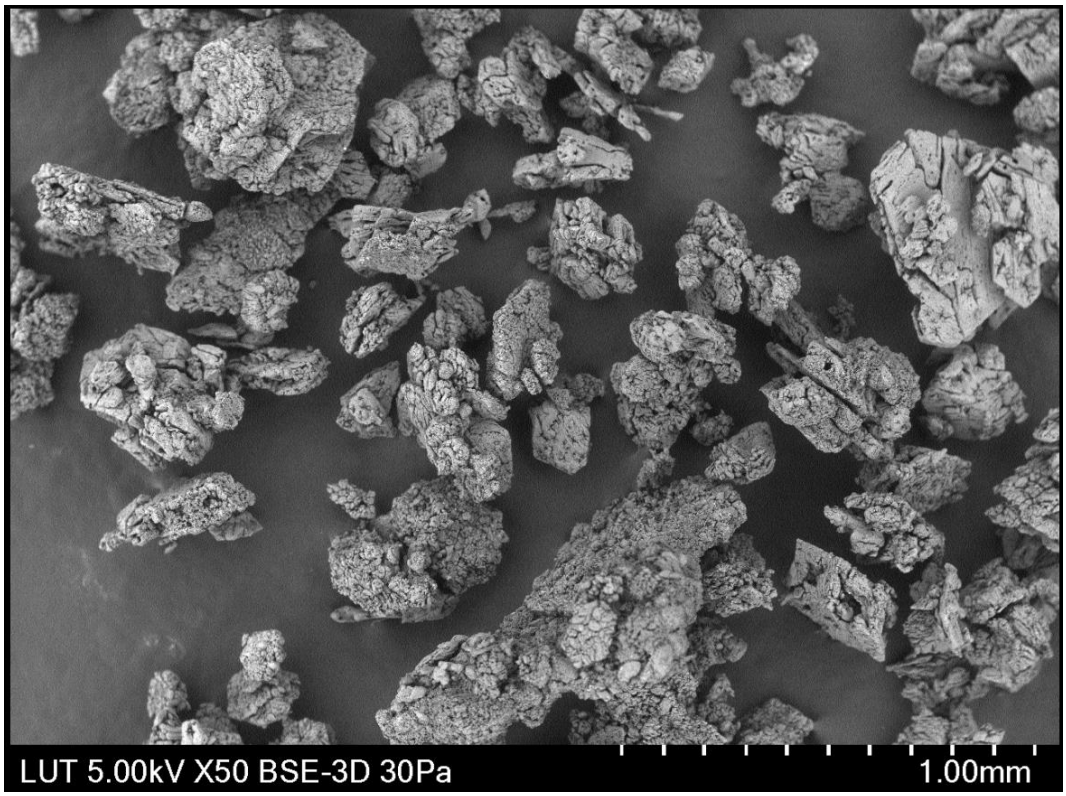

Figure 48 SEM pictures of the normally washed crystals from batch 12.6 cooling rate 2

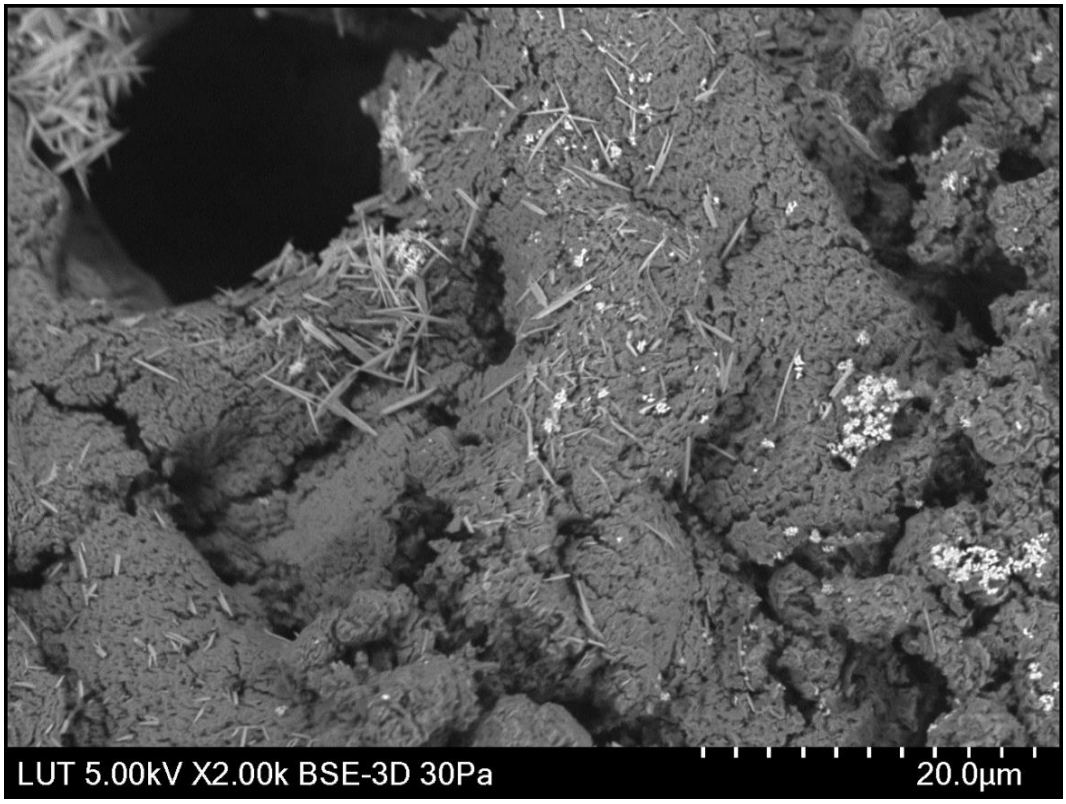

Figure 49 SEM pictures of the normally washed crystals from batch 12.6 cooling rate 2

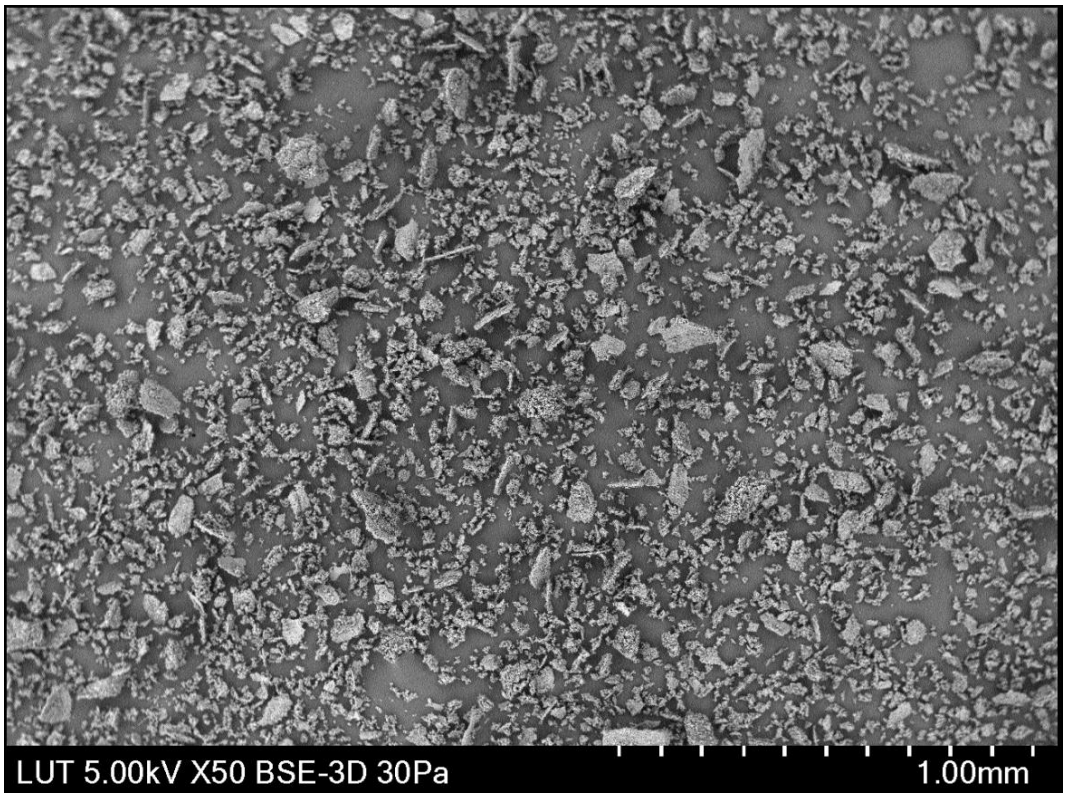

Figure 50 SEM pictures of the thoroughly washed crystals from green liquor cooling rate 1

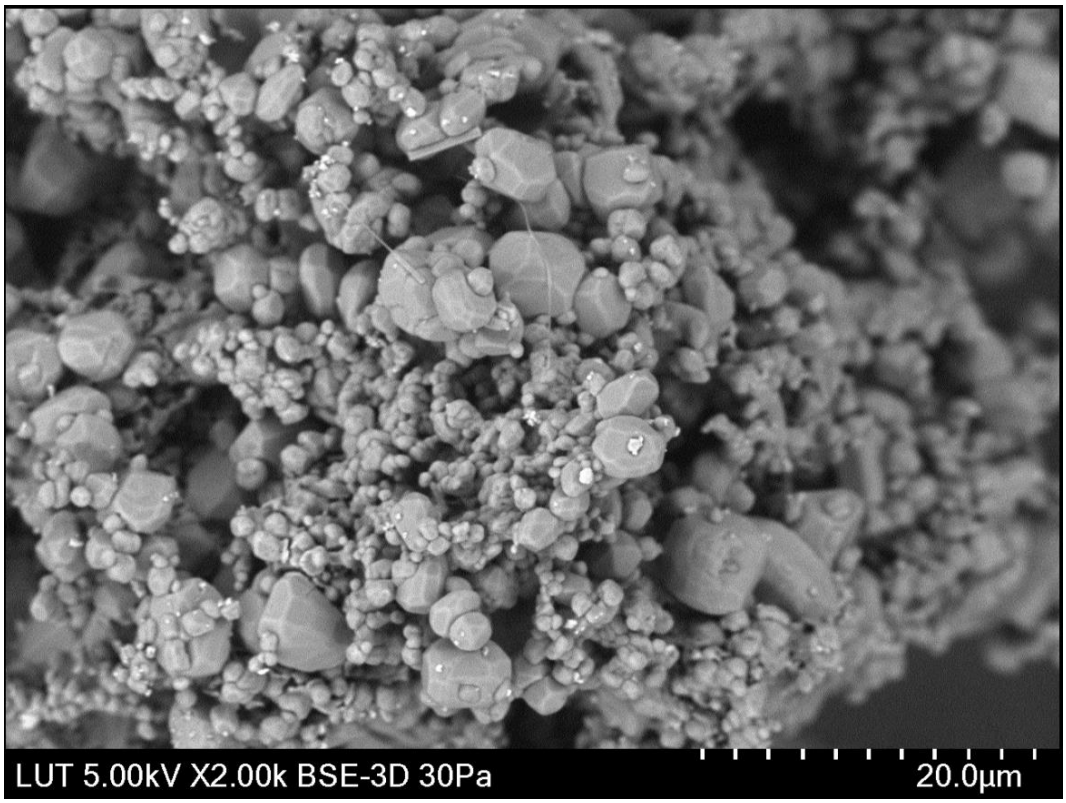

Figure 51 SEM pictures of the thoroughly washed crystals from green liquor cooling rate 1

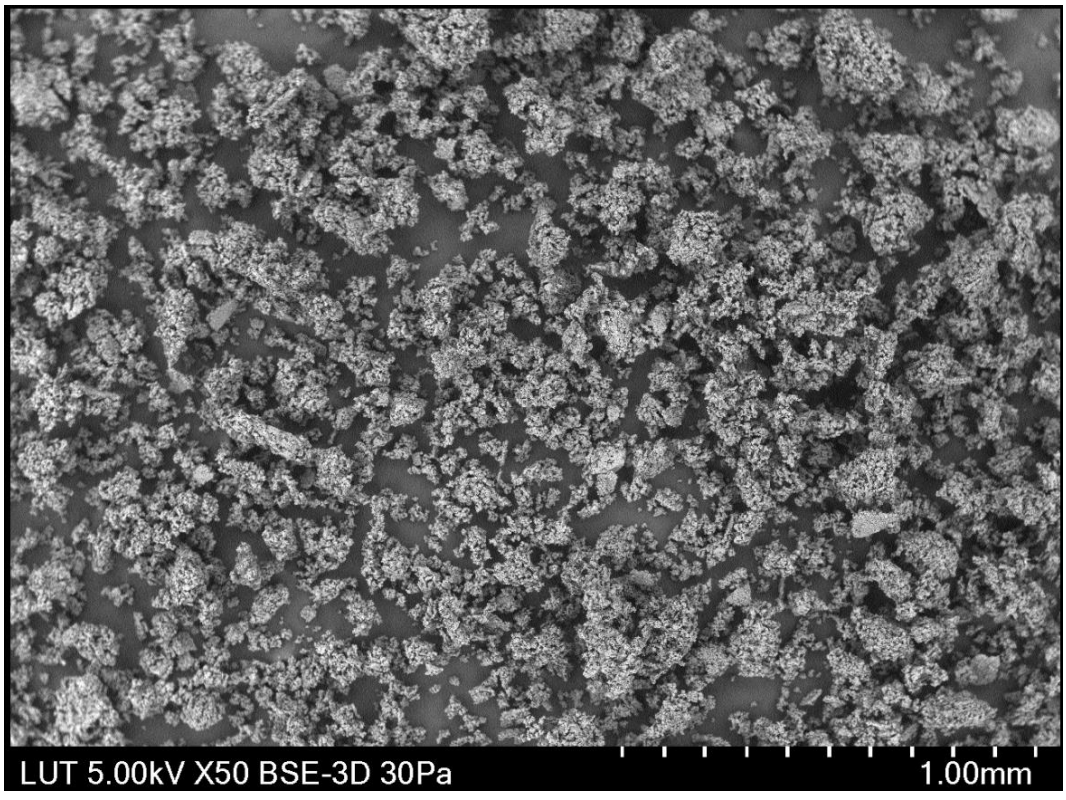

Figure 52 SEM pictures of the normally washed crystals from green liquor cooling rate 1

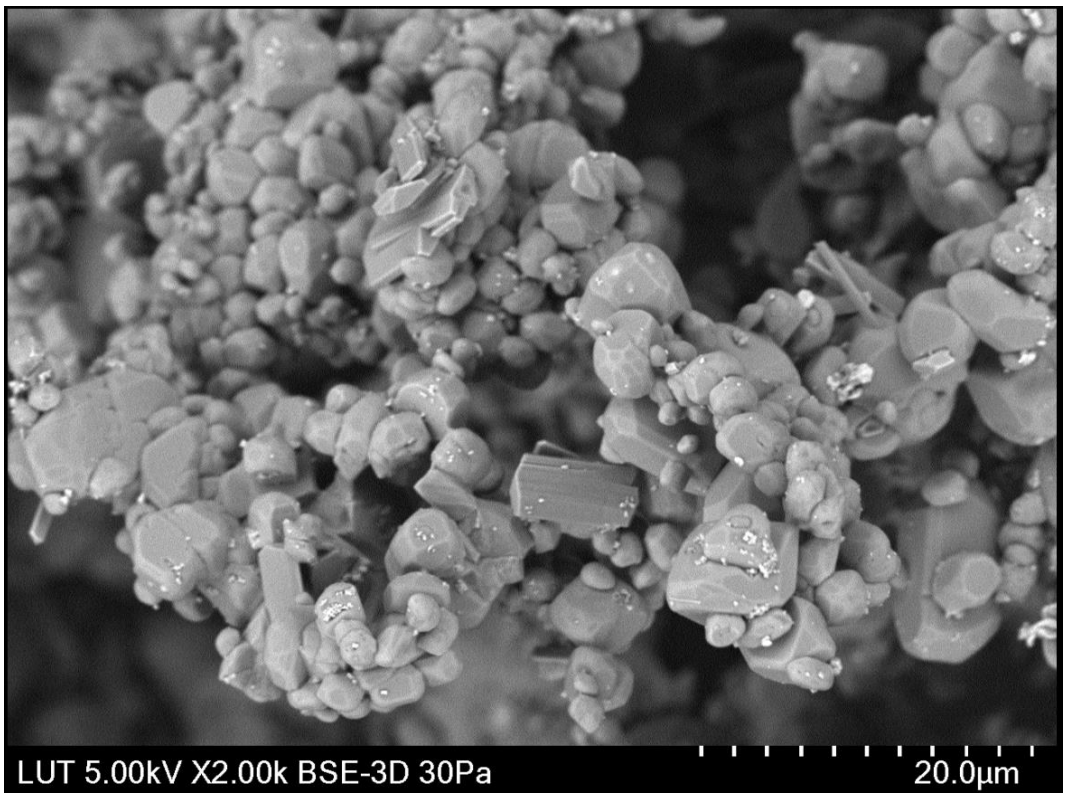

Figure 53 SEM pictures of the normally washed crystals from green liquor cooling rate 1

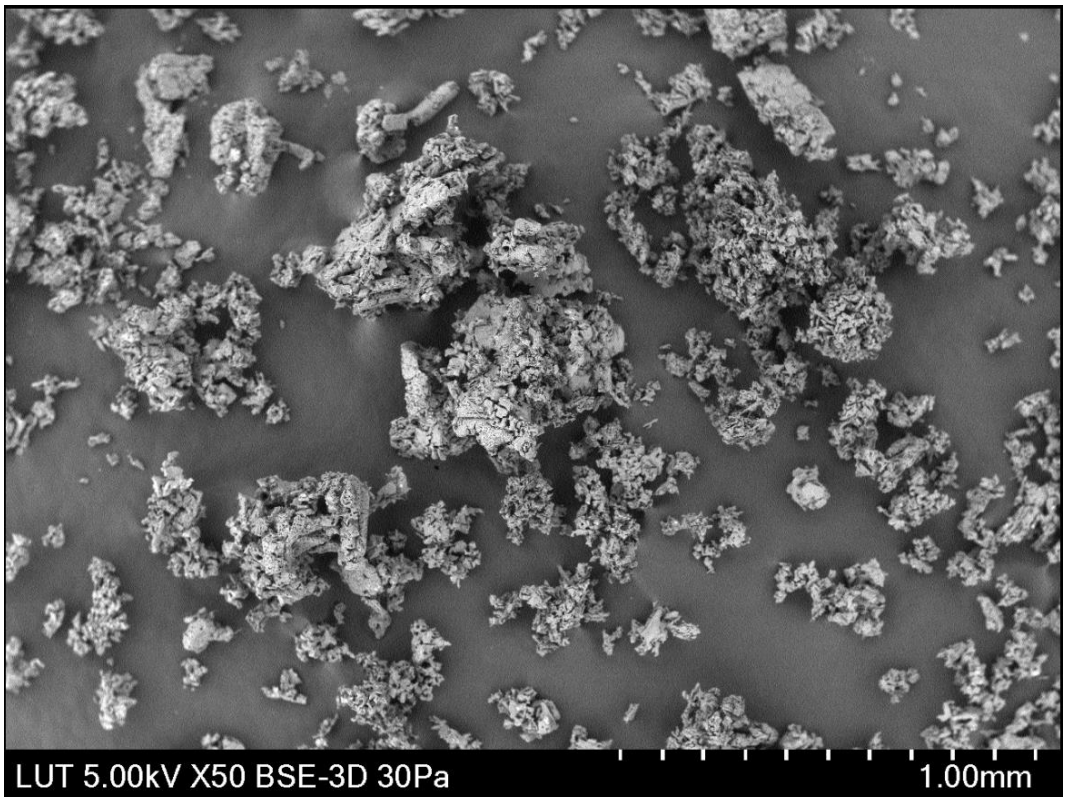

Figure 54 SEM pictures of the normally washed crystals from green liquor cooling rate 2

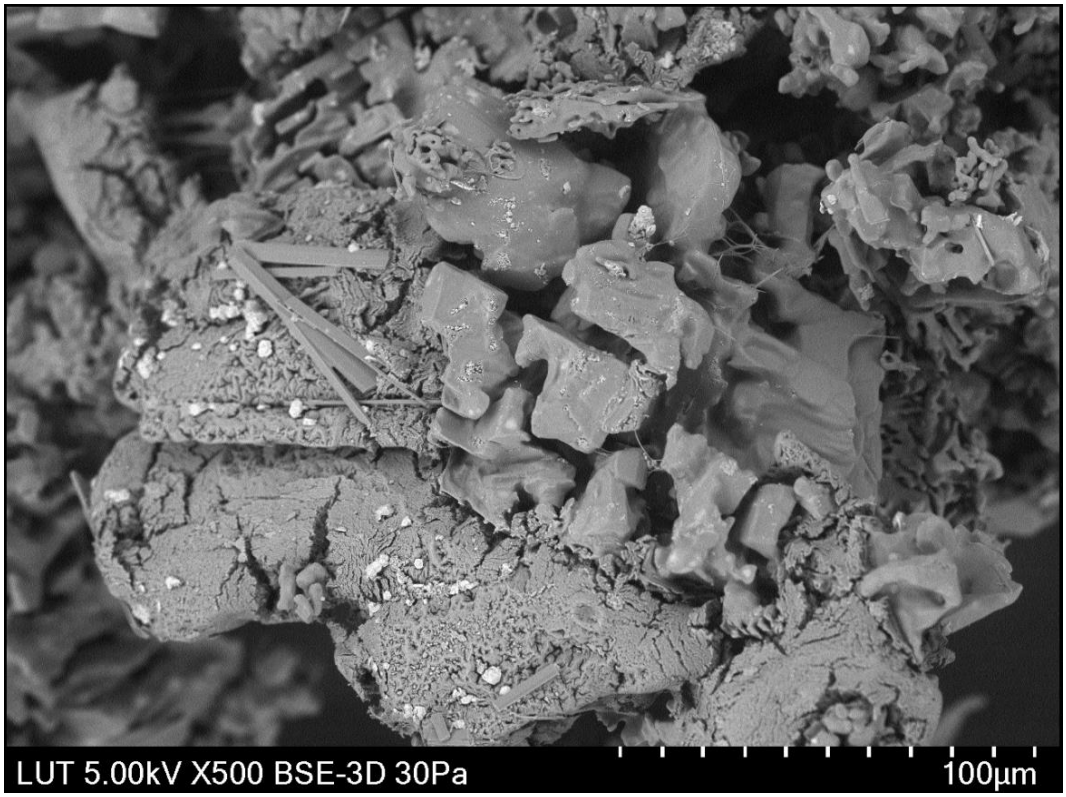

Figure 55 SEM pictures of the normally washed crystals from green liquor cooling rate 2